AD-A159 133 A THEORETICAL APPROACH TO THE CALCULATION OF ANNEALED IMPURITY PROFILES O..(U) STANFORD UNIV CALIF SOLID-STATE ELECTRONICS LAB A CHU JUN 77 1/2

UNCLASSIFIED SU-SSEL-77-012 ECOM-77-2684-1 F/G 20/2 NL

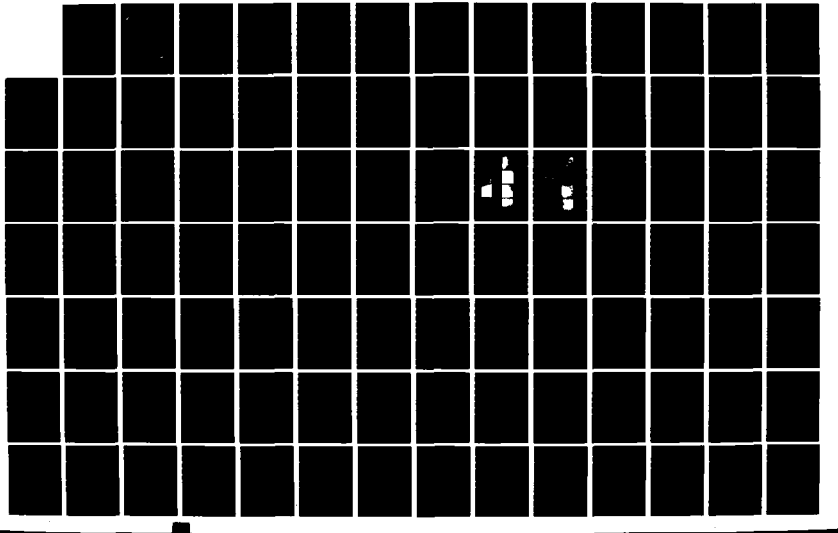

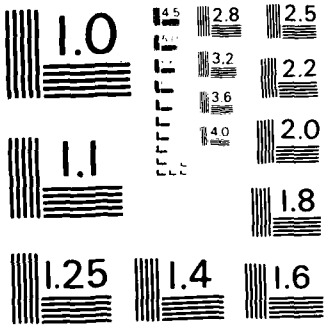

(1)

AD A159133

Research and Development Technical Report

ECOM - 77-2684-1

A THEORETICAL APPROACH TO THE CALCULATION OF ANNEALED IMPURITY PROFILES OF ION IMPLANTED BORON INTO SILICON

by

Alejandro Chu

Solid State Laboratory
Stanford Electronics Laboratories
Stanford, California 94305

June 1977

Interim Report for Period 1 November 1976 - 30 April 1977

Distribution Statement

Approved for Public Release, Distribution Unlimited

Prepared for

ADVANCED RESEARCH PROJECTS AGENCY
1400 Wilson Boulevard
Arlington, Va. 22209

Contract Nos. DAA-B07-75-C-1344 and DAA-B07-77-C-2684
ARPA Order No. 2985

ECOM

UNITED STATES ARMY ELECTRONICS COMMAND · FORT MONMOUTH, N.J.

SECURITY CLASSIFICATION OF THIS PAGE

AD-A159133

REPORT DOCUMENTATION PAGE

Form Approved
OMB No 0704-0188
Exp Date Jun 30, 1986

1a REPORT SECURITY CLASSIFICATION Unclassified	1b RESTRICTIVE MARKINGS
2a SECURITY CLASSIFICATION AUTHORITY	3 DISTRIBUTION / AVAILABILITY OF REPORT
2b DECLASSIFICATION / DOWNGRADING SCHEDULE	
4 PERFORMING ORGANIZATION REPORT NUMBER(S) SU-SSEL-77-012	5 MONITORING ORGANIZATION REPORT NUMBER(S) ECOM-77-2684-1
6a NAME OF PERFORMING ORGANIZATION Stanford University Stanford Electronics Lab 6b OFFICE SYMBOL (If applicable)	7a NAME OF MONITORING ORGANIZATION ECOM
6c ADDRESS (City, State, and ZIP Code) Stanford, CA 94305	7b ADDRESS (City, State, and ZIP Code) Ft. Monmouth, NJ
8a NAME OF FUNDING / SPONSORING ORGANIZATION DARPA 8b OFFICE SYMBOL (If applicable)	9 PROCUREMENT INSTRUMENT IDENTIFICATION NUMBER DAAB-07-75-C-1344 DAAB-07-77-C-2684
8c ADDRESS (City, State, and ZIP Code) 1400 Wilson Blvd Arlington, VA 22209-2308	10 SOURCE OF FUNDING NUMBERS PROGRAM ELEMENT NO / PROJECT NO / TASK NO / WORK UNIT ACCESSION NO

11 TITLE (Include Security Classification)
A Theoretical Approach to the Calculation of Annealed Impurity Profiles of Ion Implanted Boron into Silicon

12 PERSONAL AUTHOR(S)
Alejandro Chu

13a TYPE OF REPORT	13b TIME COVERED	14 DATE OF REPORT (Year, Month, Day)	15 PAGE COUNT
Technical	FROM 1/11/76 TO 3/4/77	June 1977	133

16 SUPPLEMENTARY NOTATION

17 COSATI CODES			18 SUBJECT TERMS (Continue on reverse if necessary and identify by block number)
FIELD	GROUP	SUB-GROUP	Materials Boron Silicon
11	3, 9		

19 ABSTRACT (Continue on reverse if necessary and identify by block number)

A multi-stream diffusion model is proposed for the calculation of the annealing behavior of boron that is ion implanted into silicon at room temperature and subsequently annealed. This model is capable of predicting both the redistribution and the electrical activation of boron during the anneal, as a realistic model should. The calculated results compare very well with extensive experimental data reported in the literature. The comparison includes samples that are implanted at room temperature with boron in the dose range from 10^{14} to 10^{16} ions/cm^2 and subsequently annealed in the temperature range from 800°C to 1000°C. This range of dose and annealing conditions includes both the typical applications of ion implantation as it is applied in the fabrication of devices and the unconventional cases of high dose implants and low temperature annealing.

20 DISTRIBUTION / AVAILABILITY OF ABSTRACT	21 ABSTRACT SECURITY CLASSIFICATION
☒ UNCLASSIFIED/UNLIMITED ☐ SAME AS RPT ☐ DTIC USERS	Unclassified
22a NAME OF RESPONSIB E INDIVIDUAL G. T. Winn	22b TELEPHONE (Include Area Code) (202) 694-5919 / 22c OFFICE SYMBOL TIO

DD FORM 1473, 84 MAR 83 APR edition may be used until exhausted
All other editions are obsolete

SECURITY CLASSIFICATION OF THIS PAGE
UNCLASSIFIED

SU-SSEL-77-012

A THEORETICAL APPROACH TO THE CALCULATION OF ANNEALED IMPURITY PROFILES OF ION IMPLANTED BORON INTO SILICON

by

Alejandro Chu

July 1977

Technical Report No. 4969-2

Prepared under

Defense Advanced Research Projects Agency
Contract DAA-B07-75-C-1344
and
National Science Foundation
Grant GH-31999

Solid-State Electronics Laboratory
Stanford Electronics Laboratories
Stanford University Stanford, California

ABSTRACT

A multi-stream diffusion model is proposed for the calculation of the annealing behavior of boron that is ion implanted into silicon at room temperature and subsequently annealed. This model is capable of predicting both the redistribution and the electrical activation of boron during the anneal, as a realistic model should. The calculated results compare very well with extensive experimental data reported in the literature. The comparison includes samples that are implanted at room temperature with boron in the dose range from 10^{14} to 10^{16} ions/cm^2 and subsequently annealed in the temperature range from 800°C to 1000°C. This range of dose and annealing conditions includes both the typical applications of ion implantation as it is applied in the fabrication of devices and the unconventional cases of high dose implants and low temperature annealing.

The annealing model is in essence a diffusion model extended to include the following situations:

(1) precipitation of boron, when the boron concentration level exceeds the solid solubility limit, in high dose implantation cases

(2) trapping of boron by the strain fields associated with dislocation dipoles that form during annealing at low temperature

In both cases, the presence of this immobile and electrically inactive boron alters significantly the redistribution and electrical activation behavior of boron during the anneal.

The presence of boron precipitates makes it necessary to include four species in the annealing model. These species are substitutional (electrically active) boron, boron-vacancy pairs (electrically inactive), positively charged vacancies, and the aforementioned immobile boron. The electrically active boron is assumed to diffuse substitutionally by means of random encounters with neutral vacancies. The boron-vacancy pair is assumed to diffuse much more rapidly. The principal interaction among the species is the reaction of active boron with positive vacancies to form BV-pairs.

The parameters in the model are a set of diffusivities and lifetimes for various species and interaction. These parameters are estimated from the examination of each diffusion and each interaction. The values of the most important parameters obey simple activation energy relations. In other cases, the modelling was either not carried to the extent necessary as to make the temperature dependence apparent, or else the parameters represent the composite effects of very complex interactions. In all cases, the mathematical model and the parameter set are universal in the sense that the same equations and parameters can be used for the prediction of ordinary diffusion, proton enhanced diffusion, and the annealing behavior of ion implanted boron at room temperature under conditions that include precipitation effects and low annealing temperature anomalies. Furthermore, in most cases of practical importance, high dose and low annealing temperature conditions are of limited interest and, as a result, the three stream diffusion model with an appropriate subset of parameters is sufficient. This reduced model is still very important and attractive because, once the parameters associated with high dose and/or low temperature anomalies are deleted, the remaining parameters have simple activation energies and are determined by the specification of a single variable: the temperature.

ACKNOWLEDGMENT

I would like to express my sincere gratitude to Professor James F. Gibbons, my research advisor, for providing his guidance in an atmosphere that awakened my interest in many areas, for formulating questions that sharpened my judgment, and for being critical in a way that encouraged my self-improvement. For these reasons, my research under his supervision has been a most meaningful academic and educational experience.

I am indebted to Dr. T. J. Magee of Stanford Research Institute for his considerable assistance with the transmission electron microscopy experiments in this thesis. I thank Dr. A. Hindmarsh of the Lawrence Livermore Laboratory and Professor O. Buneman for their advice in the area of numerical analysis. I am grateful to Dr. K. Saraswat and my colleagues, E. Ammar, A. Lidow, T. Herman, A. Gat, and F. Wu, for their assistance or comments on this work. In particular, I am much obliged to Dr. J. R. Anderson for his valuable discussions on the diffusion of boron in silicon.

Finally, I would like to thank my family. I am especially grateful to the following members: my parents from whom I learned perseverance, my sister Anna who provided the financial support that made possible my first studies in the United States, and my wife Cira who gives me constant enouragement.

The financial support of the Santa Rosa Division of the Hewlett-Packard Company is gratefully acknowledged. This work was supported jointly by the Defense Advanced Research Projects Agency under Contract No. DAA-B07-75-C-1344 and the National Science Foundation under Contract No. GH-31999.

CONTENTS

CONTENTS (Cont)

CONTENTS (Cont)

TABLES

ILLUSTRATIONS

ILLUSTRATIONS (Cont)

Furthermore, it is possible that ordinary diffusion, proton enhanced diffusion, and the annealing of boron are indeed the same problem with different excitation and initial condition. With this preliminary discussion, we turn the attention back to the consequences of a perturbation of the boron-silicon system at equilibrium with proton bombardment.

Fladda et al [11] have shown that substitutional boron in a diffused sample can be rapidly removed from their lattice sites by proton bombardment at room temperature. This same result can be achieved if the diffused sample is replaced by an ion implanted boron doped sample that was fully annealed. However, if an unannealed ion-implanted sample is used, no change in the fraction of substitutional boron can be detected even for proton doses as high as 10^{17} protons/cm^2. Similar results can be obtained at higher temperatures. Figure 3 shows profiles from a boron diffused sample irradiated by 10 KeV protons at 550°C for two hours, as determined by SIMS and electrical resistivity measurement [12]. The impurity distribution is characterized by the presence of a dip in the electrical carrier profile near the proton range and by some diffusion of the tail of the profile. This dip is not observed in the total boron concentration. The enhanced diffusion of the tail is more pronounced at higher temperatures such as 850°C or 900°C. If the proton dose is increased, then a peak starts to emerge from the bottom of the dip. This peak is attributed [13] to pileup of immobile boron (complexes, precipitates, dislocation trapping, etc.). To elucidate this issue, we analyze the annealing of damage produced by the room temperature irradiation of a 5×10^{15} protons/cm^2 dose on an annealed sample. The transmission electron micrograph shows the formation of lineated defects, that we identify as dislocation dipoles [19].

c. Profiling Measurements

Figure 4 shows a collection of isochronally annealed Boron profiles (35 min) at 800°C to 1000°C and the corresponding electrical carrier profiles for implantation doses* of 10^{14} to 10^{16} ions/cm^2, after

*The calculation based on the integration of the SIMS profiles shows that the actual implanted doses are ~ 30%, ~ 16%, and 30% higher than the nominal doses of 10^{14}, 10^{15}, and 10^{16} ions/cm^2.

system, the equilibrium condition can be altered by an excess vacancy concentration produced by proton irradiation. Since the production of vacancies that result from collision is a complicated problem, it is pertinent to elaborate upon the conditions under which excess vacancies are produced. Obviously, we want to avoid producing severe damage to the crystal, since in this case the recovery of equilibrium will be a much more complicated matter.

Energetic light ions such as protons or boron produce diffuse disorder clusters. These clusters are isolated because, even at room temperature, there is a certain amount of annealing that prevent the overlapping of individual disorder clusters. In contrast, if the implantation is performed at liquid nitrogen temperature, then the disorder clusters will overlap and an amorphous layer will form. This is a direct consequence of the negligible annealing at low temperature. An amorphous layer is also observed if the implanted ion is heavy. In this case, even if the implantation is carried out at room temperature and the implanted dose is moderate, the size of the disorder clusters are so extended that they will overlap.

In a Proton Enhanced Diffusion (PED), generally the substrate is held at an elevated temperature and the diffusion occurs under a steady proton bombardment. In view of this continuous excitation and the criterion of thermal equilibrium, we can classify the PED as a non-equilibrium-steady state problem. We shall see that the annealing of ion-implanted boron bears some resemblance and some differences with this case. As in the proton case, vacancies produced by the light boron damage give rise to an initial nonequilibrium condition; and, in contrast with the PED case, the perturbation is not at steady state. Hence, annealing of ion-implanted boron is a transient problem with a nonequilibrium initial condition. In this analysis, the simplest case is the ordinary diffusion occurring under thermal equilibrium, then in increasing order of difficulty: PED, a steady state nonequilibrium problem, and finally the annealing of ion-implanted Boron, a transient problem.

This analysis provides a natural way of conceiving how the enhanced diffusion at the outset of the anneal can turn into ordinary diffusion at a later time. In this interpretation, it is simply a transient problem reducing to the thermal equilibrium condition.

Table 1

A COMPARISON OF DIFFUSION COEFFICIENTS AT VARIOUS TEMPERATURES OBTAINED UNDER DIFFERENT CONDITIONS, AFTER HOFKER ET AL [2]

Annealing Temp. (°C)	D (cm^2 s^{-1})			
	N(ξ,0): Not Annealed Distribution		N(ξ,0): Annealed Distribution	from Kurtz
	10^{14} dose: ions cm^{-2}	10^{15} dose: ions cm^{-2}		
800	---	---	$1.5 \cdot 10^{-15}$	$5.2 \cdot 10^{-16}$ (extrapol.)
900	$1.7 \cdot 10^{-14}$	$1.4 \cdot 10^{-14}$	$1.4 \cdot 10^{-15}$	$1.3 \cdot 10^{-15}$ (extrapol.)
1000	$4.8 \cdot 10^{-14}$	$5.2 \cdot 10^{-14}$	$1.8 \cdot 10^{-14}$	$1.7 \cdot 10^{-14}$
1100	$1.9 \cdot 10^{-13}$	$1.5 \cdot 10^{-13}$	---	$1.7 \cdot 10^{-13}$

b. Proton Irradiation

In the preceding review, we have examined situations in which the boron-silicon system is near thermal equilibrium conditions. In other words, equilibrium has been achieved with respect to temperature and all possible chemical reactions in the system. We purposely exclude the attainment of equilibrium with respect to the distribution of matter within the system in this definition. In what follows, we turn the attention to the perturbation of the equilibrium condition. First, we discuss the use of protons to create an excess vacancy concentration, and then we compare the differences between a proton enhanced diffusion and the annealing problem with respect to thermal equilibrium.

The purpose of perturbing a system at equilibrium with an excitation is to observe the subsequent response. Generally, a system under perturbed condition will expose the driving forces that will enable the system to return to equilibrium, hence elucidating physical mechanisms hidden under thermal equilibrium conditions. In the boron-silicon

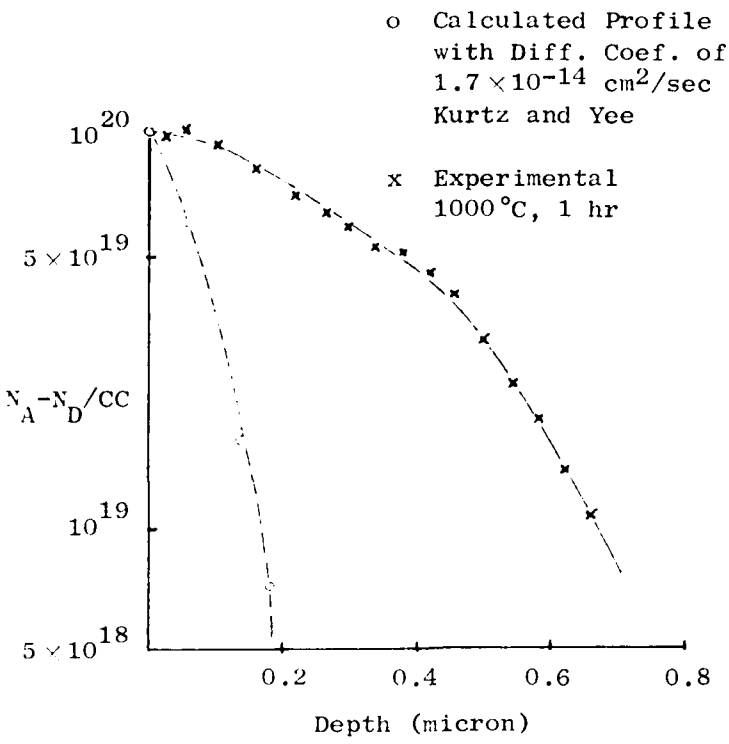

Fig. 2. THE HIGH CONCENTRATION ANOMALY--COMPARISON OF EXPERIMENTAL DIFFUSION PROFILE WITH THE CALCULATED PROFILE USING THE DIFFUSION COEFFICIENTS DETERMINED IN LOW CONCENTRATION EXPERIMENTS, AFTER NICHOLAS [7].

During annealing, the redistribution of boron is anomalous. At the beginning, the diffusion rate is high. However, as the annealing proceeds, the diffusion rate decreases to values obtained in ordinary diffusion experiments [2]. The relative importance of this transient effect is shown in Table 1, after Hofker et al [2]. The diffusion coefficients in the second and third columns are obtained from curve fitting the experimental profiles after 35 min of annealing with calculated profiles originated from the as-implanted profiles. The values in the fourth column are obtained from fitting experimental profiles at longer annealing times with calculated profiles originated from annealed profiles. Agreement of the values in the fourth column with the diffusion coefficients in column five, obtained in ordinary diffusions, indicate that, once the ion implanted impurities are on substitutional sites, the diffusion mechanism is indistinguishable from ordinary diffusion.

concentrations under thermal equilibrium conditions, the electrically active Boron concentration approaches the total boron concentration. In contrast, under nonequilibrium thermodynamic conditions such as at the completion of a boron implant of a proton irradiation or before the completion of an anneal, the active boron concentration will differ substantially from the total boron concentration, as we will see.

a. Ordinary Diffusion

At low concentrations, the diffusion of impurities into near intrinsic silicon substrates obeys Fick's laws, hence the diffused profile from a constant concentration source is represented by a complementary error function. At high concentrations, boron and many Group III and Group V impurities diffuse abnormally fast. This high concentration anomaly [3-7] is depicted in Fig. 2; after Nicholas [5]. Another anomaly is the effect of substrate background doping. If the substrate is doped a-priori with arsenic or phosphorus, the a-posteriori diffusion of boron is greatly reduced [6,7]. These diffusion anomalies can be represented by the following equation, after Crowder et al [8].

$$D/D_i = p/p_i \qquad (1)$$

where D and p symbolize diffusion coefficient and hole concentration, respectively, and the subscript i denotes intrinsic condition. This equation can be derived [8] assuming that the diffusion of boron is proportional to the total vacancy concentration, which is in turn Fermi level dependent. An alternate derivation by Anderson and Gibbons [9] has also been published and is, in fact, consistent with the annealing model we will develop here.

There are other anomalies, such as the enhancement in diffusion in mechanically polished substrates and diffusion in the presence of oxidation. These cases require an alternative mechanism to explain the enhanced diffusion, for instance, Nicholas [7] and Parker [10] propose that vacancies are generated from the nonconservative motion of dislocation.

Next, we will examine the experiments on the lattice location of ion-implanted boron. These experiments reveal that at the initial stages of annealing only a small fraction of boron is on substitutional sites. This fraction gradually increases to 100% toward the end of the anneal. Then, we review experiments on the electrical activity of the implanted Boron and show that this data is in good agreement with the channeling data.

It is evident from these experiments that there is a nonsubstitutional fraction of boron during annealing. Naturally, this inactive boron need not be in a single type of defect or complex. Whereas, in many cases it does seem that a single type of defect is responsible for the electrical inactivity, in other cases it is apparent that more than one form of inactive boron is required. To study this possibility, we performed a group of experiments on the evolution of implantation damage during an isothermal annealing to elucidate this issue. The global transmission electron microscopy results indicate that, when the presence of more than one form of inactive boron is evident, the second form is either boron trapped by defects formed during annealing or boron precipitate, if the solid solubility limit was exceeded by the boron concentration.

1. Experiments on Diffusion

The study of diffusion depends heavily on the determination of concentration profiles. Whereas some profiling techniques are based on the identification of the species chemically present, others are based on the electrical effect of the ionized specie present in the substrate. In the first category, we find the use of radiotracers, secondary ion mass spectrometry, Auger, backscattering, and ESCA. In the second category, the techniques are two point or four point resistance measurements, CV profiling, and Hall-mobility measurements. In general, these methods do not give the depth information unless they are used in conjunction with a layer removal technique such as anodic oxidation and oxide stripping or sputtering with an argon ion beam. The data that we will review were obtained using SIMS for the determination of total boron concentration profiles in the substrate and Hall-mobility measurement to determine the ionized, electrically active boron profiles. For moderate

temperature under conditions that include the most relevant cases in device fabrication; i.e., dose range of 10^{14} to 10^{15} ions/cm^2 and annealing temperature range between 900°C to 1000°C. The primary input to the annealing model is the history of the substrate summarized by two distributions: the as-implanted boron profile (either computed or determined experimentally) and the distribution of energy deposited into nuclear processes by the boron ions. Damage is a product of this energy distribution. Our goal is to use this basic information (which is available for various combinations of projectiles and targets with acceleration voltage as a parameter) to predict the isothermal annealing of boron implanted into Si at room temperature (the most common application). Specifically, we wish to determine the evolution of the electrically-active boron in both time and space. A realistic annealing model should predict ordinary diffusion, proton enhanced diffusion, and naturally be consistent with the collection of experiments that we will review hereafter.

B. A Summary of Relevant Experimental Data

The purpose of reviewing relevant experiments is to establish that, despite the complexity of the actual situation, a model containing only four interacting species is capable of explaining the major features of the annealing behavior. These species are: substitutional boron, boron vacancy pairs, positively charged vacancies, and immobile boron (B trapped by defects or B precipitate). In what follows, we will show that with these four species we can model both the diffusive redistribution of ion implanted boron and the electrical activation of the implanted boron during annealing.

The experiments we will review can be grouped in three major areas: diffusion, electrical activation, and implantation damage. In the first area, we will examine diffusion anomalies, proton enhanced diffusion, and the redistribution of profiles during annealing. A vacancy mechanism is likely to account for the global features in these experiments. However, other features will require additional explanations. This is the case for the abnormal structures in low-temperature and short-time anneals.

shows that this enhancement in diffusion is a transient and that eventually, as the electrical activity approaches 100%, diffusion will gradually slow down and the ordinary thermal diffusion rate of 1.3×10^{-15} cm^2/sec will be obtained.

5. The Need for an Annealing Model

The example in the preceding section is from a common industrial application. It serves the purpose of showing the need for a realistic annealing model. Such a model should provide not only reasonable predictions of the annealed boron profile, but also a reasonable prediction of the evolution of electrical activity versus time. At present, empirical procedures are used to arrive at the implantation conditions and annealing schedule that will achieve the desired profiles. In this empirical process, the accurately calculated as-implanted profiles are only used as approximations to the desired profiles. And the annealing schedule is selected from a proven set of conservative schedules.

In contrast, given a suitable annealing model, the device designer can utilize the calculated as-implanted profiles and from these determine the annealed profiles for one or more annealing schedules. Furthermore, such a model will enable the entire ion implantation process to be modelled on a computer, which may lead to the eventual development of more sophisticated applications of ion implantation in device fabrication.

6. Cases to be Studied

The principal impurities used in the fabrication of silicon devices are boron (for p-type regions), phosphorus and arsenic (for n-type regions). In this group, B has attributes that make it the most widely implanted impurity. For instance, the implantation of B for threshold shifting in MOS devices and the implantation of the boron doped base into a pre-prepared substrate with the E and C structures are possible because of the light damage and the long range characteristics of ion implanted boron. We chose in the present work to study the annealing behavior of ion-implanted boron into silicon at room

thermal equilibrium. Therefore, it is not surprising to find that the redistribution of boron during annealing cannot be predicted with a simple diffusion model that utilizes diffusion coefficients derived from ordinary diffusion experiments under thermal equilibrium conditions. For instance, Fig. 1 shows an as-implanted profile for boron in silicon together with this same profile after 35 minutes of annealing at 900°C. Both profiles were determined experimentally by Hofker et al [2]. These authors show that, to fit the annealed profile with the calculated profile that result from the diffusion of the as-implanted boron distribution, the diffusion coefficient should be set equal to $1.4 \times 10\text{-}14$ cm^2/sec. This value is an order of magnitude higher than 1.3×10^{-15} cm^2/sec, the diffusion coefficient determined from ordinary diffusion experiments extrapolated to 900°C. Further annealing

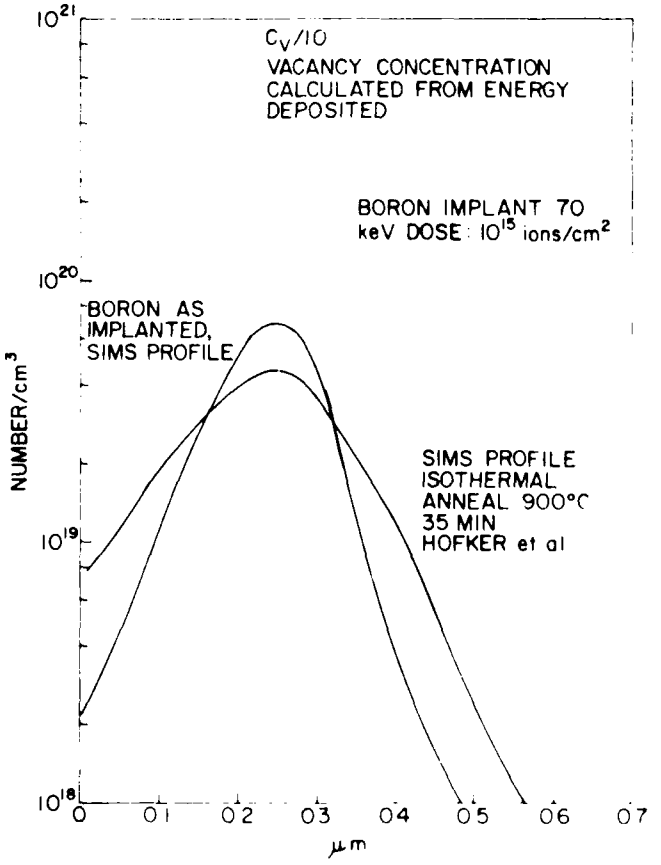

Fig. 1. AS-IMPLANTED B PROFILE AND THE ANNEALED PROFILE AT 900°C FOR 35 MIN, AFTER HOFKER ET AL [2].

lattice, forming as a result a disorder cluster around the ion track. Furthermore, since the process just described is far away from thermal equilibrium, only some of the implanted impurities will be located on substitutional sites, after the implantation. In general, a larger fraction will be found in interstitial positions and still other impurity atoms will form complexes with simple lattice defects (lattice vacancies and interstitials). Furthermore, the doping characteristics of the impurity may be overwhelmed by the damage. As a result, the as-implanted substrate will usually exhibit an electrical carrier concentration far below that which would be predicted simply from the implanted impurity concentration profile. In other words, only a small percentage of the implanted impurities contribute to electrical carriers.

3. The Anneal

In order to obtain the expected electrical properties, it is necessary to anneal the implanted material at an elevated temperature. During annealing, some vacancies will be annihilated by silicon interstitials, divancies will anneal out, stress created by the damage clusters will be relieved by the formation of dislocation loops and vacancy clusters, there will be migration of defects, transformation of complexes, etc., and, most importantly, a relocation of impurities on substitutional sites accompanied by spatial redistribution. After the anneal, the substrate will still retain residual dislocation networks, but for silicon at least, the mobility and electrical activity (ration of electrically active to the totality of implanted impurities) are comparable to bulk-doped samples, and hence this process is adequate for device fabrication.

4. The Spatial Redistribution of Impurities During Annealing

In order to examine further the spatial redistribution of Boron during the anneal, we observe that, at the outset of the anneal, the implanted Boron distribution is in the presence of an abnormally high concentration of lattice defects, mostly vacancies. Consequently, as annealing begins, the defects migrate and transform, and the redistribution of boron is occurring simultaneously under conditions far away from

Chapter I

THE ANNEALING OF ION IMPLANTED BORON INTO SILICON AT ROOM TEMPERATURE

A. Introduction

1. The Problem

Ion implantation is a technique [1] for introducing selected impurities into a substrate material in a controlled fashion. It is based on the generation of a mass analyzed ion beam followed by the acceleration of these ions in an electric field directed toward the substrate material. This scheme is easily controlled with electronic instrumentation. As a result, it is possible to achieve repeatably high purity ion beams, to implant ions to an accurate dose, and to impart precise kinetic energy to the ions, thus controlling reproducibly their stopping points in the substrate. These advantages are complemented by the availability of a theoretical model from which one can compute accurately the as-implanted distribution of impurity atoms. However, this latter advantage is somewhat fictitious, because the implanted ions may produce substantial damage in the (crystalline) substrate as they come to rest. To repair this damage, an anneal has to follow the implantation. During this anneal, a diffusive redistribution of the implanted impurities will occur and, as a result, the actual impurity profile may differ substantially from the as-implanted profile. The quantitative prediction of this redistribution problem is the principal subject of this thesis.

2. The Implantation of Ions

To elaborate on the nature of this problem, it is first useful to remark that the distribution of implanted ions in the solid substrate depends on both the acceleration voltage and mass relations between the implanted ion and the atoms of the target. Stopping of an energetic ion occurs as a result of collisions between the ion and the electrons and atoms of the target. If these collisions are sufficiently energetic, host atoms will be displaced from lattice sites, thus leaving vacancies behind. These displaced atoms may in turn displace other atoms in the

τ_V	Lifetime of vacancies
V^+	Positively charged vacancies
V^o	Neutral vacancy
x	Space
Δx	Spatial increment
$\vec{y}$	Vector
y_i, y_j	The i^{th} and j^{th} components of vector $\vec{y}$
$\dot{y}_i$	The time derivative of the i^{th} component of $\vec{y}$

EA	Electrical activity, fraction of ionized impurities to the total number of implanted impurities
E_F	Fermi energy level in the band gap
E_{V+}	Energy level of the positive vacancies in the band gap
f_i	i^{th} function
i	Integer index
j	Integer index
J	Jacobian matrix
J_{ij}	Element in the Jacobian matrix
k	Constant
k_o	Equilibrium constant in the B-BV-pair reaction
K	Boltzmann's constant, 8.62×10^{-5} eV/°K
$K_1, K_2, K_3, K, K', K_V, K_V'$	Scaled parameters
l	Superscript denoting left
p	Hole concentration in hole/cm^{-3}
p_i	Hole concentration under intrinsic conditions
r	Superscript denoting left
SSL	Solid solubility limit
T	Temperature in degrees kelvin
τ	Lifetime of BV-pairs
τ_{DAM}	Time constant associated with the release of vacancies from the primary implantation damage
τ_{dd}	Time constant associated with the trapping of boron by dislocation dipoles
τ_{diss}	Time constant associated with the dissolution of boron precipitates
τ_{prec}	Time constant associated with the precipitate of boron
τ_{rel}	Time constant associated with the release of boron from the annealing dislocation dipoles

SYMBOLS

B^-	Ionized boron
B^-V^+	Boron vacancy pair
B_{prec}	Boron precipitate
B_I	Immobile boron
$B_{trapped}$	Boron trapped by dislocation dipoles
c	Superscript denoting center
C	Concentration in $\#/cm^3$
C_B	Concentration of electrically active boron in $\#/cm^3$
C_{BI}	Concentration of immobile boron
$C_{B_{prec}}$	Concentration of boron precipitates
$C_{B_{total}}$	Total boron concentration
$C_{B_{trapped}}$	Concentration of boron trapped by dislocation dipoles
C_{BV}	Concentration of boron-vacancy pairs
C_{dd}	Threshold concentration level of boron for the formation of dislocation dipoles
C_{SSL}	Concentration at the solid solubility limit
C_{V^+}	Concentration of positively charged vacancies
$C_{V^+_{eq}}$	Equilibrium concentration of positively charged vacancies
D	Diffusion coefficient in units of cm^2/sec
Di	Diffusion coefficient under intrinsic conditions
D_B	Diffusion coefficient of electrically active boron
D_{BV}	Diffusion coefficient of boron-vacancy pairs
D_{exp}	Diffusion coefficient measured in an experiment
D_V	Diffusion coefficient of vacancies
Damage(x)	Damage profile computed from the distribution of energy deposited into atomic processes in ion implanted silicon

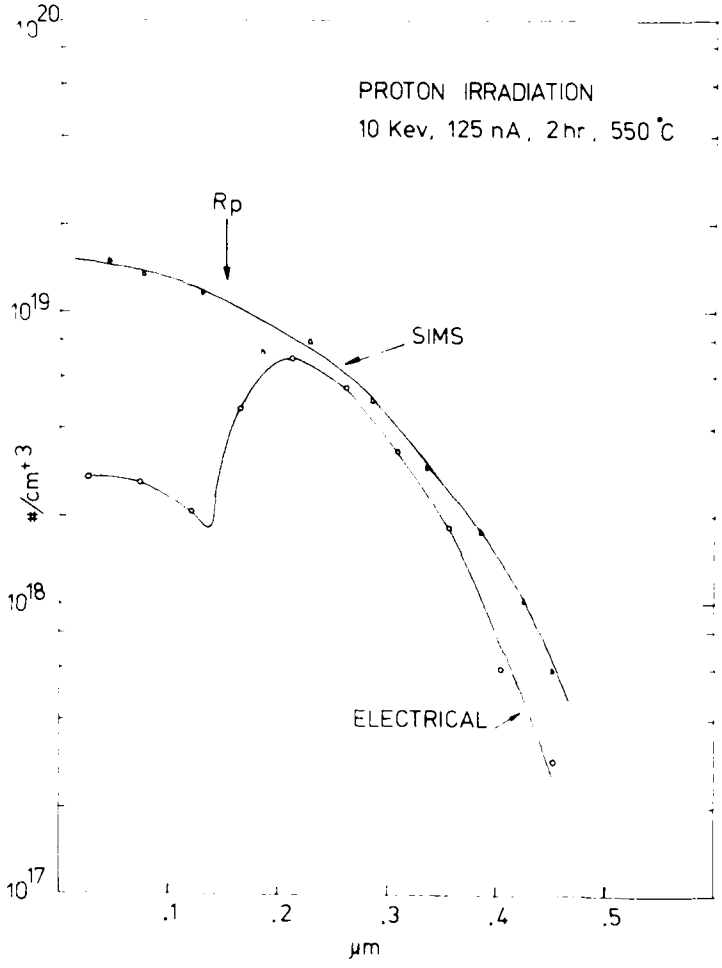

Fig. 3. A COMPARISON OF TOTAL BORON PROFILED DETERMINED EXPERIMENTS USING SIMS WITH THE ELECTRICAL CARRIER PROFILE THAT RESULT AFTER TWO HOURS OF IRRADIATION WITH 10 KeV PROTON, AFTER ANDERSON ET AL [12].

Hofker et al [2,14]. Figure 5 displays the juxtaposition of the annealed profiles with the as-implanted boron profiles for each dose, permitting the comparison of the profiles as the annealing temperature is varied (after Hofker et al).

Inspection of these figures indicates that:

(1) 100^{+} electrical activity is attained after 35 minutes of annealing a temperature of 900°C or higher and for implanted doses of 10^{15} ions/cm^2 or lower.

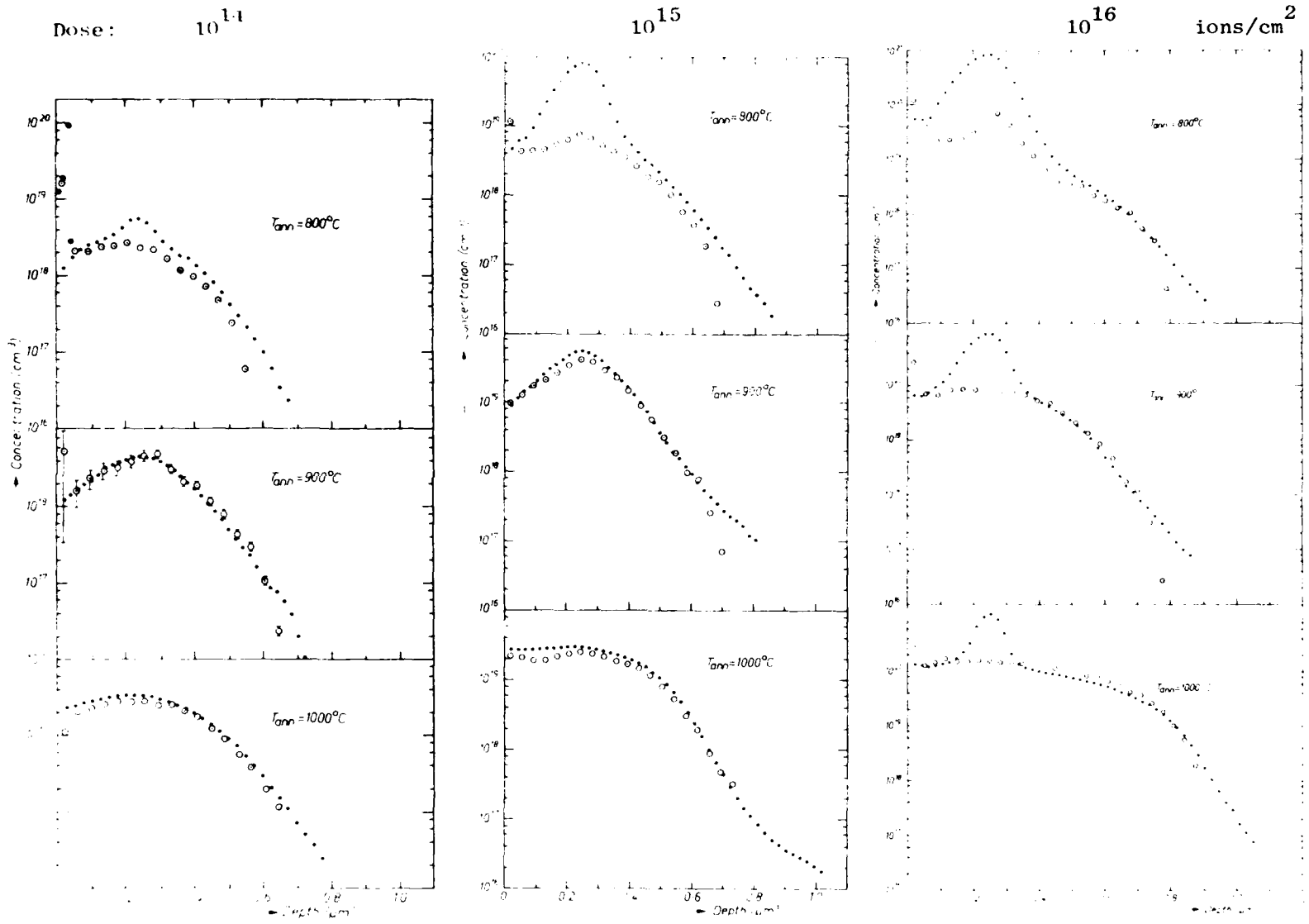

Fig. 1. CONCENTRATION PROFILE OF BORON AND THE CORRESPONDING CHARGE CARRIER PROFILES OBTAINED AFTER ANNEALING AT DIFFERENT TEMPERATURES FOR 35 MIN, AFTER HOFKER ET AL [14].

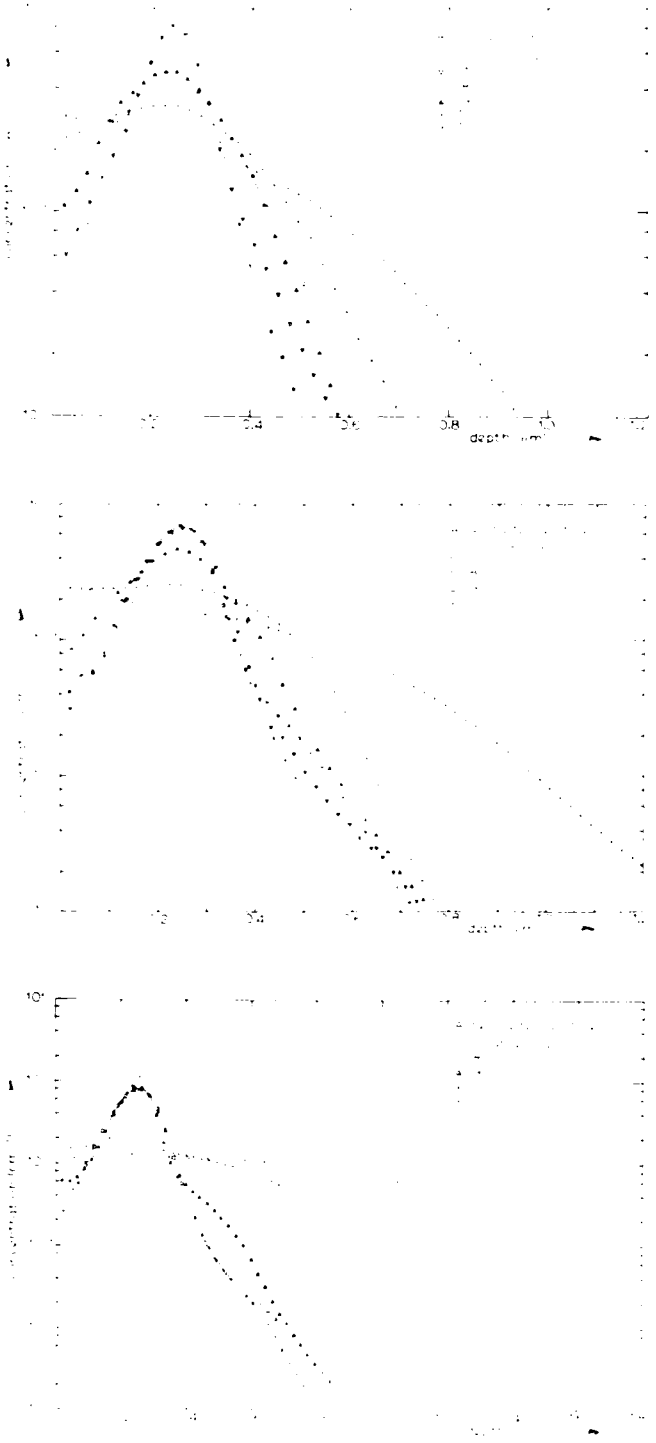

Fig. 5. CONCENTRATION PROFILES OF A BORON IMPLANTATION WITH A DOSE OF (a) 10^{14} IONS/CM^2, (b) 10^{15} IONS/CM^2, (c) 10^{16} IONS/CM^2, AND AT AN ENERGY OF 70 KeV BEFORE AND AFTER ANNEALING (ANNEALING DURATION: 35 MIN); AFTER HOFKER ET AL [2].

(2) In the 10^{16} ions/cm^2 cases, the boron peak concentration exceeds solid solubility. Therefore, there will be precipitation of boron.

(3) In the lower dose cases, when the anneal is carried out at 800°C, there is a fraction of boron that is electrically inactive and does not diffuse, hence similar to a precipitate. However, the boron concentration is below the solid solubility limit for these cases.

2. Experiments on the Lattice Location of Boron

The techniques used in the experiments that we will review are really indirect measurements that permit the inference that a fraction of boron is on substitutional sites. For instance, the carriers observed in an electrical resistance measurement are assumed to arise from the ionization of impurity atoms located on substitutional sites. However, substitutionality can also be measured independently by the channeling technique.

This method is based on the interactions of a low dose proton or Helium ion beam with the crystal lattice. This choice of ions is important because light mass ions at low doses produce negligible damage to the crystal. As a result, the probing ion will contribute with little error to the measurement. The quantitative measurement is based on the detection of backscattered ions with a solid state detector. These backscattered ions are the result of wide angle collisions of the light incident ions with heavier atoms in the substrate. During the measurement, the incident beam is directed along the channels of the crystal, hence the interactions with the substrate come primarily from (low impact parameter) collisions with off-lattice-site atoms (nonsubstitutional atoms). The calculation of the fraction of nonsubstitutional atoms is based on the comparison of the detector yield under channelled condition with the random yield, when the crystal is oriented randomly with respect to the incident beam. The substitutional fraction of atoms is the complementary fraction to unity. There are complicating factors that make the interpretation more difficult. For instance, the presence of lattice damage and flux peaking effects [15] can result in errors that are significant.

a. Channeling Experiments

Figure 6a shows the results of a channeling experiment by North and Gibson [16] on the lattice location of ion implanted boron in silicon. They determined that upon isochronal annealing at a sequence of monotonically increasing temperatures, the substitutional fraction of boron decreases first to a small fraction at temperatures between 500°C and 700°C and then it increases smoothly to near 90%, at higher annealing temperatures. Also, in Fig. 6a the fraction of substitutional boron can be compared with the percentage of electrical carriers produced by the implanted impurity dose. The agreement between the two curves is excellent above 700°C. The difference at lower temperatures is attributed by the authors to the compensation effect of intrinsic damage produced by the implantation. Although such an explanation is reasonable and transmission electron micrographs on samples of equivalent preparation do show [17] the presence of a high concentration of vacancy clusters and dislocation loops, there is perhaps insufficient attention given to the consequences of dechanneling of the probing beam by said defects. Certainly, a correction of the data to include this effect will result in a lower fraction of substitutional boron in this region.

Basically, this experiment indicates that annealing proceeds with the conversion of nonsubstitutional, electrically inactive boron into Boron that is electrically active and located on substitutional sites. A more detailed inspection of Fig. 6a reveals that between 500°C and 700°C the electrical activity as well as the concentration of substitutional boron decreases to a minimum. This phenomenon is known as negative or reverse annealing, and occurs near the recrystalization temperature of Silicon for boron implanted in the dose range of 10^{14} to 10^{15} ions/cm^2. Transmission Electron Microscopy (TEM) work by Bicknell [17] indicates that negative annealing is accompanied by the formation of lineated defects.

The effect of an increase in dose is a decrease in the fraction of substitutional boron and a lower initial electrical activity. This result is depicted in Fig. 6b after Fladda et al [11] and in Fig. 6c after Seidel and McRae [18].

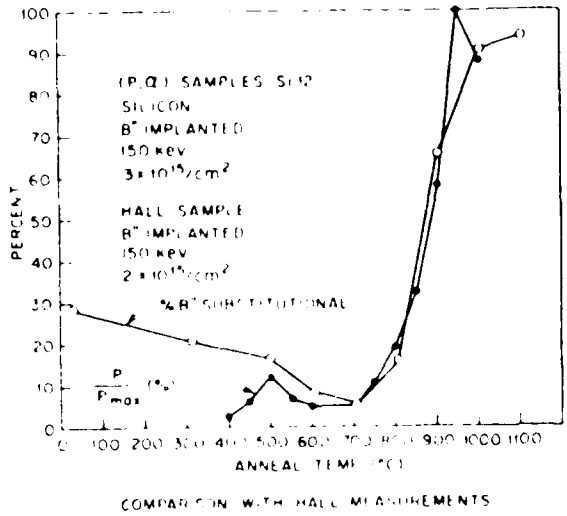

a. The percentage of the boron atoms which occupy substitutional lattice sites as a function of annealing temperature. Also shown is the carrier concentration expressed as a percentage of the maximum number of observed carriers determined from Hall measurements on a sample implanted to a fluence of $2 \times 10^{15}/cm^2$. After North and Gibson [15].

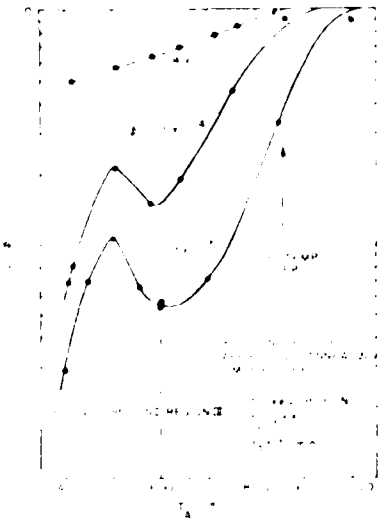

c. Isochronal data in reduced form. The ratio of the free carrier content from Hall measurements to the dose is plotted against the annealing temperature for three doses. The maximum free carrier content is nearly equal to the measured dose $p_m = \phi$. After Seidel and MacRae [18].

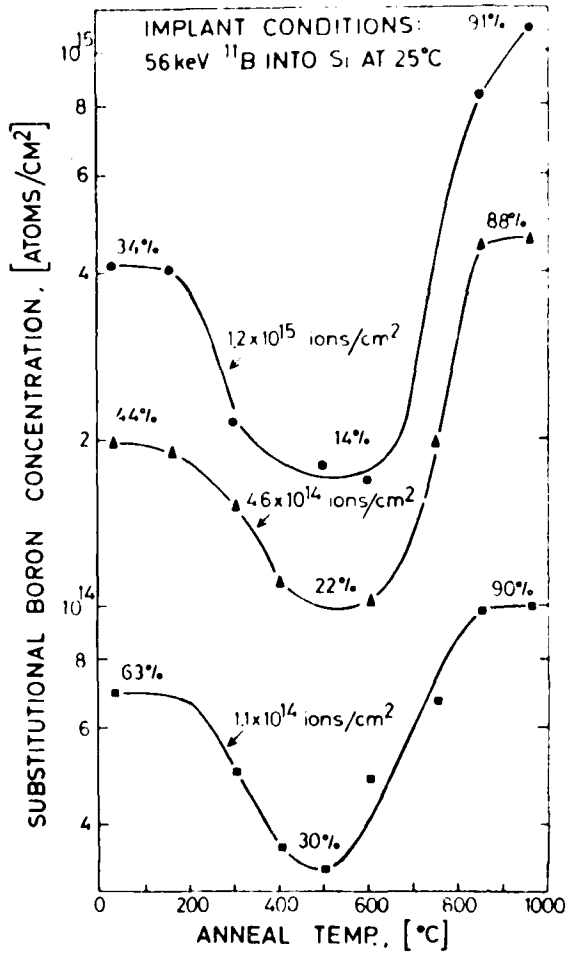

b. Anneal behavior of 56-keV room-temperature boron implants in silicon. The variation of the substitutional concentration with anneal temperature is shown for three different boron doses: ● 1.2×10^{15} ions/cm^2, ▲ 4.6×10^{14} ions/cm^2, and ■ 1.1×10^{14} ions/cm^2. At a few selected temperatures, the substitutional concentration is also given in percent of the implanted dose. After Fladda et al [11].

Fig. 6. EFFECT OF DOSE ON THE FRACTION OF ION IMPLANTED BORON ON SUBSTITUTIONAL LOCATION DURING ANNEALING.

3. Transmission Electron Microscopy

The interpretation of transmission electron micrographs is a very sophisticated topic. A thumbnail sketch shows two types of experimentally observed patterns. A DIFFRACTION PATTERN is formed by projecting all the electrons that emerge from the sample onto the observation screen, analogous to the low power magnification case in a light microscope. The observed pattern consists of a central spot and a series of secondary spots and/or rings depending on whether the substrate is still crystalline or amorphous. These structures are a consequence of the existence of or the lack of periodicity in the arrangement of the atoms and the constructive and destructive interference of the electron diffraction patterns from the individual atoms on the observation screen. The other type of pattern is the DARK or BRIGHT FIELD MICROGRAPH which is obtained by permitting only those electrons that form a selected dark or bright area of the DIFFRACTION pattern to reach the observation screen. TEM is an effective technique for the study of implantation damage and the annealing behavior. Bicknell [17] correlated the damage with electrical activity resulting from a succession of 30 minute isochronal anneals at temperatures between 300 °C and 1100 °C. Naturally, the electrical activity result follows the behavior described previously, namely, a general increase in electrical activity interrupted by reverse annealing between 500 °C to 600 °C, the temperature range over which amorphous silicon recrystalizes. Although no amorphous layer is produced in this experiment, severe migration and reordering of implantation induced defects occur. This is indicated by the rapid growth of lineated defects in the micrographs. Bicknell interpreted negative annealing as precipitation of boron and the lineated defect as a product of the precipitation. Further annealing at higher temperature show the disappearance of lineated defects and the emergence of loop defects. At even higher temperatures, these loops grow in size and decrease in number. Figure 7, after Bicknell, shows a schematic summary of the result and the interpretation. As mentioned previously, we are interested in the correlation of implantation damage with electrical activity in an isothermal anneal. In particular, we speculate whether the lineated defects will be present in isothermal annealing at 800 °C and 900 °C for

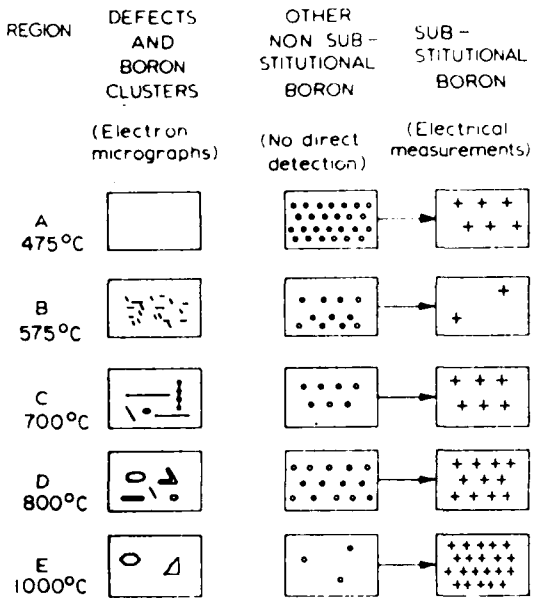

Fig. 7. SCHEMATIC SUMMARY OF RESULTS AND THEIR INTERPRETATION, AFTER BICKNELL [17].

length of time consistent with the electrical activation of boron. Next, we will present the isothermal annealing results.

a. The Isothermal Annealing of Implantation Damage

Representative bright field transmission electron micrographs obtained on isothermally annealed samples at 800°C and 900°C are shown in Figs. 8 and 9. The samples were implanted with 70 keV boron to doses of 10^{14} and 10^{15} ions/cm^2. These implantation and annealing conditions are identical to those of Hofker et al [2,14] and close to those of Seidel and MacRae [18]. Consequently, the present TEM study [19] can be correlated with the electrical activation and profiling work by the previously cited authors. We can identify two distinct damage annealing stages in the 800°C isothermal anneals. The first stage is characterized by the appearance of a high concentration of 150 to 200 Å diameter vacancy dislocation loops inclined to the (100) plane, as shown in Figs. 8b and 9b, at 5 minutes. The maximum loop density occurs at a depth of approximately 1800 Å, in agreement with calculations of the location of the primary loops is estimated to be approximately 10^{19} and 10^{20}

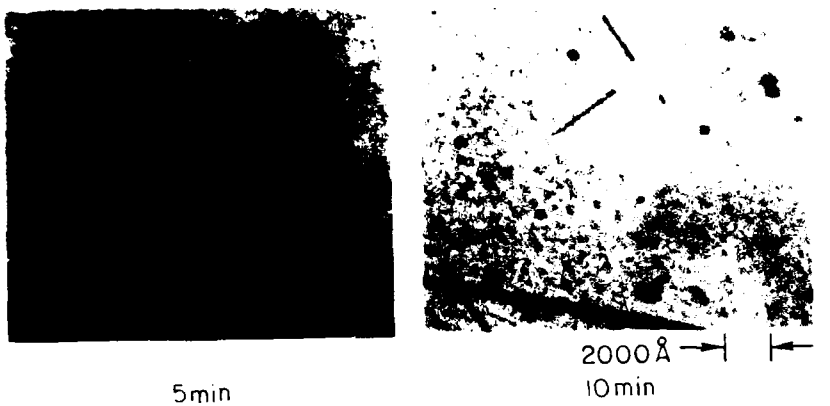

None observable defects at 15 and 35 min

(a)

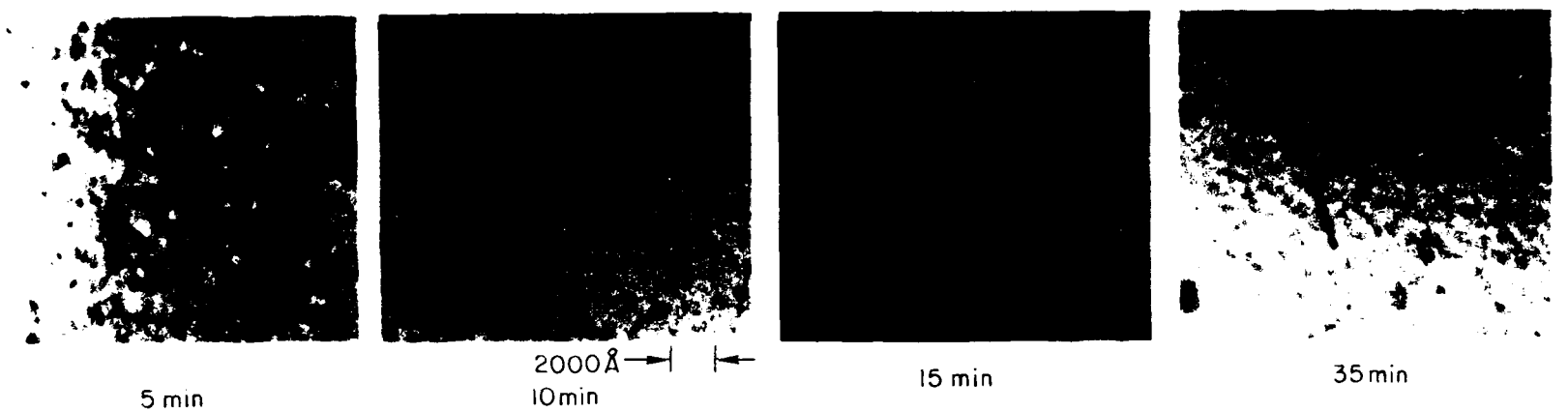

(b)

Fig. 8. TRANSMISSION ELECTRON MICROGRAPHS OF 70 keV BORON IMPLANTED INTO 100 SILICON AND SUBSEQUENTLY ANNEALED FOR 5, 10, 15, AND 35 MIN AT (a) 900°C AND (b) 800°C; IMPLANTED DOSE = 10^{14} IONS/CM^2.

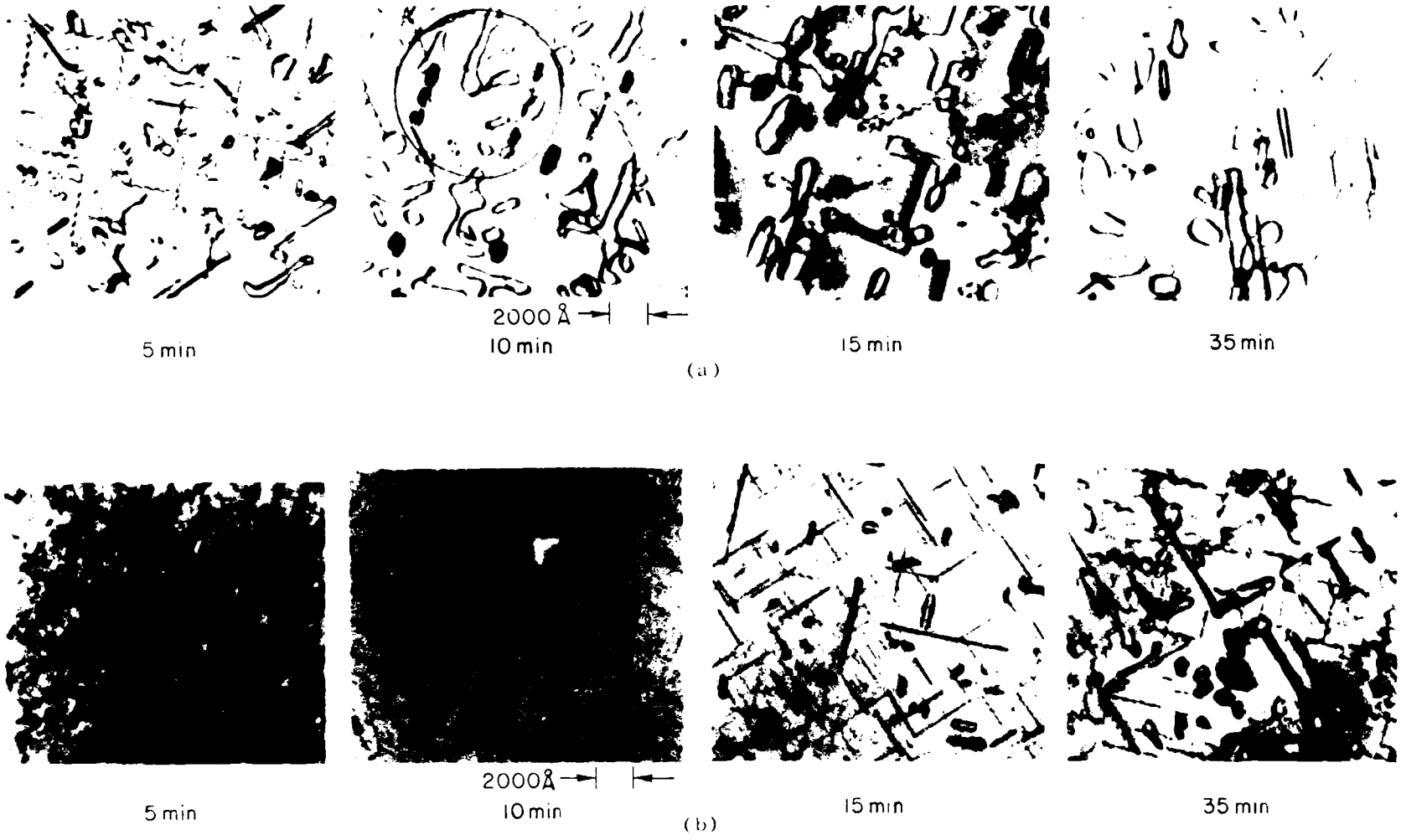

Fig. 9. TRANSMISSION ELECTRON MICROGRAPHS OF 70 keV BORON IMPLANTED INTO 100 SILICON AND SUBSEQUENTLY ANNEALED FOR 5, 10, 15, AND 35 MIN AT (a) 900°C AND (b) 800°C; IMPLANTED DOSE = 10^{15} IONS/CM^2.

vacancies/cm^3 for implantation doses of 10^{14} and 10^{15} ions/cm^2, respectively. These figures are about an order of magnitude lower than the concentration of Frenkel Pairs, computed from the distribution of energy deposited by the implanted boron into atomic processes. A fraction of this difference can be attributed to the recombination of vacancies and silicon interstitials. Since both calculations in this comparison are subject to some error, we consider that the figures are in reasonable agreement. These bound vacancies are released upon annihilation of the primary loops between 5 and 10 minutes of annealing.

The second stage of damage annealing appears within 10 minutes of annealing. It is characterized by the emergence of lineated defects that are distributed about a position deeper than the primary damage peak and coincident with the boron range, in agreement with Pelous et al [20]. The presence of lineated structures in boron implanted into silicon has been reported by a number of authors [21-24]. Previously, they have been identified as rod shaped defects or boron precipitates in conflict with the solid solubility limit. We interpret the observed contrast of these defects to be due to dislocation dipoles [25] and support Pelous's [20] suggestion that the pinning of boron by long range interactions between boron and secondary line defects is a likely possibility. The comparison of total boron concentration and electrical carrier concentration profiles for 35 minutes of annealing at 800°C does indicate that the entire inactive fraction of boron is immobile. If we associate this fraction of immobile boron with the dislocation dipoles* in Figs. 8b and 9b at 35 minutes, a simple calculation involving defect density shows that there are approximately 10^4 pinned boron atoms per dislocation dipole. Proceeding with this interpretation, we reason that the electrical activation of boron at 800°C is controlled by the annealing of dislocation dipoles. The 900°C annealing results indicate that, as annealing time increases, the dislocation line density decreases and dissociation of dipoles occur. Large secondary loops have been shown to originate from dipoles, as illustrated

*The residual damage other than dislocation dipoles in Fig. 2b does not retain boron, as inferred by their presence at 900°C 35 min 100 elect.

(circled region in Fig. 9a). Many of the secondary loops, dislocation ring structures, and arrays remain in the lattice as residual damage after 35 minutes. At this time, the electrical activity is near 100%, therefore, this residual damage does not trap boron. Presumably, at 900°C, the two stages of annealing apparent in the 800°C cases occurred at earlier points in time.

The experimental evidence on hand does not permit a detailed explanation on the exact nature of how these dislocation dipoles trap boron atoms. There are, however, strong indications that the formation of dislocation dipoles require the presence of both a high concentration of Boron and a high concentration of vacancies. For instance, the existence of dislocation dipoles in high concentration diffusions [26] indicates that the formation mechanism requires a boron concentration above a certain level. We can also infer that, in addition to the boron, a large concentration of vacancies is required to form the dislocation dipoles. This deduction follows from the observation that the dislocation dipole density is much higher in the implanted case than in the diffused case. To give further support to this point, we recourse to a micrograph in which various dislocation dipoles are emerging, each one from a vacancy cluster. Furthermore, we performed [19] another irradiation experiment in which an annealed ion implanted sample was subsequently irradiated with protons followed by a short 10 minute anneal at 800°C. The transmission electron micrograph of this sample shows that, prior to the proton bombardment, as described previously, dislocation dipoles formed and annealed out at 900°C. After the 5×10^{15} protons/cm^2 bombardment at room temperature, the micrograph shows that dislocation dipoles were formed again, presumably when the vacancy concentration was greatly increased by the proton irradiation.

Given the number of boron atoms to be associated with a dislocation dipole (approximately 10^4 boron/dd), we visualize the impurities as being located in a cloud imbedded in the strain field of the dislocation dipole. Upon annealing, the dislocation dipoles dissociate, releasing the boron atoms. As mentioned in a previous section, as annealing proceeds, some dislocation dipoles produce secondary defect loops and the residual damage that remains in the crystal is ineffective for trapping boron atoms.

C. The Annealing Model

In the preceding section, we reviewed a group of experiments that encompassed electrical behavior and redistribution of boron under conditions of ordinary diffusion, proton irradiation, and boron introduced in the substrate by ion implantation. Before we develop our annealing model, it is pertinent to highlight some of the models proposed to explain some of these experiments.

As mentioned previously, there is not an unanimous agreement on the nature of the diffusion of boron in silicon. Details of this interstitial-vacancy-controversy are well documented in the literature. Some arguments in favor of an interstitial mechanism can be found in an excellent review article by Seeger and Chick [27], and numerous quantitative models based on the monovacancy mechanism extended to cover different diffusion anomalies are available [28-30]. Basically, a monovacancy mechanism is a single stream diffusion model where the impurity diffusion coefficient is linearly dependent upon the total vacancy concentration. Therefore, substitution of the expression for the variation of the positive vacancy concentration with the Fermi level in the bandgap by Longini and Green [31] yield an impurity diffusion coefficient dependent on the Fermi level, hence on the impurity concentration and/or substrate doping.

Also based on vacancies but in a different manner, recently Anderson and Gibbons [9] proposed a two stream model for the diffusion of boron in silicon. The two species are: substitutional boron and boron vacancy pair.

In this formulation, the diffusion of boron is a weighted process with contributions from a slow and a fast diffusing species, substitutional boron and boron vacancy pair, respectively. And, the charged monovacancies come into play through the following chemical reaction:

$$B^- + V^+ = B^-V^+ \qquad (2)$$

For instance, an increase in the positive vacancy concentration with the position of the Fermi level approaching to the valence band edge manifest as a shift of the reaction to the right, hence increasing the population

of BV-pairs, the fast diffusant. This increase, in turn, causes an increase in the overall diffusion. As we can see, this approach can also predict the doping anomalies, and it is possible to derive from this formulation the basic expression in Eq. (1):

$$D/Di = P/Pi$$

This two stream diffusion model has also been shown to give reasonable predictions of proton enhanced diffusion. This result is important for two reasons. First, one would expect that a realistic model should apply to both ordinary diffusion and proton enhanced diffusion. Second, because there are many similarities between the PED case and the annealing problem, that it is likely that the basic two stream approach may be applicable to the annealing behavior of ion-implanted boron.

We should also mention at this point that Baruch et al [32] proposed an interstitial counterpart of the two stream diffusion model for the prediction of proton enhanced diffusion. For ordinary diffusion, they propose a shift from the interstitial diffusion mechanism to a vacancy mechanism. Thus far, maybe all three approaches appear to be nearly equivalent, however, when we examine them in regard to the ion-implantation related experiments, it will be apparent that extending the basic two stream model with boron vacancy pairs to include positive vacancies may result in an annealing model capable of predicting the diffusive redistribution of boron during annealing.

1. Choice of Diffusion Model

The single species approach is incapable of accounting for both the substitutional and nonsubstitutional form of boron. In the two stream diffusion approach, the BV-pair or boron interstitial are naturally associated with the nonsubstitutional boron. However, internal friction [33] and photoconductivity experiments [34] have indicated that boron interstitials anneal out near 300°C; therefore, it is unlikely that they are present at 600°C. Recently, Watkins [35] reported the experimental evidence of an Electron Paramagnetic Resonance (EPR) peak that he tentatively identified as related to BV-pairs. However, in his experiments, this peak is only stable up to 260°K.

Table 3

THE ANNEALING CASES

Temperature °C	Dose: ions/cm^2 10^{14}	10^{15}	10^{16}
800	Low Annealing Temperature Cases		High
900	Typical Annealing		Dose
1000	Cases		Cases

(a) The species are: substitutional boron, electrically active and a slow diffusant; BV-pair, electrically inactive and a fast diffusant, and positive vacancies.

(b) A reaction exists between B, BV-pairs, and positive vacancies. The kinetics of this reaction governs the time evolution of the populations of active boron and BV-pairs. Therefore, it also governs the electrical activation and indirectly the redistribution.

(c) The diffusion of boron is a weighted process with contributions of BV-pairs, the fast diffusant, and substitutional boron, the slow diffusant.

(d) Under thermal equilibrium, the concentration of positive vacancies is a function of the temperature and the Fermi level in the bandgap.

6. High Dose Cases

The high dose cases are represented in the left-hand column in Table 3. The canonical case representing this group is the 10^{16} ions/cm^2 dose implant, annealed at 900°C. In this case, the peak boron concentration is 8×10^{20} atoms/cm^3 and the solid solubility limit at 900°C is $1.1\ 10^{20}$ atoms/cm^3; therefore, we expect the boron atoms to precipitate. The

(c) Under thermal equilibrium, because the lifetime of vacancies is short compared to other time constants in the diffusion process, it is possible to approximate that the vacancy concentration is the thermal equilibrium concentration.

(d) During the annealing of room temperature boron implants, it is possible to model the vacancy perturbation arising from the implantation as a vacancy pulse superimposed on a background vacancy concentration at equilibrium with the substrate.

(e) In many instances, the effect of the vacancy pulse (arising from the annealing of vacancy clusters and vacancy loops) on the overall annealing is not significant. This effect is only apparent in short anneals at high annealing temperature.

(f) This description of vacancies does not apply to the annealing of boron that is implanted at liquid nitrogen temperature or the case of the implantation of a heavy ion.

5. Summary of the Typical Annealing Cases

Within the group represented by this canonical case, annealing will proceed as described with the following trends as temperature and implantation dose are varied. An increase in annealing temperature will result in a decrease in the reaction time constant. Consequently, annealing will be faster (a shorter transient is equivalent to a faster attainment of equilibrium conditions). An increase in implantation dose produces proportionally higher boron concentrations but lower initial electrical activity as observed by Fladda et al [11] and Seidel and Mac Rae [18]. Therefore, annealing time will be longer than for a lower dose case annealed at the same temperature. This situation holds true until the increased dose causes a peak boron concentration to exceed the solid solubility limit at the annealing temperature. Under these circumstances, annealing will no longer obey the description given above, instead it will follow the global features of high dose cases represented in the left-hand column in Table 2.

We conclude the discussion of the first canonical case which is representative of the cases in the lower left-hand corner of Table 3 by summarizing that:

In this expression, Damage(x) is the vacancy distribution computed from the distribution of energy deposited into nuclear processes, k is a constant adjusted to produce the total number of vacancies calculated in Fig. 11, and τ_{dam} in the exponential factor determines the duration of the generation of vacancies.

In this section, we modelled three processes that take place during the annealing of room temperature implantation of boron into silicon. These processes are: the release of vacancies from vacancy clusters and vacancy loops, the absorption of vacancies by the bulk and the surface to restore the equilibrium vacancy concentration and the spontaneous breakup of BV-pairs. During the anneal, the great majority of vacancies generated are absorbed by the substrate and the smaller remaining fraction may increase the population of BV-pairs only if the time constant associated with the generation of vacancies is comparable to the lifetime of BV-pairs. At annealing temperatures below 1000°C, the lifetime of BV-pairs is long compared to the duration of the generation of vacancies. Consequently, the boron-BV-pair reaction finds essentially the concentration of positive vacancies at equilibrium. At 1000°C and above, the lifetime of BV-pairs is short; therefore, there is some overlap between the generation of vacancies and the breaking up of BV-pairs. For this reason, the shape of the annealed profile is modified by the localized enhancement in diffusion caused by the vacancies that arise from the annealing of vacancy clusters and loops. This effect is only observable at short annealing times. At longer annealing times, it is masked by ordinary diffusion which is more important at 1000°C and above. It is appropriate to emphasize that this description pertains to the annealing of a silicon substrate implanted with boron ions at room temperature. The behavior of vacancies under implantation conditions that produce an amorphous layer will certainly be different.

The major results in this section can be summarized as:

(a) Under thermal equilibrium, the concentration of neutral vacancies is a function of temperature only [36].

(b) Under thermal equilibrium, the concentration of positive vacancies is a function of temperature and the Fermi-level in the bandgap [36].

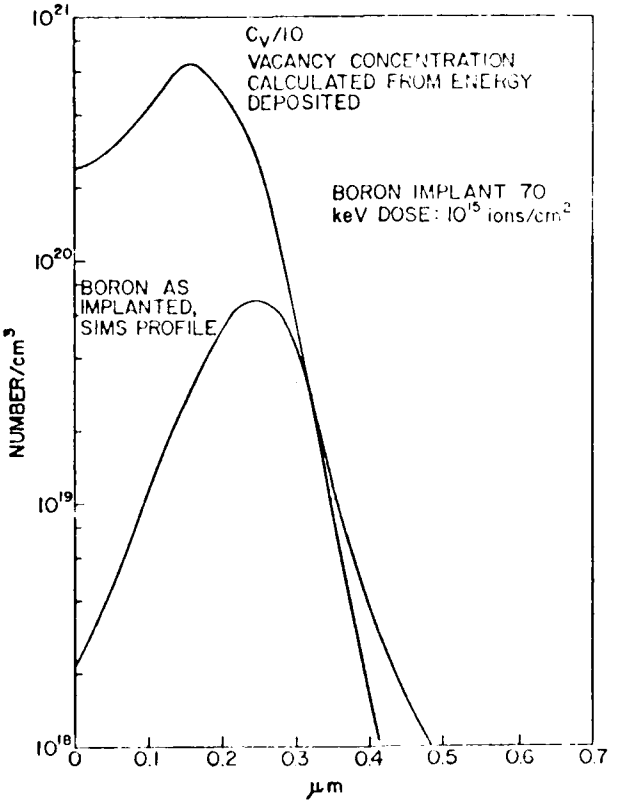

Fig. 11. THE CALCULATED VACANCY CONCENTRATION PROFILE PRODUCED BY THE IMPLANTATION OF BORON.

above the equilibrium vacancy concentration. Consequently, the substrate is severely stressed and it is incapable of sustaining such an extraordinary excess vacancy concentration. As a result, the vacancies coalesce in vacancy clusters and vacancy loops to relieve the stress in the lattice. Transmission electron micrographs reveal that bound vacancies will be released from the vacancy clusters and vacancy loops as these defects anneal out and that the background vacancy concentration will reach thermal equilibrium very rapidly. This result is in agreement with the backscattering work by Westmoreland et al [39]. The process we just described can be modelled with the vacancy generation pulse in Eq. (10), that we propose.

$$\text{Vacancy Generation Rate} = k\ \text{Damage}(x)\ \exp(-t/\tau_{DAM}) \qquad (10)$$

E_{V^+} = energy level of positive vacancies, 0.35 eV above the valence band edge

E_F = Fermi level

K = Boltzmann constant

T = temperature in degrees Kelvin

The Fermi level is, in turn, dependent on the concentration of active boron through the Fermi-Dirac statistics. It is apparent now that the Fermi level dependence of the concentration of positive vacancies is the mechanism responsible for the high-concentration and substrate-doping anomalies observed in ordinary diffusions under thermal equilibrium conditions.

Under nonequilibrium conditions, if the perturbation is small, the bulk and the surface of the semiconductor will absorb or generate vacancies to restore the equilibrium vacancy concentration. We model the rate for the attainment of equilibrium using the departure from equilibrium as the driving force and a time constant τ_V, see Eq. (9):

$$\text{Rate for the Attainment of Equilibrium} = \frac{C_{V^+} - C_{V^+_{eq}}}{\tau_V}$$

where τ_V is the vacancy lifetime. The values that τ_V take are small compared to other time constants associated with diffusion. Consequently, in those cases where the vacancies are only slightly perturbed, it is possible to approximate that the vacancy concentration is the equilibrium concentration.

Naturally, when the perturbation is large, the aforementioned approximation may no longer be adequate. For instance, Fig. 11 shows the vacancy concentration produced by the implantation of boron ions at 70 keV into silicon. This profile is computed from the number of Frenkel-pairs produced by the implantation; which is, in turn, calculated from the distribution of energy deposited into atomic processes by the energetic ions [38] and by assuming that 12 eV are required to produce a Frenkel-pair. The calculated vacancy profile is many orders of magnitude

$$\text{Reaction Rate} = \frac{C_{BV} - k_o C_B C_V}{\tau} \tag{5}$$

This term will be used in the mathematical formulation of the annealing model. The time constant τ determines the rate of the BV-pair-substitutional boron reaction. Therefore, indirectly it also determines the rate of the anneal and the diffusive redistribution.

4. The Positively Charged Vacancies

The presence of positive vacancies in this model has important implications. For instance, rearranging Eq. (4), we obtain:

$$\frac{C_{BV}}{C_B} = k_o C_{V^+} \tag{6}$$

In this expression, we can appreciate that the concentration of positive vacancies determines at equilibrium the relative concentrations of active boron and BV-pairs, hence the overall diffusion.

Vacancies exist in the silicon lattice in various charged states. The neutral vacancy is a nonionized flaw; therefore, according to the analysis by Shockley and Moll [36], its equilibrium concentration is a function of the temperature only. We use the expression in Eq. (7), after Seidel and MacRae [37]

$$C_{V^o_{eq}} = 5\ 10^{25} \exp(-1.7\ \text{eV}/KT) \tag{7}$$

The positive vacancy is, on the other hand, an ionized flaw. Consequently, its equilibrium concentration is a function of both temperature and the Fermi level in the bandgap:

$$C_{V^+_{eq}} = C_{V^o}(T) \exp\left(\frac{E_{V^+} - E_F}{kT}\right) \tag{8}$$

where

C_{V^o} = concentration of neutral vacancies [Eq. (7)]

concentration above the equilibrium level. Fladda et al [11] observed that a given dose of protons removes a fixed amount of boron from substitutional sites, rendering the boron electrically inactive. Furthermore, they observed that doubling the proton dose will, in turn, double the number of boron atoms removed from substitutional sites. This correspondence between the number of boron atoms rendered inactive with the proton dose or indirectly with the number of vacancies produced, leads us to infer the existence of a chemical reaction between a substitutional boron and a vacancy. Since BV-pairs are the inactive boron, it is apparent that a substitutional boron reacts with a (positive) lattice vacancy to form a BV-pair. Because the BV-pair is electrically neutral and the substitutional boron is ionized negatively, the presence of the positive vacancy is necessary in order to preserve the conservation of charge in the proposed reaction:

$$B^- + V^+ \rightleftharpoons B^-V^+ \tag{3}$$

Let us elaborate on the implications of this reaction. We just saw that a proton implant drives the vacancy concentration above the equilibrium level forcing the reaction in Eq. (3) to the right. And, we recall that during annealing the high BV-pair concentration forces the reaction in Eq. (3) to the left. When the reactions in opposing directions cancel each other, the reaction is at equilibrium. Under this special circumstance, a simple algebraic expression exists relating the concentrations of reactants and product:

$$C_{BV} = k_o C_B C_{V^+} \tag{4}$$

where k_o is the equation constant, a function of temperature. Whereas the equality of the members in this equation is indicative of equilibrium, the inequality is a measure of the departure from thermodynamic equilibrium. Consequently, the kinetics of this reaction can be modelled by the driving force represented by the departure from equilibrium and a time constant τ, as indicated in Eq. (5):

of BV-pairs, and enhanced diffusion, see Fig. 10b. On the other hand, at the completion of the anneal, we find a thermal equilibrium situation characterized by high electrical activity, a large population of substitutional boron, and ordinary diffusion. We insert these dichotomous attributes in the figure as mnemonics for our next argument. By inspection of Fig. 10b, we can interpret annealing as a transient process going from a nonequilibrium state toward an equilibrium state in which a large initial population of BV-pairs transform into electrically active substitutional boron. The comparison of the diffusive attributes with the population of BV-pairs and substitutional boron at the outset and end of the anneal lead us to infer that BV-pairs are fast diffusants and substitutional boron are slow diffusants. With this interpretation, the diffusive behavior during annealing becomes a weighted process with contributions from a fast and electrically inactive species, the BV-pair, and a slow and electrically active fraction, the substitutional boron. Hence, a large population of BV-pairs lead to enhanced diffusion, whereas a large population of substitutional boron produces ordinary diffusion.

In summary, annealing is governed by the driving forces that arise from a nonequilibrium state. These driving forces produce the spontaneous conversion of BV-pairs into substitutional boron. And, the electrical activation and diffusive behavior are consequences of the dichotomous attributes of BV-pairs and substitutional boron with respect to electrical activity and diffusion.

3. The 'Boron-Boron Vacancy Pair' Reaction

In the preceding section, we concluded that the spontaneous conversion of BV-pairs into substitutional boron governed the annealing behavior. Now, we will examine this conversion problem in greater detail. The transformation of BV-pairs into substitutional boron comes gradually to an end as the equilibrium conditions are attained. We can now address the question whether it is possible to perturb the equilibrium condition and force the transformation in the reverse direction? The answer is yes. It is possible to perturb the equilibrium by implanting protons. Protons are light ions. Therefore, the damage they produce is also light, consisting mainly of simple defects that raise the vacancy

this particular case, it does appear that all the inactive boron is in the form of boron-vacancy pairs. During annealing, as we can appreciate from observing the monotonic nature of the electrical activity versus time curve, it is possible to relocate the nonactive boron on substitutional sites, hence increasing the electrical activity to near 100% in 35 min. During annealing, a succession of events take place: there is annihilation of vacancies by interstitials, annealing of divacancies, formation of vacancy clusters and vacancy dislocation loops as a means of releasing stress created by the vacancy clusters in the crystal lattice, and, most importantly, there is relocation of inactive boron on substitutional sites accompanied by redistribution. This conversion of electrically inactive boron to electrically active boron is represented in Fig. 10b by the arrow crossing the electrical activity curve which is the boundary between the two forms of boron. As the annealing proceeds, the fraction of electrically active boron increases gradually while the impurity atoms diffuse in the crystalline substrate. Finally, at the end of the 35 min, we find that the implanted distribution has displaced significantly and it is now represented by the deeper boron profile in Fig. 10a. An attempt to predict this diffusive redistribution would be to take the diffusion coefficient of boron in silicon at the annealing temperature of 900°C, which is $1.4\ 10^{-15}$ cm^2/sec, and use this number to calculate where the implanted profile will diffuse to after 35 minutes have elapsed. This calculation shows that the profile would move only very slightly. Hofker et al [2] show that, in order to fit the experimental profile obtained after the annealing, the diffusion coefficient in the aforementioned calculation has to be increased to $1.7\ 10^{-14}$ cm^2/sec, which is one order of magnitude higher than the ordinary diffusion rate. These calculations clearly indicate the presence of <u>enhanced diffusion</u> during annealing. Further annealing indicates that the enhanced diffusion is only transitory because, as the electrical activity approaches to 100%, the enhanced diffusion reduces to ordinary diffusion.

2. <u>The Spontaneous Conversion of BV-Pairs</u>

At the outset of the anneal, we encounter a nonequilibrium situation characterized by low electrical activity, a large population

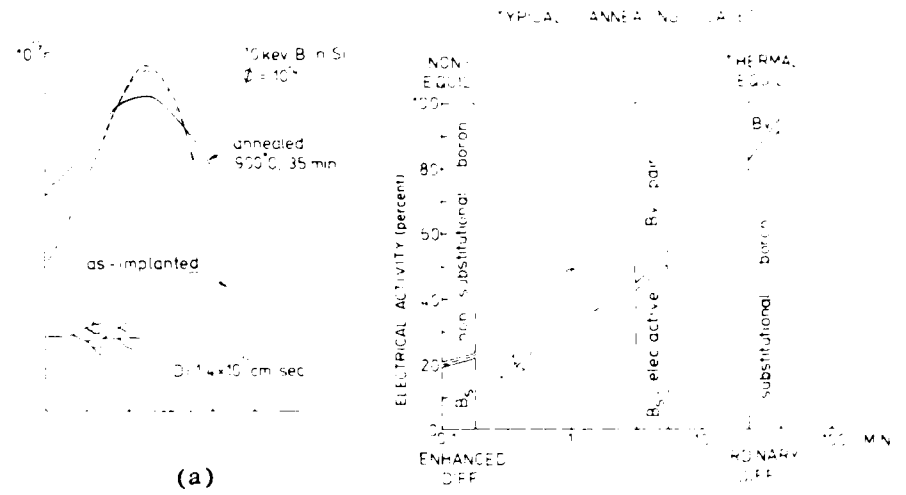

Fig. 10. THE ELECTRICAL ACTIVATION AND REDISTRIBUTION BEHAVIOR OF BORON IN TYPICAL ANNEALING CASES.

The process we just described is far away from thermal equilibrium. Therefore, only a small fraction of boron atoms will be located on substitutional sites, a larger fraction will be on interstitial sites, and other boron atoms will form complexes with simple defects, i.e., vacancies and silicon interstitials. Consequently, the electrical activity at the completion of the implant is far below what one would expect from the implanted dose. This situation is depicted in Fig. 10b at the origin of the time axis, in the horizontal direction. The electrical activity is represented on the vertical axis. At any instant in time, the fraction of boron that contributes to electrical carriers is represented by the ordinate of the electrical activity curve. On the other hand, the nonelectrically active boron is represented above the curve by the distance between the 100% activity line and the ordinate of the curve. Therefore, we can also interpret Fig. 10b as a bar graph describing the relative concentrations of active and inactive boron. In general, the nonelectrically-active boron need not be in a single form; however, in

produced by the 10^{16} ions/cm^2 doses exceed the solid solubility limit at all the annealing temperatures in the table. Therefore, boron will precipitate. And, the precipitated phase is characteristic of the high dose implantation cases. The remaining cases are represented in the upper left-hand corner of the table and they are characterized by the trapping of boron atoms by dislocation dipoles that form during the early stages of annealing. At 800°C, these dislocation dipoles do not anneal out completely in 35 minutes. Therefore, they are incapable of releasing the boron atoms trapped in the associated strain fields.

These three groups have distinct characteristics that will manifest in the electrical activation as well as in the redistribution of the implanted boron. In the discussions that will follow, we will select canonical cases representative of each of the aforementioned groups. Our exposition will concentrate on each of the three canonical cases and on the global features in the anneal when implantation dose and annealing temperature are varied.

1. The Typical Annealing Cases

We first examine the 10^{14} ions/cm^2 dose, 70 keV boron implant annealed at 900°C for 35 minutes. This is a relatively simple case. In the insert in Fig. 10a, we depict the silicon surface coincident with the origin of the horizontal axis representing depth in tenth of microns into the substrate material. The 70 keV boron beam is directed toward the surface from left to right. As these energetic ions penetrate the target, their stopping in the substrate is produced by collisions with electrons and host atoms. In this process, some collisions are sufficiently energetic that host atoms are displaced from their lattice sites leaving vacancies behind; the displaced atoms may in turn displace other atoms. This process leaves a disorder cluster around the ion track. The insert in Fig. 10a represents one disorder cluster. Since this collision process is random in nature, not all the implanted boron ions will stop at the same depth. Instead, the ions will come to rest at different depths with different probabilities. Thus, after the implant, the distribution of implanted ions is represented by the impurity concentration profile shown in Fig. 10a. The peak concentration is 8×10^{18} atoms/cm^2 for the 10^{14} ions/cm^2 dose implant in this example.

Table 2

ISOCHRONAL ANNEALING RESULTS
Annealing Time = 35 min

Anneal Temp °C	Dose: ions/cm^2 10^{14}	10^{15}	10^{16}
800	Boron Adsorption Near Profile Peak ~25% Activity		Boron < 16%
900	Three Stream Duffusion Model Applies		Precipitates when 40%
1000	(B^-, V^+, B^-V^+) 100% Activity		$C_B > C_{SS}$ 65%

When the annealing is performed isochronally for 35 min, in this range of temperatures the electrical activity (at the completion of the anneal) will vary from a small fraction to near 100%, depending on the particular implantation dose and annealing temperature. In other words, the ratio of implanted boron that contribute electrical carriers (holes) to the totality of implanted boron ions is a function of implantation dose, annealing temperature, and time. The understanding of these relationships is one of our principal objectives.

This collection of implantation doses and annealing temperatures illustrated in Table 2 covers a very wide range of conditions. For instance, most applications of ion implantation in device fabrication are performed under conditions represented in the lower left-hand corner of this table. These cases are very relevant because the electrical activities approach to near 100% after 35 minutes of ar ing. Among the remaining cases in this table, we can distinguish two groups. The first group is composed of high dose implants represented by the right-hand column of the table. In these cases, the peak impurity concentration

in order to predict the annealing behavior under all the annealing temperature and implantation dose ranges that we are interested in.

2. The Immobile and Nonsubstitutional Boron

A comparison of the electrical carrier concentration profiles and the total boron profiles for various implantation doses and annealing temperatures is depicted in Fig. 4. It is apparent from the inspection of these cases that, in the high dose and/or low annealing temperature cases, there is a fraction of electrically active boron that is IMMOBILE. This new fraction is present near the peak of the boron profile. In the high dose, 10^{16} ions/cm^2 cases, the boron peak exceeds the solid solubility limit; therefore, the immobile boron is a precipitate. However, in the moderate dose cases, the peak boron concentration does not exceed the solid solubility limit; hence, this immobile boron is not a precipitate in the conventional sense. We propose that this immobile boron consists of boron atoms trapped by dislocation dipoles that form during the annealing.

D. Development of the Model

In the preceding sections, we reviewed a group of experiments related to ion-implantation and our interpretation of these experiments. In this section, we will use the four species inferred previously (substitutional boron, boron-vacancy pairs, positive vacancies, and immobile boron) to formulate a model capable of describing the overall annealing behavior of boron implanted into silicon at room temperature. Specifically, we wish to explain the redistribution and the electrical activation of the implanted boron. In the course of this discussion, the key attributes in the annealing will be apparent and the global features that result, when the implantation dose and anneal temperature are varied, will also follow naturally.

The cases to be studied are shown schematically in Table 2. In the horizontal direction, we show boron implantation doses varying from 10^{14} to 10^{16} ions/cm^2. For a 70 keV boron implant, this dose range will lead to peak concentrations between 10^{19} to 10^{21} atoms/cm^3. In the vertical direction, we show annealing temperature ranging between 800°C to 1000°C.

We are faced with a difficult decision. Until more evidence on the stability and positive identification of the BV-pair is available, we proceed with the examination of the boron-BV-pair two stream diffusion models extended to include the diffusion of vacancies. This extension is necessary because, in general, the migration of vacancies during annealing cannot be safely neglected. In this three-stream diffusion model, the electrical activity becomes the ratio of substitutional boron to the sum of BV-pairs and B substitutional. The stoichiometry of the reaction, namely, one substitutional to boron and one vacancy to form one BV-pair can correspond to the fixed proportion of boron removed from substitutional sites per unit dose of proton irradiation in the experiments by Fladda et al [11]. Furthermore, let us examine qualitatively if the diffusion attributes of the substitutional boron and BV-pair are consistent with the redistribution of ion-implanted boron during annealing. The small fraction of substitutional boron at the outset of the anneal implies a large fraction of BV-pairs, the fast diffusant. Annealing proceeds then with the conversion of nonsubstitutional boron or BV-pairs into substitutional boron as indicated by the experiments on the lattice location of boron. Therefore, the redistribution during annealing is characterized by an initial fast diffusion caused by a large fraction of BV-pairs reducing gradually to a slow diffusion when the population of substitutional boron predominates. This prediction is in agreement with the anomalous transient diffusion observed in annealing experiments. Qualitatively, there is an obvious relation between the overall diffusion coefficient and the electrical activity. Furthermore, if the chemical reaction in Eq. (2) is the dominant annealing mechanism, then it is possible to relate the lifetime of the BV-pairs to the annealing time at a particular temperature. This is the kind of reasoning that we use to determine the values of the parameters in the model; some of them not determined previously, others we will obtain by alternative means.

In summary, the three stream diffusion model appears to contain the global features for explaining the annealing behavior of ion implanted boron into silicon. We shall see later that it will be necessary to extend this model to include other forms of nonsubstitutional boron

experimental annealing result shows in Fig. 12a that there is diffusion of the tail in the impurity concentration profile, but the central portion near the peak remained unchanged. Furthermore, in the same figure we can appreciate from the inspection of the annealed electrical carrier profile that the immobile boron is also electrically inactive. At the outset of the anneal, especially at this high dose, the electrical activity is quite low (≈12%); therefore, nearly all the implanted boron is electrically inactive. From these facts, we conclude that the composition of the inactive boron is mostly boron precipitate and a much smaller fraction of BV-pairs. The experimental evidence on hand does not indicate whether the boron precipitate is formed directly from the implanted boron once the solid solubility limit is exceeded or whether BV-pairs are first formed and then followed by precipitation. We choose the second possibility for the sake of convenience in our mathematical model. This arbitrary choice does not modify the end result because precipitation takes place very rapidly regardless of the boron source. Consequently, in this interpretation, annealing of this canonical case will proceed as follows. At the outset, the low activity is due to a large fraction of BV-pairs, from which the fraction above the solid

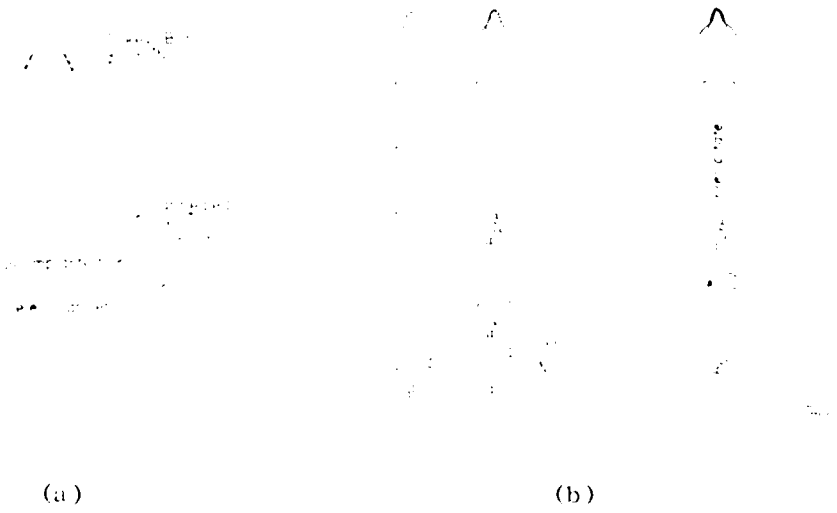

(a) (b)

Fig. 12. THE ELECTRICAL ACTIVATION AND REDISTRIBUTION BEHAVIOR OF BORON IN HIGH DOSE CASES.

solubility limit precipitates very rapidly. After a short time, we find the situation depicted in the insert in Fig. 12b: the annealing profile at this time differs very slightly from the implanted profile. Near the profile peak, the boron has precipitated and it is immobile. The remaining boron, which is composed mainly of BV-pairs, has diffused very slightly in this short time. Later in time, annealing proceeds with two mechanisms. One mechanism is the conversion of BV-pairs into electrically active boron accompanied by redistribution as described in the first canonical case. The other mechanism is the dissolution of precipitated boron. The dissolution takes place because the redistribution of boron removes boron from the areas of high concentration, thus upsetting the equilibrium concentrations of precipitated and nonprecipitated boron with respect to solid solubility. This nonequilibrium situation is, in turn, corrected by the dissolution of precipitates. Whereas the B-BV pair reaction reaches equilibrium conditions in the course of annealing, dissolution is a slow process at 900°C and, after 35 min of annealing, there is still a large fraction of boron precipitates. This situation is depicted in the insert to the left in Fig. 12b. The boron precipitate remains essentially unchanged, however, the fraction of BV-pairs diffused as they converted into substitutional boron. Hence, the total boron concentration profile exhibits a shoulder-like structure in agreement with the experiment. Furthermore, we can also predict that subsequent annealing will produce diffusion of the tail of the profile at ordinary diffusion rate because the B-BV pair reaction reached equilibrium conditions, and the electrical activation will be extremely slow because equilibrium with respect to solid solubility is only slightly perturbed by the slow diffusion at 900°C. To elaborate further on this subject, we can contrast this case with a higher annealing temperature case. As the annealing temperature is increased, the solid solubility limit increases and diffusion becomes more important. Consequently, the dissolution of boron precipitates will occur more readily and a higher rate of electrical activation results. For instance, at 1100°C, the electrical activity approaches 100% after 35 minutes of annealing. In summary, annealing of high dose implants occur as a result of two mechanisms. The boron-BV pair reaction governing the redistribution behavior and the dissolution

of boron precipitates governing the annealing time. We model the precipitation and dissolution kinetics by assuming again a rate proportional to the departure from equilibrium as the driving force and a time constant. Thus, the precipitation rate becomes:

$$\text{Precipitation Rate} = + \frac{C_{BV} - \text{Solid Solubility Limit (SSL)}}{\tau_{prec}} \qquad (11)$$

and likewise the dissolution rate results in a more complicated relation:

$$\text{Dissolution Rate} = \begin{cases} C_{B_{total}} > \text{SSL} & - \dfrac{\text{SSL} - (C_{BV} + C_B)}{} \\ C_{B_{total}} \leq \text{SSL} & - \dfrac{C_{B_{prec}}}{\tau_{diss}} \end{cases} \qquad (12)$$

The upper branch accounts for the situation depicted in Fig. 13a, in which the fraction of precipitates below the solid solubility limit (SSL) indicated by the bracket should decay to zero. Similarly, the

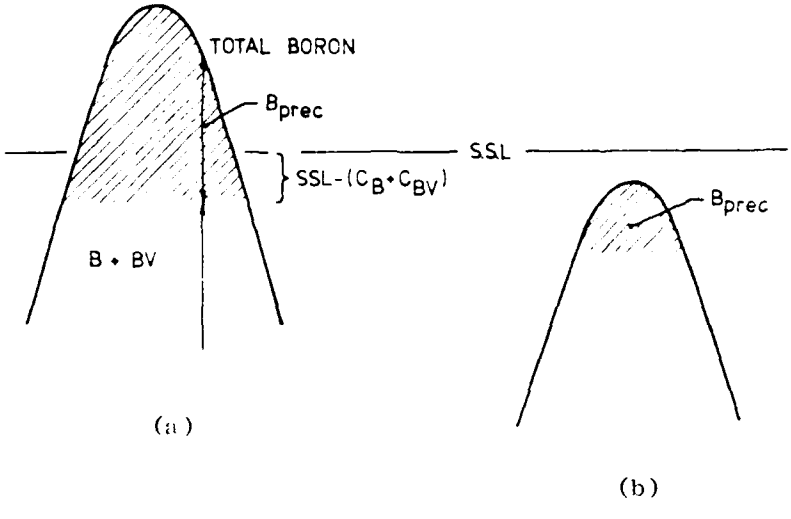

Fig. 13. THE DISSOLUTION RATE OF PRECIPITATES.

lower branch represents the case in Fig. 13b when the total boron concentration is below the solid solubility limit. In this case, if there is a precipitate, it should decay spontaneously to zero.

By inspection of these equations, we can verify that the rates reduce to zero at equilibrium.

7. Low Temperature Annealing

We will examine now the low temperature annealing cases in which 'metastable boron precipitates' form as a result of the trapping of boron by dislocation dipoles. The canonical case representative of this group is the 10^{14} ions/cm^2 dose implant annealed at 800°C. In this example, the boron peak concentration is 8×10^{18} atoms/cm^3, which is below 10^{19} atoms/cm^3, the solid solubility limit at 800°C. However, the experimental profile that results after 35 minutes of annealing shows again the shoulder-like structure in Fig. 14a. The electrical carrier profile shows a behavior very similar to the high dose cases with the presence of true precipitates. In essence, it appears that there is again a threshold level of concentration, resembling a solid solubility

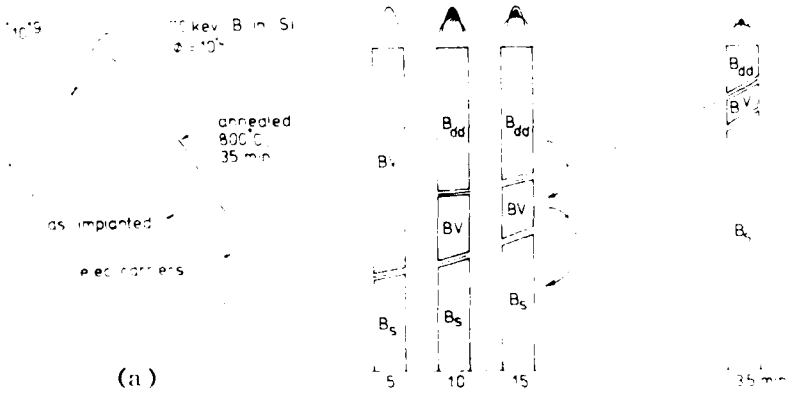

Fig. 14. THE ELECTRICAL ACTIVATION AND REDISTRIBUTION BEHAVIOR OF BORON IN LOW ANNEALING TEMPERATURE CASES.

limit, above which concentration the boron becomes immobile and electrically inactive. The boron in this case is certainly not a precipitate in the conventional sense. An analysis of transmission electron micrographs and electrical activation results indicate that this boron is trapped by dislocation dipoles that form and evolve during annealing. A more detailed description of this issue was given in a previous section. Our objective here is to describe the role and participation of the trapped boron in the low temperature annealing. At the outset of the anneal, the large concentration of vacancies generated by the implantation coalesce into vacancy clusters and loops, as indicated by the 5 minute transmission electron micrograph in Fig. 9b. We assume that the low electrical activity is due to a large concentration of BV-pairs, as shown in Fig. 14b. As annealing proceeds, the micrograph corresponding to 10 minutes of annealing (Fig. 9b) indicates that the vacancy clusters break up and two events take place. One is the migration of vacancies in the bulk and to the surface. The other is the formation of dislocation dipoles in the substrate. The consequences of this annealing stage is the attainment of equilibrium concentration for the vacancies and the trapping of boron atoms by the dislocation dipoles. This is depicted in Fig. 14b, and we can see that the trapped boron, immobile and electrically inactive, is formed at the expense of the BV-pairs. Apparently, the formation of dislocation dipoles is very fast in time, and the boron immobilized by these defects is the fraction of boron that exceeds a critical concentration. From these premises, we model the trapping of boron as a chemical reaction with a reaction rate represented by:

$$\frac{C_{BV} - C_{dd}}{\tau_{dd}} \qquad (13)$$

where C_{dd} represents the aforementioned critical concentration.

There are other evidences of the existence of this critical concentration level. For instance, dislocation dipoles have only been observed in high concentration diffusions and not at lower concentrations. Furthermore, since dislocation dipoles form when they are about 100 Å long (Bicknell et al [17]), we can estimate the concentration

level for which two boron atoms are 100 Å appart. Such a calculation yields a boron concentration of 10^{18} atoms/cm^3, which is consistent with the observed threshold.

Once the boron has been trapped by the dislocation dipoles, further annealing proceeds with two distinct mechanisms. One is the B-BV pair reaction, as in the other cases that we already examined. The other mechanism is the release of trapped boron atoms from the dislocation dipoles as they anneal out. The transmission electron micrograph at 15 minutes of annealing indicates that the dislocation dipoles have decreased in number and increased somewhat in length. Hence, we would expect a release of trapped boron atoms. We do not have clear evidence of how the trapped boron becomes active. However, the faster diffusion, inferred from Table 2 on the behavior of the annealed distribution, appears to indicate that the trapped boron becomes a BV-pair, the fast diffusant. It is conceivable that a vacancy migrates to the neighborhood of a boron atom imbedded in the strain field of a dislocation dipole. When the dislocation dipole is annealing out, the strain field is weakened and the vacancy may approach the boron atom to form a boron vacancy pair. It is also possible that the dislocation dipoles emit vacancies as they anneal out, hence increasing locally the probability for the formation of BV-pairs. The global features characteristic of this case are depicted in Fig. 14b. The inserts below the graph represent schematically the evolution of defects, among which are the dislocation dipoles, capable of trapping boron atoms in their strain fields. In the electrical activity graph, we show, using a bar graph representation, the fractions of immobile boron, BV-pairs, and electrically active boron. The arrows connecting these fractions represent the continuous release of trapped boron from the dislocation dipoles as they anneal out and the conversion of BV-pairs into active boron. The inserts above the electrical activation graph indicate the evolution of the redistribution behavior that results from the presence of immobile boron, BV-pairs (fast diffusant), and substitutional boron (slow diffusant). The shoulder-like structure at annealing times of 15 and 35 minutes are consequences of the immobility of the trapped boron near the profile peak and the mobility of the BV-pairs responsible for the faster diffusion of

the profile's tail. We can appreciate at this point that the major difference between this present case and the high dose case originates from the fact that, whereas the dissolution of boron precipitates in the high dose case is a consequence of the removal of boron from the areas of high concentration, in the low annealing temperature case the release of boron is the result of the annealing of dislocation dipoles. The release of boron from the strain fields associated with the dislocation dipoles is a complicated matter. The individual strain fields may overlap and produce a nonlinear relation between the number of boron atoms associated with a dislocation dipole and the dislocation dipole density. However, as we will see, despite the complexity in the real situation, the simple exponential release rate in Eq. (14) is capable of capturing the key features under consideration:

$$\text{B Release Rate} = \frac{C_{B_{trapped}}}{\tau_{dd}} \tag{14}$$

This equation is mathematically identical to the expression for the dissolution of the precipitate when the boron concentration is below the solid solubility limit. Therefore, Eq. (12) can be used in the high dose as well as in the low annealing temperature cases, provided the appropriate parameters are substituted.

Let us examine now the global features of the anneal when implantation dose or annealing temperature are increased with respect to the canonical case that we just studied. An increase in dose produces a proportional increase in the dislocation dipole density. The time evolution of the defects is depicted in Fig. 9b. The principal difference with the canonical case is the formation of residual damage from the annealing of the dislocation dipoles. In contrast with the dipoles, the residual damage does not trap boron atoms. Annealing of the higher dose case at the same annealing temperature of 800°C requires a longer annealing time because a larger fraction of boron is trapped by the defects. The other situation of interest is when the annealing temperature is increased. At a higher temperature, annealing becomes more rapid. For instance, Fig. 8 shows that the dislocation dipole density

after 5 minutes of annealing at 900°C is equivalent to 35 minutes of annealing at 800°C. Presumably, at higher temperature, the sequence of events in the 800°C anneal depicted in the micrographs in Fig. 8b at 5, 10, and 15 minutes occur at earlier times in the 900°C anneal. Consequently, annealing in this case is not dominated by the time required to release the trapped boron but, instead, is governed by the B-BV pair reaction time constant. This is indeed the situation idealized by the first canonical case in which the presence of boron trapped by the dislocation dipoles is assumed to be negligible.

8. Summary

We describe in this chapter the annealing behavior of boron that is ion implanted at room temperature into silicon, in the dose range of 10^{14} to 10^{16} ions/cm^2 and annealed in the temperature range of 800°C to 1000°C. This wide range of implantation dose and annealing temperatures include from the typical annealing cases of ion implantation in the fabrication of devices to the unconventional situations in which the annealing is dominated by boron precipitates (high dose implantation) and/or boron trapped by dislocation dipoles (low temperature annealing).

To model the redistribution and electrical activation of boron, we propose a model composed of substitutional boron (electrically active and slow diffusant), boron-vacancy pair (electrically inactive and fast diffusant), and the positively charged vacancy. The overall diffusion of boron is then composed of a slow and electrically active fraction, the substitutional boron, and a fast and electrically inactive fraction, the boron vacancy pair. The diffusive and electrical attributes of boron and the BV-pair enable the overall diffusion of boron to assume the dichotomous characteristics that pertain to the prevalent specie in the diffusion. For instance, the implanted boron react with nearby vacancies to form BV-pairs. This dominant population of BV-pairs is responsible for the low electrical activity and enhanced diffusion at the outset of the anneal. During the anneal, the BV-pairs break up spontaneously into its constituents until the thermodynamic equilibrium is reached. At equilibrium, the opposing rates in the reaction cancell and the remaining

fraction of BV-pairs is small compared to the population of substitutional boron. For this reason, the diffusion is slow and the electrical activity is high at the completion of the anneal. This annealing behavior is characteristic of the typical annealing cases. In order to include the precipitation effects of high dose implants, and the low annealing temperature anomalies caused by the trapping of boron by dislocation dipoles, it is necessary to expand this basic model to include the immobile boron and additional reaction-kinetic terms. In the next chapter, we will utilize these premises to formulate a mathematical model for the annealing of ion implanted boron at room temperature, under the described conditions of implantation dose and annealing temperature.

Chapter II

THE ANNEALING MODEL

In this chapter, we will develop the mathematical model for predicting the annealing behavior of ion implanted boron into silicon. Because annealing is a very complex problem, the first chapter was devoted to the description and definition of the problem, to the analysis of relevant experiments pertinent to annealing. From these experiments, we inferred the key attributes of the annealing problem. The results of these inferences are summarized in Table 4. In the left-hand side of the table, we show the species and their electrical and diffusive characteristics. To the right, we indicate the reactions the species participate in, which annealing behavior a particular reaction determines, and when this reaction prevails. It is apparent that the kinetics of the dominant reaction and the electrical and diffusive attributes of reactants and products determine the electrical activation and the redistribution features, respectively. For this reason, it is important to relate the reaction that prevails with the corresponding implantation and annealing conditions. This cross-reference is provided by Table 3, which is repeated here from the preceding chapter.

Table 3

THE ANNEALING CASES

Temperature °C	Dose: ions/cm^2 10^{14}	10^{15}	10^{16}
800	Low Annealing Temperature Cases		High
900	Typical Annealing		Dose
1000	Cases		Cases

Table 1

KEY ATTRIBUTES IN THE ANNEALING PROBLEM

Species	Symbol	Diffusant	Electrically	Reaction	Determines	Dominant
Substitutional Boron	B	slow	active	$B^- + V^+ = B^-V^+$	Redistribution behavior and electrical activation of mobile boron	ORD DIFF ENH DIFF Annealing in the absence of precipitates and disl. dip.
Positive Vacancies	V^+	fast	active			
Boron Vacancy Pair	BV	fast	inactive			
B Precipitate	B_{PREC}	immobile	inactive	Precipitation dissolution	Equilibrium of high dose implements	Ann. in the presence of precp.
Trapped Boron	B_{DD}	immobile	inactive	Trapping and release of B by disl. dip.	Equilibrium of low annealing temperature	Ann. in the pres. of disl. dip.

A. The Mathematical Model

The quantitative description of the ideas summarized in Table 4 is represented below by Eq. (15). In essence, this set of equations performs the bookkeeping of each of the species in time and space with regard to entries such as diffusion, chemical reactions, etc.

RATE OF CHANGE IN CONC. = DIFFUSION + REACTIONS

$$\frac{\partial C_B}{\partial t} = D_B \frac{\partial^2 C_B}{\partial X^2} - \text{REAC} \tag{15a}$$

$$\frac{\partial C_{V^+}}{\partial t} = D_V \frac{\partial^2 C_{V^+}}{\partial X^2} - \text{REAC} - \begin{Bmatrix}\text{DISS}\\ \text{REL}\end{Bmatrix} + \text{GEN} - \text{EQ} \tag{15b}$$

$$\frac{\partial C_{BV}}{\partial t} = D_{BV} \frac{\partial^2 C_{BV}}{\partial X^2} + \text{REAC} - \begin{Bmatrix}\text{PREC}\\ \text{TRAP}\end{Bmatrix} + \begin{Bmatrix}\text{DISS}\\ \text{REL}\end{Bmatrix} \tag{15c}$$

$$\frac{\partial C_{Bi}}{\partial t} = + \begin{Bmatrix}\text{PREC}\\ \text{TRAP}\end{Bmatrix} - \begin{Bmatrix}\text{DISS}\\ \text{REL}\end{Bmatrix} \tag{15d}$$

where

C = atomic concentration in $\#/cm^2$

D = diffusion coefficient in cm^2/sec

and the subscripts denote

B = substitutional boron, electrically active

V^+ = positively charged vacancy

BV = boron vacancy pair

Bi = immobile boron, a boron precipitate in the high dose implantation cases or a boron trapped by dislocation dipoles in the low temperature annealing cases

The brackets in Eq. (12) denote alternative choices. The upper selection in the brackets corresponds to high dose implantation cases, and the lower selection pertains to low annealing temperatures. The analytical expression of the various reactions in Eq. (15) are summarized in Eq. (16).

$$REAC = -\frac{C_{BV} - k_o C_B C_{V^+}}{\tau} \tag{16a}$$

$$PREC = \frac{C_{BV} - C_{SSL}}{\tau_{PREC}} \tag{16b}$$

$$TRAP = \frac{C_{BV} - C_{DD}}{\tau_{DD}} \tag{16c}$$

$$DISS = \begin{cases} C_{B_{TOTAL}} > C_{SSL} & -\dfrac{C_{SSL} - (C_{BV} + C_B)}{\tau_{DISS}} \\ C_{B_{TOTAL}} \leq C_{SSL} & -\dfrac{C_{Bi}}{\tau_{DISS}} \end{cases} \tag{16d}$$

$$REL = -\frac{C_{Bi}}{\tau_{REL}} \qquad C_{B_{TOTAL}} > C_{SSL} \tag{16e}$$

$$GEN = \frac{Damage(x)}{\tau_{DAM}} \exp(-t/\tau_{DAM}) \tag{16f}$$

$$EQ = \frac{C_{V^+} - C_{V^+_{eq}}}{\tau} \qquad C_{V^+_{eq}} = C_{VO} \exp\left(\frac{E_{V^+} - E_F}{kT}\right) \tag{16g}$$

where

k_o = equilibrium constant, a function of temperature only (cm^3)

τ = reaction time constant

C_{SSL} = solid solubility limit, function of temperature

C_{DD} = concentration threshold for the formation of dislocation dipoles

τ_{PREC} = precipitation time constant

τ_{DD} = time constant for the trapping of boron by dislocation dipoles

τ_{DISS} = time constant for the dissolution of B precipitate

τ_{REL} = time constant for the release of boron from the dislocation dipoles that anneal out

Damage(x) = primary damage profile computed from the energy deposited into nuclear processes

τ_{DAM} = time constant for the release of vacancies from vacancy clusters

$C_{V^+_{eq}}$ = equilibrium concentration of positive vacancies

τ_V = lifetime of vacancies

C_{V^0} = equilibrium concentration of neutral vacancies

E_{V^+} = energy level of positive vacancy in the band gap

E_F = Fermi energy level

K = Boltzmann constant

T = temperature in degree Kelvin

The reasons for representing boron precipitates (high dose implants) and boron trapped by dislocation dipoles (low annealing temperatures) as one single species in Eq. (15) are threefold. First, we recall that boron precipitates and trapped boron are both electrically inactive and immobile. Second, a comparison of Eq. (16b) with (16c) and Eq. (16d) with (16e) reveals that, with the exception of the parameters, the analytical expressions are respectively identical. Third, the only case in which boron precipitate and trapped boron are simultaneously present is when the 10^{16} ions/cm^2 dose boron implant is annealed at 800°C. In this case, the electrical activation of boron due to the release of boron trapped by dislocation dipoles is so slow that the distinction between the two forms of boron becomes unnecessary. In this case also, the diffusion is so slight

transmission electron micrographs of samples annealed at low temperatures for short times (Figs. 9 and 10). However, for the case of the precipitates present in high dose implants, this is strictly an assumption. An alternative approach of assigning fractions of the as-implanted boron profiles to the BV-pairs and immobile boron could be as adequate. Transmission electron micrographs also indicate that the high vacancy concentration in Fig. 11 will condense first into vacancy clusters and vacancy dislocation loops imbedded in a background of vacancies at equilibrium concentration. Then, these defects will anneal, transform, and release vacancies very rapidly. For this reason, we use the equilibrium concentration of positive vacancies as the initial condition. In most instances, the release of vacancies from the annealing defects has little overlap in time with the boron-BV-pair reaction. Therefore, the effects are negligible. And, when the vacancies released from the vacancy clusters and dislocation loops do interact with the annealing, we use the generation term in the vacancy equation to model a pulse of vacancies that is distributed in space in accordance with the energy deposition profile.

In summary, the initial conditions are:

$$
\begin{aligned}
C_B(x,o) &= 0 \\
C_{BV}(x,o) &= \text{As-Implanted Boron Profile} \\
C_{V^+}(x,o) &= C_{V^+_{eq}}(E_F) \\
C_{BI}(x,t) &= 0
\end{aligned}
\tag{23}
$$

We recall that the primary input to the model is the history of the substrate summarized by two distributions: the as-implanted boron profile and the distribution of energy deposited into nuclear processes by the boron ions. We can appreciate now that, in this implementation of the annealing problem, the as-implanted B profile becomes an initial condition, while the energy deposition profile becomes the space dependence of the vacancy generation term.

(a) a set of parameters as estimated in the preceding section

(b) a set of initial conditions, one for each of the independent variables:

$$\left.\begin{matrix} C_B(x,t) \\ C_{BV}(x,t) \\ C_{V^+}(x,t) \\ C_{BI}(x,t) \end{matrix}\right\} \quad \text{for} \quad t = 0 \tag{22}$$

Naturally, the initial conditions are particular to a specific problem. In this section, our objective is to elaborate on those initial conditions pertinent to the annealing of B in Si.

The detailed discussion with regard to the overall annealing behavior can be found in Chapter I. In that discussion, special attention is devoted to the state of the boron-silicon system at the outset of the anneal. In particular, the initial state of the silicon substrate containing the as-implanted boron atoms is carefully analyzed. For this reason, we can formulate the initial conditions of interest by simply recalling the results in Chapter I.

The as-implanted profile as determined by secondary ion mass spectrometry is shown in Fig. 11. The vacancy concentration profile is calculated from the Frenkel-pairs produced by the 70 KeV incident boron ions as they deposit energy into atomic processes [38] along their trajectories. In what follows, we will make the conservative assumption that as the boron atoms come to rest they will all combine with nearby vacancies to form BV-pairs, which are electrically inactive. Hence, at the outset of the anneal, the electrical activity is zero. Although a nonzero activity is more reasonable, it will also require an initial profile for the electrically active boron. At present, we do not wish to introduce this unknown. In other words, the initial profiles of boron and BV-pair are the null and the as-implanted profiles, respectively. With regard to the immobile boron present in high dose implant and low annealing temperature cases, we assume that the initial concentration profile is identically zero. This is in agreement with the

For these reasons, the only requirement for the value of this time constant is for it to be small. We choose both parameters to be 1 sec arbitrarily.

10. Time Constant Associated with the Dissolution of Precipitates and the Release of Boron from Dislocation Dipoles

In the high dose implant cases, the dissolution is so slow compared to the 35 minute anneal that τ_{DISS} is chosen to be 10^8 sec, an arbitrarily large value. In the low annealing temperature cases, we estimate τ_{REL} from the electrical activation data by Seidel and MacRae [18]. According to these authors, the time to reach 90% electrical activity at 800°C are 6×10^3 and $1.8\ 10^5$ sec for implantation doses of 10^{14} and 10^{15} ions/cm^2, respectively. We use the values of $2.4\ 10^4$ and $3.6\ 10^5$ sec in the calculation.

In summary, Table 6 presents the global features of the annealing problem by displaying the relation of implantation dose and annealing temperatures to the parameters in the model, hence to the various mechanisms that prevail during annealing. The parameters associated with the annealing of damage, high dose implants, and low annealing temperatures are estimated from a more limited amount of data. Functionally they account for the formation of the immobile and electrically inactive phase of boron and the subsequent transformation into BV-pairs. Hereafter, the behavior of the BV-pairs is governed by the set of parameters in Table 5. This other subset of parameters describe the redistribution and electrical activation of ion implanted boron. They describe ordinary diffusion with high dose anomalies. They describe the enhanced diffusion of boron and subsequent reduction to ordinary diffusion. And, they describe the enhancement in diffusion produced by proton implants. This subset of parameters in the model encompass the main issues in the annealing problem and their importance cannot be overstated.

C. The Initial Conditions

To solve the initial value problem described by the set of coupled partial differential equations, we need the following:

8. Threshold Concentration Level for the Formation of Dislocation Dipoles

We use this parameter to represent the trapping of boron by dislocation dipoles. It is obvious that, functionally, this threshold level will produce the desired fraction of electrically inactive and immobile boron that we propose to be trapped by dislocation dipoles. Physically, this parameter represents the composite effects of a sequence of complex events depicted by the transmission electron micrographs; viz., the formation of dislocation dipoles and the trapping of boron. As a consequence, C_{DD} cannot be obtained from simple physical arguments. The value of 4×10^{18} cm^{-3} for C_{DD} at 800°C is first obtained from the inspection of Fig. 4 (10^{14} dose) and then varied to optimize the fit to experimental data. At higher temperatures, in the lower left-hand side of Table 6d, we can infer from the transmission electron micrographs at 900°C that the formation of dislocation dipoles and their subsequent annealing occurs so rapidly that the effects on annealing are not observable. It is for this reason that the corresponding values of C_{DD} are not estimated. At the right-hand side of Table 6d, we assume that all the immobile boron are precipitates that arise from exceeding the SSL. For this reason, we use the values of the solid solubility limit for C_{DD} in this region of the table. Lastly, TEM indicates the presence of dislocation dipoles during the 900°C annealing in the case of the 10^{15} ions/cm^2 dose implant. And, we find that, by incorporating the effects of dislocation dipoles in the conventional annealing model, we can improve slightly the fit between the calculated and the experimental profiles. We use the value of 5×10^{19} cm^{-3} for C_{DD} in this case.

9. Time Constants Associated with Precipitation and the Trapping of Boron by Dislocation Dipoles

In the low annealing temperature cases, the sequence of transmission electron micrographs show that the trapping of boron by dislocation dipoles occurs early during annealing. In the high dose implant cases, we assume that the precipitation of boron takes place rapidly.*

*It is possible that precipitation has occurred prior to annealing.

In summary, with the exception of τ_V, which is assumed to be constant, all the other parameters are functions of temperature only. To emphasize this dependence, we use the following representation. The dotted lines within the matrix (a) in Table 6 enclose sets of values that are invariant with implantation dose, but dependent on the annealing temperature. As mentioned previously, the parameters that follow hereafter are associated with anomalies arising from the annealing of implantation damage, high dose implants, and low annealing temperatures.

6. τ_{DAM}, Damage Annealing Time Constant

This parameter characterizes the time evolution of vacancy clusters during annealing. Figures 9 and 10 show the presence of these vacancy sources in the transmission electron micrographs corresponding to 5 minutes of annealing at 800°C. At 800°C and 900°C, because of the longer lifetime of BV-pairs ($>$ 10 min), the release of vacancies from vacancy clusters ($<$ 10 min) does not alter the boron-BV-pair reaction significantly. On the other hand, at 1000°C the lifetime of BV-pairs is only 140 sec. Consequently, the simultaneous generation of vacancies slows down the conversion of BV-pairs into active boron, prolonging locally the enhanced diffusion. This effect is only observable at high temperatures and short annealing times because, at longer annealing times, it is masked by ordinary diffusion. In our calculations, we use the value of 40 sec for τ_{DAM} at 1000°C (see Table 6b).

At lower temperatures, we can deduce from transmission electron micrographs and the lifetime of BV-pairs that the bounds of τ_{DAM} are larger than 40 sec and smaller than 550 sec, respectively.

7. Solid Solubility Limit (SSL)

The solid solubility limit is a function of temperature only. Table 6c shows the values we use in the calculation. These values are comparable to the experimental values by Vick et al [43].

Table 8

THE ESTIMATION OF THE LIFETIME OF BV-PAIRS

	x Measured from the Annealing of 10^{14} Dose Implants (μm)	τ Estimated from D_{BV} Used (sec)	τ Estimated from Enhanced Diffusion Coefficient (sec)	τ Used (sec)
800°C	0.110	3000	---	2780
900°C	0.079	230	1150	550
1000°C	0.180	270	540	140

repeat the calculation using the enhanced diffusion coefficient determined by Hofker et al; the results of this second estimation are shown in the third column. An alternative way to obtain the value of τ is to solve the set of diffusion equations with initial conditions for an ordinary diffusion. Then, the values of τ are chosen to fit experimental ordinary diffusion profiles. The values of τ we use in the calculations are presented in the fourth column of Table 9.

5. The Lifetime of Vacancies

The lifetime of vacancies is estimated from the diffusion length of vacancies. We use the diffusion length of 1.78×10^{-6} cm at 750°C, after Tsuchimoto et al [42]. The corresponding value of τ_V computed from this diffusion length and the diffusion coefficient estimated previously is $8.3\ 10^{-5}$ sec, approximately 10^{-4} sec. It is apparent that τ_V is much smaller than τ. Consequently, provided that this strong inequality is preserved, the annealing calculations will be rather insensitive to the actual value of τ_V. For this reason, the lack of more data on the diffusion length of vacancies does not create a problem, and we can use the value of 10^{-4} sec for τ_V at all temperatures. It is evident that, if more data were available, then we could have estimated a vacancy lifetime that is temperature dependent.

$$C_{V^+_{eq}} = C_{V^o} \exp\left(\frac{E_{V^+} - E_F}{kT}\right)$$

where $E_{V^+} = 0.35$ eV above the valence band edge. The Fermi level is calculated using approximations to the Fermi-Dirac integral of order 1/2 (Blakemore [41]). Hence, doping degeneracies are accounted for. It is worthwhile to emphasize that the apparent concentration-dependent diffusion coefficient of boron is achieved in this model through the Fermi level. A high substitutional boron concentration shifts the Fermi level closer to the valence band edge, thus increasing the concentration of positive vacancies ($E_V = 0.35$ eV above the valence band). This, in turn, increases the ratio of BV-pairs to substitutional boron, increasing the overall diffusion of boron.

4. τ, The Lifetime of BV-Pairs

This parameter is estimated from the diffusion length associated with the BV-pairs, the fast diffusing specie of finite lifetime. If we assume that the distance x travelled by the profile tail is twice the diffusion length, then we can solve for τ in the following expression:

$$x = 2\sqrt{D_{BV}\,\tau}$$

where the distance x is measured from the isochronal annealing profiles in Fig. 5a, after Hofker et al. The values of x at annealing temperatures in the range of 800°C to 1000°C are shown in the first column of Table 8. It is appropriate to comment that the values of x thus obtained are more representative of the enhanced diffusion at 800°C than at 1000°C. The reason for this is that, for a fixed annealing time of 35 minutes, the contribution of ordinary diffusion is less significant at lower temperatures than at higher temperatures. Consequently, the estimate of τ at 1000°C is probably an upper limit. The values of τ calculated in this manner using the values of D_{BV} estimated previously are shown in the second column of Table 8. As a comparison, we

2. The Equilibrium Constant in the Thermodynamic Reaction

At thermal equilibrium, the concentrations of reactants and products of the boron-BV-pair reaction are given by the following thermodynamic equation:

$$C_{BV} = k_o C_B C_V \tag{4}$$

The equilibrium constant k_o of this reaction can be calculated from Eq. (4) as follows. Under equilibrium conditions, such as in an ordinary diffusion, the electrical activity is near 100%. Assuming again an electrical activity of 98% and rearranging Eq. (4), we obtain the following expression for k_o:

$$k_o = (C_{BV}/C_B)\left(1/C_{V+}\Big|_{\text{equil., intrinsic}}\right) \tag{20}$$

where C_{V+} is the equilibrium concentration of positive vacancies under intrinsic conditions. The value of C_{V+} is obtained from Eq. (8) with the Fermi energy level at the middle of the energy band gap. Consequently, C_{V+} is a function of temperature only.

This choice of C_{V+} and the method for selecting D_{BV} insure that, when the electrical activity reaches 98%, the overall diffusion coefficient will approach to the value obtained from ordinary diffusion experiments under intrinsic conditions. From a different viewpoint, this choice of C_{V+} is responsible for the modelling of high dose and substrate doping effects by allowing the actu l concentration of positive vacancies to alter the position of active to inactive boron [Eq. (6)].

3. Equilibrium Concentration of Positively Charged Vacancies

The equilibrium concentration of positive vacancies C_{V+}^{eq} is dependent on the energy level E_{V+}, the Fermi energy level E_F; the temperature T and the concentration of neutral vacancies C_{VO}, which is a function of temperature only [36].

Table 7

THE ESTIMATION OF D_{BV}

	Enhanced Diffusion Coefficient by Hofker et al (cm^2/sec)	D_{BV} Estimated from the Diffusion of Annealed Profiles (cm^2/sec)	D_{BV} Estimated from the Ordinary Diffusion Coefficient (cm^2/sec)	D_{BV} Used (cm^2/sec)
800°C		$7.5\ 10^{-14}$	$2.51\ 10^{-14}$	10^{-14}
900°C	$1.4\ 10^{-14}$ $1.7\ 10^{-14}$	$7\ 10^{-14}$	$6.5\ 10^{-14}$	7×10^{-14}
1000°C	$1.5\ 10^{-13}$	$9\ 10^{-13}$	$8.5\ 10^{-13}$	$3.56\ 10^{-13}$

alternative, Anderson and Gibbons estimate the value of D_{BV} to be 5.7×10^{-14} cm^2/sec at 750°C from proton enhanced diffusion experiments. Another alternative method of estimating the value of D_{BV} is based on the following relation between diffusion and electrical activity:

$$D_{exp} = D_{BV} \text{ (1 - electrical activity)} \tag{19}$$

where D_{exp} is the diffusion coefficient measured in an experiment, hence the subindex.

The discussion and derivation of this relation is carried out in Appendix B. To estimate D_{BV}, we solve Eq. (19) under equilibrium conditions. For this reason, we assume that the electrical activity is 98% and we use for D_{exp} the experimental diffusion coefficients measured under equilibrium conditions by Hofker et al [2] and Kurtz (see Table 1). The values of D_{BV} thus estimated are shown in the second and third columns of Table 7, respectively. In the fourth column, we show the values used in the present work.

Table 6

THE RELATION OF THE PARAMETERS TO THE
IMPLANTATION DOSE AND ANNEALING TEMPERATURE

$D_B, D_V, D_{BV}, k_o, \tau, \tau_V$

	10^{14}	10^{15}	10^{16}
800			
900			
1000			

ions/cm^2

(a)

τ_{DAM} (sec)

	40 sec	
40 sec	40 sec	40 sec

(b)

SSL (#/cm^3)

7×10^{18}	7×10^{18}	7×10^{18}
$1.1\ 10^{20}$	$1.1\ 10^{20}$	$1.1\ 10^{20}$
$3.3\ 10^{20}$	$3.3\ 10^{20}$	$3.3\ 10^{20}$

(c)

C_{DD} (#/cm^3)

4×10^{18}	4×10^{18}	4×10^{18}
	$5\ 10^{19}$	1.1×10^{20} (SSL)
		3.3×10^{20} (SSL)

(d)

$\tau_{PREC} - \tau_{DD}$ (sec)

1 sec

Arbitrarily small

(e)

$\tau_{DISS} - \tau_{REL}$ (sec)

$2.4\ 10^4$	$3.6\ 10^5$	10^{8*}
	700	10^8
		10^8

*Arbitrarily large

(f)

contain the preexponential factors and the activation energies. This set of parameters is the backbone of the annealing model. These parameters control the redistribution and electrical activation of boron. They are the dominant parameters in the ordinary diffusion of boron and in the typical annealing cases of ion implanted boron into silicon. In high dose implantation and low annealing temperature cases, these parameters control the redistribution and electrical activation of the boron arising from the dissolution of boron precipitates or the boron released from the annealing of dislocation dipoles. As discussed previously, the modelling of precipitation and dissolution as well as the trapping of boron by dislocation dipoles and the subsequent release require additional parameters such as solid solubility limits, time constants, and so on. These parameters are generally obtained from more empirical considerations. A summary of all the parameters and their relation to implantation dose and annealing temperature is given in Table 6. In this manner, Table 6 displays mainly the parameters associated with anomalies, while Table 5 contains the parameters controlling the main diffusion mechanism. The data in Table 6 is arranged in six separate groups. Each group is a matrix displaying the behavior of the parameter as implantation dose (horizontal) and annealing temperature (vertical) are varied.

We shall now discuss the methods used in the estimation of the parameters in Tables 5 and 6.

1. Diffusion Coefficients--Only Functions of Temperature

We assume that substitutional boron diffuses by the same mechanism as the self diffusion of silicon. Therefore, we use the self diffusion coefficient of silicon [40] for D_B. For positive vacancies, we use the diffusion coefficient proposed by Seidel and MacRae [37]. Finally, the diffusion coefficient for BV-pairs is estimated from various diffusion experiments. Hofker and coworkers measure the enhanced diffusion of ion implanted boron after 35 minutes of annealing. The enhanced diffusion coefficient they obtain is shown in the first column in Table 7. Since these are average values, they provide only lower limits for the value of D_{BV} at the respective temperatures. As an

Table 5

THE TEMPERATURE DEPENDENT PARAMETERS

Parameter	800 °C	900 °C	1000 °C	D	Q (eV)	Source
D_B cm^2/sec	$7.35\ 10^{-21}$	$8.32\ 10^{-19}$	$4.477\ 10^{-19}$	9000	-5.13	Fairfield et al [40]
D_V cm^2/sec	$9.4\ 10^{-8}$	$4.5\ 10^{-7}$	$1.68\ 10^{-6}$	9	-1.7	Seidel and MacRae [37]
D_{BV} cm^2/sec	10^{-14}	$7\ 10^{-14}$	$3.56\ 10^{-13}$	$6.65\ 10^{-5}$	-2.09	
k_o cm^3	$3.025\ 10^{-12}$	$1.34\ 10^{-13}$	$9.68\ 10^{-15}$	4×10^{-28}	+3.3817	
τ sec	2782	550	140	$1.515\ 10^{-5}$	+1.76	
τ_V sec	10^{-4}	10^{-4}	10^{-4}			
C_{V^o} $=/cm^3$	$5.4\ 10^{9}$	$1.25\ 10^{11}$	$1.75\ 10^{12}$	5×10^{25}	-3.4	Seidel and MacRae [37]

on a digital computer. The results of the integration are concentrations of each of the species as functions of time and space. Details concerning the solution are given in Appendix A. In order to evaluate the effectiveness of the model, we have to compare the calculated results with experimental data. In this respect, while the electrical carrier concentration profile can be compared directly with the calculated active boron profile at corresponding times, the comparison with other experimental data requires some algebraic manipulations. For instance, the total boron concentration determined experimentally using Secondary Ion Mass Spectrometry (SIMS) is to be compared with the summation in Eq. (17).

$$C_{B_{total}}(x,t) = C_B(x,t) + C_{BV}(x,t) + C_{BI}(x,t) \qquad (17)$$

And, the electrical activation curve is to be compared with the spatial integration of the calculated active boron profile in Eq. (18).

$$ea(t) = \int_0^{+\infty} C_B(x,t)\, dx$$

B. The Selection of Parameters

The mathematical model presented in the preceding section is the result of inferences drawn from the discussions in Chapter I. Basically, the complex annealing problem is broken into three simpler cases. Then, the reactions dominant in each of the aforementioned cases are identified. The kinetics of these reactions are then modelled by first order approximations involving parameters with physical interpretations. Our objective in this section is to estimate the numerical values of these parameters.

In typical annealing cases, the problem is less complicated and the experimental data is more abundant. Consequently, it is possible to apply thermodynamic and physical considerations in the estimation of the parameters. Table 5 gives a summary of the estimated values of the parameters, which are functions of temperature only. The last two columns

that the dissolution of boron precipitates is negligible (see Fig. 5). In other cases, either boron precipitate or trapped boron is present. Consequently, by defining the immobile boron to represent either boron precipitate or trapped boron, we do not lose generality and we do gain simplicity in the mathematical formulation of the model.

In summary, we propose a mathematical model for predicting the redistribution and electrical activation of ion implanted boron that is subsequently annealed. The general model in Eq. (15) is aimed toward solving the annealing problem under the implantation and annealing conditions in Table 3. These conditions are by no means too restrictive; in fact, most applications fall into the subcategory of "typical annealing cases" in Table 3. To solve the simple annealing cases, as discussed in Chapter I, only three species are required. Consequently, Eq. (15) can be simplified by dropping the last equation and the associated coupling terms from the remaining equations. The importance of this simpler case is threefold. First, the annealing mechanism in this simpler case is also present in more complicated cases. Second, in these cases, after 35 minutes of isothermal annealing, the enhanced diffusion reduces to ordinary diffusion. Hence, this set of equations should also apply to ordinary diffusion if appropriate initial conditions are used. Third, the enhanced diffusion mechanism at the outset of the anneal is also responsible for the enhancement in diffusion produced by proton implants. Consequently, the three species model should be capable of predicting ordinary diffusion, proton enhanced diffusion, and the simpler annealing cases in Table 3. And, if the three species model is extended to include boron precipitate and boron trapped by dislocation dipoles, then the more general model in Eq. (12) can also predict the high dose implant and low annealing temperature cases in Table 3.

Let us outline now the necessary steps for solving the equations of the annealing model. First of all, a set of parameters is to be estimated based on thermodynamic considerations and experimental data. Then we will recall the discussions in Chapter I and establish the initial conditions for the annealing problem. With these elements, we can now integrate the set of coupled partial differential equations. This is an initial value problem, and the solution is implemented using numerical analysis methods

Chapter III

COMPARISON OF CALCULATED AND EXPERIMENTAL RESULTS

With the choice of parameters and initial conditions described in the preceding chapter, we can proceed to solve the annealing behavior of ion implanted boron into silicon. The results of the calculations corresponding to the cases in Table 3 can be structured in three canonical groups:

(1) typical annealing cases

(2) high dose cases

(3) low annealing temperature cases

Each group has characteristic features that are manifest in the equations, reaction kinetic terms, and parameters. And, these characteristics features are consequences of special conditions present at certain implantation dose and/or annealing temperatures. For these reasons, we present the results of the calculations following the same organization.

A. Typical Annealing Cases

The result of the calculation with the initial condition corresponding to the 10^{14} ions/cm^2 dose implant and the parameters for the 900°C anneal is shown in Fig. 15. The atomic concentration is represented on the vertical logarithmic scale, and the depth in microns into the silicon substrate is represented linearly on the horizontal axis. The as-implanted profile determined experimentally by Hofker et al [2] is represented by the dotted line. Upon annealing, the BV-pairs in this profile diffuse and convert into substitutional boron. Hence, a sequence of electrically active boron profiles will develop with time. Figure 15 shows calculated profiles after 1, 3, 10, and 35 minutes of annealing with corresponding electrical activities of 10, 28, 65, and 94 percent. The total boron concentration at 35 minutes is represented by triangles; the fit to the solid line representing the experimental SIMS profile is excellent. Since the ordinary diffusion of boron at 900°C would only

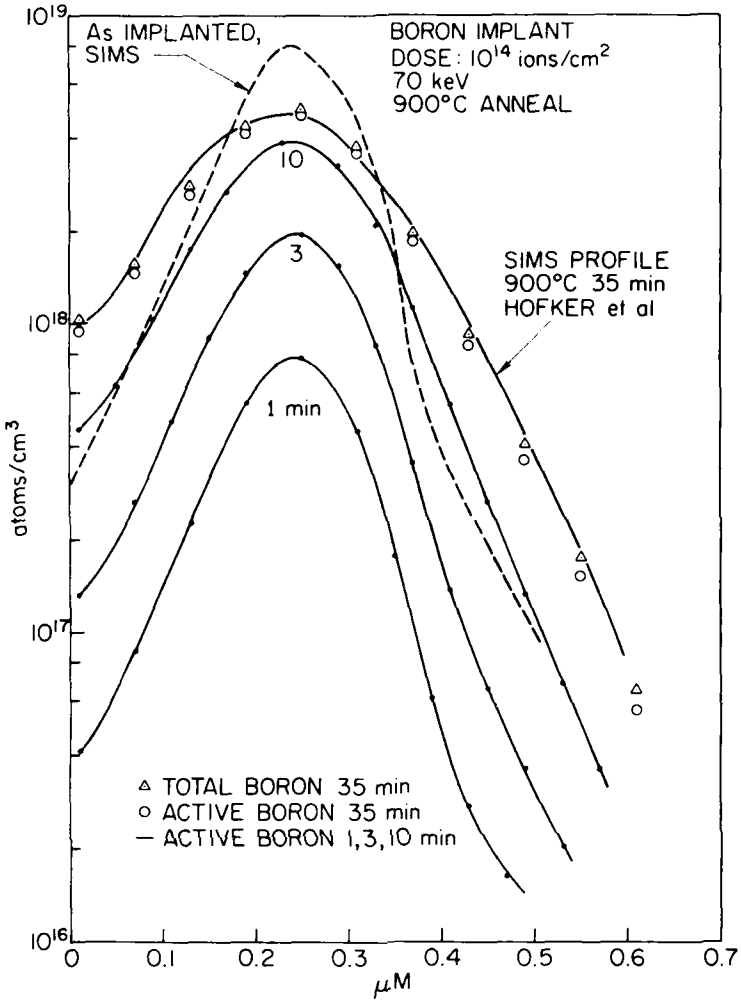

Fig. 15. THE ANNEALING OF A 10^{14} IONS/CM^2 DOSE B IMPLANT AT 900°C. The comparison of calculated and experimental results.

modify the as-implanted profile very slightly, the fit between the calculated results and the deeper experimental profile is indicative of the existence of enhanced diffusion which progressively diminishes to the ordinary diffusion rate as the electrical activity approaches 100%. The calculated results are thus in good agreement with the experimental observations of Hofker and coworkers [2].

Figure 16 shows the results of the calculation for the 10^{15} ions/cm^2 dose, which produces an order of magnitude increase in the impurity and damage profiles. We show again the evolution of the calculated

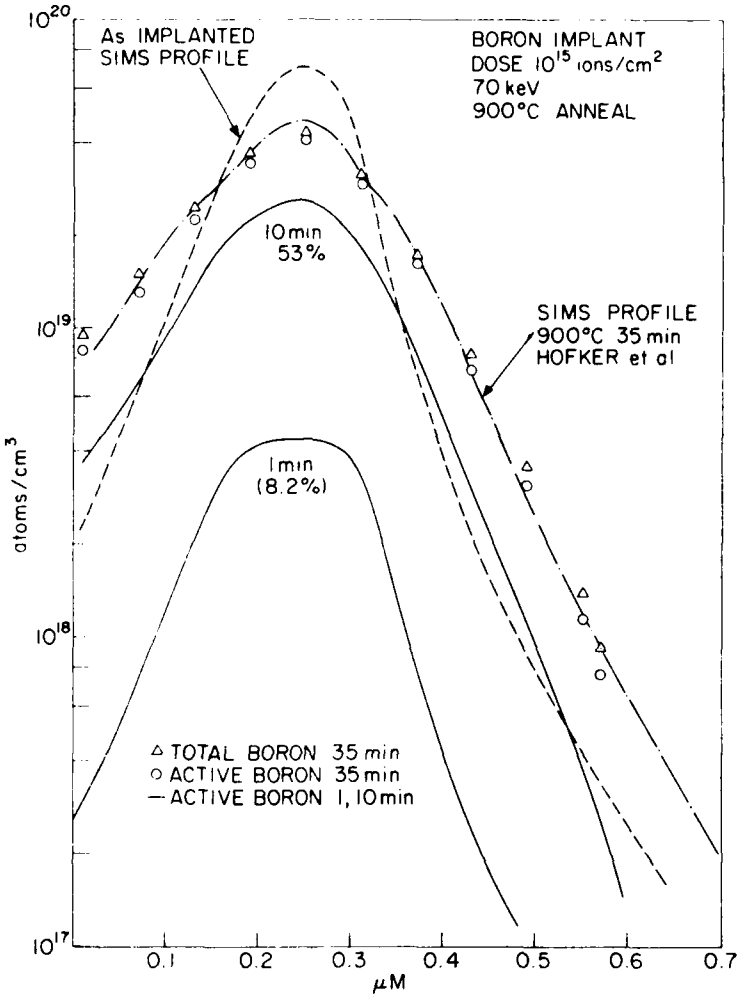

Fig. 16. THE ANNEALING OF A 10^{15} IONS/CM^2 DOSE B IMPLANT AT 900°C. The comparison of calculated and experimental results.

active boron concentration with time, and we compare the calculated to tal boron concentration represented by triangles with the experimental SIMS profile represented by the solid line. Again, the fit is excellent. We wish to comment that this basic result can be obtained from two alternative calculations, by including or excluding the trapping effects of boron by dislocation dipoles, although there is a slight loss of accuracy if the effects of the dislocation dipoles are neglected. Figure 16 depicts the results of the calculation that includes the trapping of boron by defects.

Next, we show the calculated results corresponding to the 10^{14} and 10^{15} ions/cm^2 dose boron implants annealed at 1000°C in Figs. 17 and 18. From the inspection of these figures, we can appreciate that at 1000°C the electrical activation of boron is more rapid. This quicker activation is the consequence of the shorter lifetime of BV-pairs at 1000°C. At this temperature, we can notice the effects of the vacancies released from the vacancy cluster that anneal very rapidly (at the outset of the anneal). This excess vacancy concentration retards the conversion of BV-pairs into active boron, hence prolonging the initial enhancement in

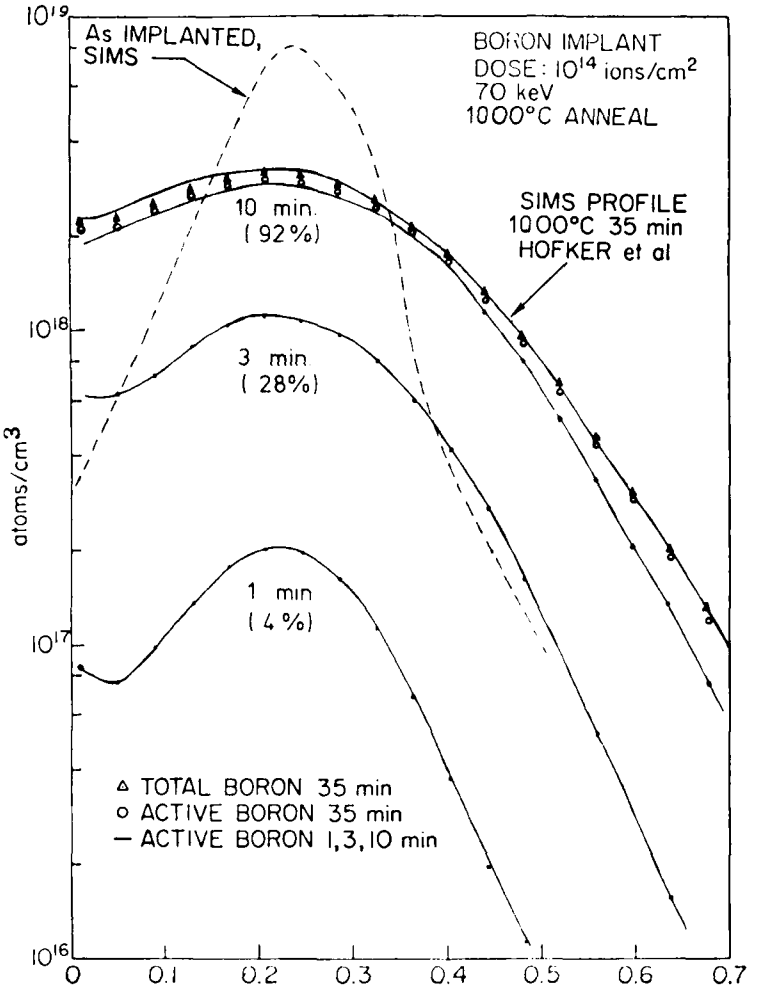

Fig. 17. THE ANNEALING OF A 10^{14} IONS/CM^2 DOSE B IMPLANT AT 1000°C. The comparison of calculated and experimental results.

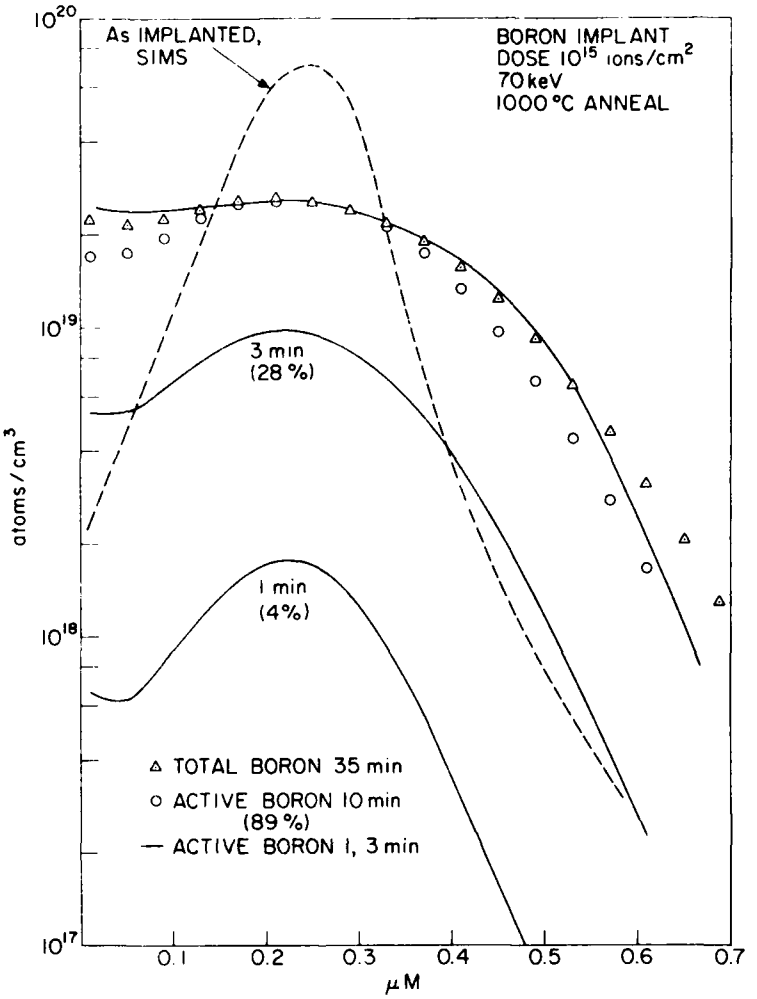

Fig. 18. THE ANNEALING OF A 10^{15} IONS/CM^2 DOSE B IMPLANT AT 1000 °C. The comparison of calculated and experimental results.

diffusion. It is for this reason that, for short annealing times, the inclusion of the generation term in the vacancy equation contributes to the improvement of the fit to the experimental data. Naturally, at longer annealing times, the enhanced diffusion is overwhelmed by the greater ordinary diffusion at higher temperatures and the aforementioned improvement becomes less noticeable. We can state from a different viewpoint that: for the case of a long annealing at high temperature, the neglect of the vacancy generation term in the calculation will not cause significant errors.

The comparison of the experimental electrical activation of boron versus time by Seidel and MacRae [18] with the calculated results from some of the previous examples is shown in Fig. 19. The agreement is good for long times. For short times, we attribute the difference to our initial condition of zero electrical activity at the outset of the anneal. As discussed previously, we expect improvements with a nonzero initial condition for the electrical activity. The nonzero initial electrical activity is generally attributed to room-temperature annealing of the implanted silicon substrate. We can apply this idea to the interpretation of the calculated electrical activity result in Fig. 19 and to obtain an alternative set of initial conditions. For instance, if t_o is the instant in time at which the desired electrical activity is attained, then the annealing prior to t_o is due to room-temperature annealing and only the electrical activation of boron <u>after</u> t_o is attributable to the annealing at the elevated temperature. In other words,

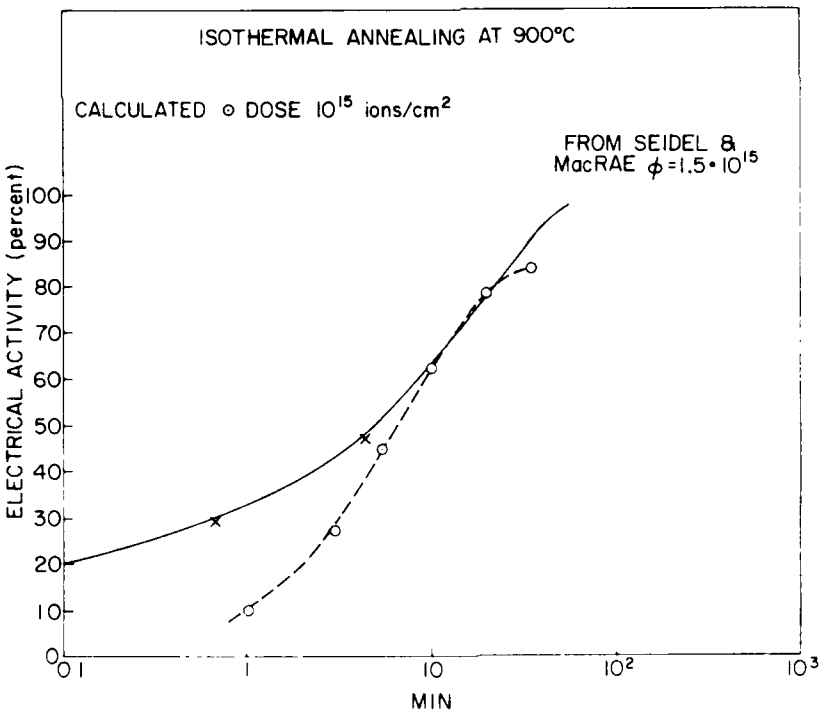

Fig. 19. THE COMPARISON OF CALCULATED ELECTRICAL ACTIVITY VERSUS TIME WITH EXPERIMENTAL ISOTHERMAL RESULTS BY SEIDEL AND MacRAE. Dose: 10^{14} ions/cm^2, 900°C.

the experimental result should be compared with the calculated result shifted in time by t_o to correct for room temperature annealing effects. Or, equivalently, a shift in time would not be required if the boron and BV-pair profiles at t_o were the initial conditions used in the calculation. To explore the validity of these arguments, we use the pertinent profiles at t_o = 2.5 minutes as initial conditions in the subsequent calculation. We find that the calculated data points represented by 'x's, thus obtained, do approximate the experimental electrical activation curve. We also verify that shifting the time axis of the original calculation by t_o produces equivalent results. Namely, subtraction of 2.5 minutes from the abscissa of each original data point (calculated using the zero initial electrical activity) moves the calculated data closely toward the experimental curve.

B. High Dose Cases

Figure 20 shows the comparison of calculated and experimental results* for the case of the 10^{16} ions/cm^2 dose boron implant annealed at 900°C. The slower electrical activation is a consequence of the small dissolution rate of boron precipitates and diffusion effects, as we will see. There are plateaus on the electrically active boron profiles calculated at 1, 3, 10, and 35 minutes. In particular, we compare the calculated electrically active boron profile at 35 minutes with the corresponding experimental electrical carrier concentration profile represented by the squares. The theoretical results are in good agreement with the experimental data. It is apparent that near the profile peak there is an immobile and electrically inactive fraction of boron. This fraction is composed of boron precipitates because the boron concentration is in excess of the solid solubility limit at the annealing temperature. Both theoretical and experimental results exhibit, upon annealing, a decrease in the width of the immobile fraction near the profile peak. This change of shape is due to the dissolution of boron

*In the 10^{16} ions/cm^2 dose cases, the annealed profiles by Hofker et al [2] have been corrected for the 30% ion yield increased in the precipitation area observed by the authors.

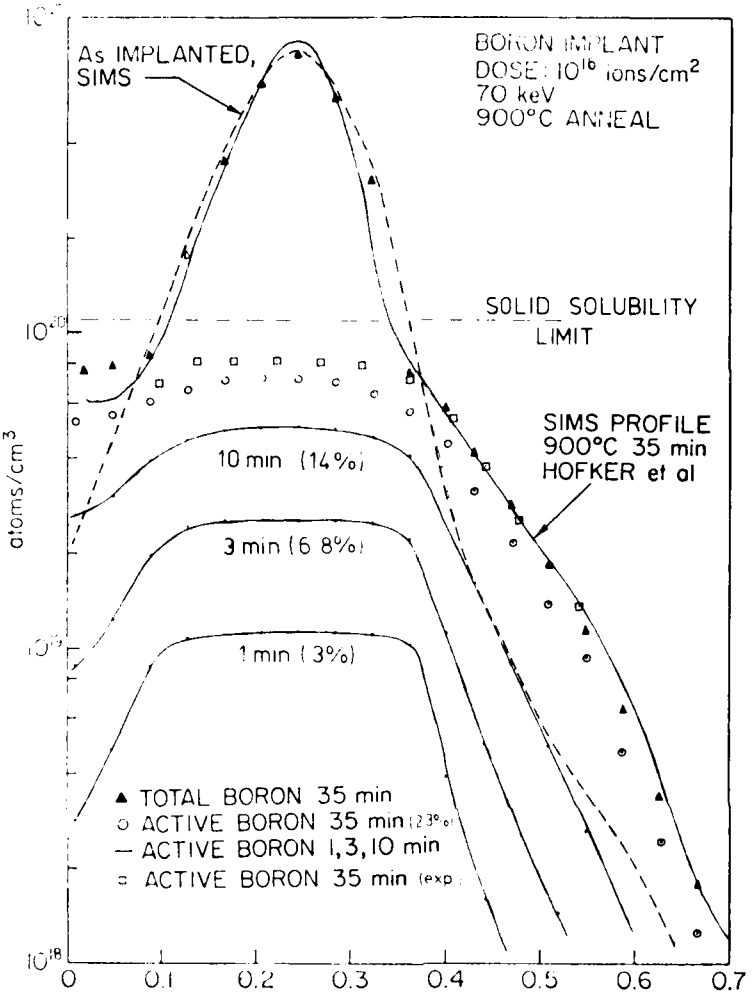

Fig. 20. THE ANNEALING OF A 10^{16} IONS/CM^2 DOSE B IMPLANT AT 900°C. The comparison of calculated and experimental results.

in this area. The dissolution takes place because diffusion has depleted the mobile boron, upsetting the equilibrium concentrations of precipitated and nonprecipitated boron. Therefore, the dissolution is not only limited by the dissolution rate of boron precipitates, but it is also governed by the diffusion process. The relative importance of this diffusion can be assessed from inspection of Fig. 21. In this figure, we compare the total calculated boron concentration at 800°C through 1000°C with the experimental SIMS profiles. It is apparent that at 800°C the diffusion is very slight and the profile peak

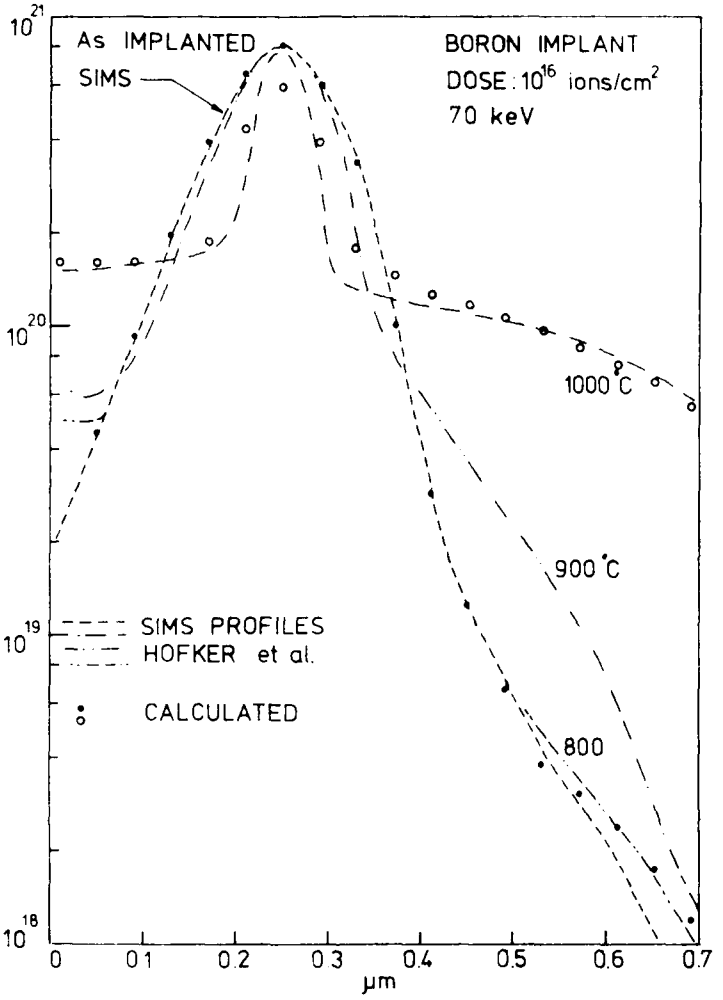

Fig. 21. THE ANNEALING OF A 10^{16} IONS/CM^2 DOSE B IMPLANT IN THE TEMPERATURE RANGE OF 800°C TO 1000°C.

remains identical to the as-implanted profile. At 900°C, the diffusion is appreciable and we can observe a decrease in the width of the top portion of the profile peak upon annealing. At 1000°C, the diffusion is important and the removal of boron from the high concentration area is quite conspicuous. In summary, the electrical activation of boron in the annealing of high dose implants is controlled by both the dissolution rate of the precipitates and by the diffusion of the mobile boron.

C. Low Annealing Temperature Cases

Figure 22 shows the comparison of the calculated and experimental results of the 10^{14} ions/cm^2 dose boron implant annealed at 800°C. We show the evolution of the calculated electrically active boron profiles at 1, 3, 10, and 35 minutes, and we compare the 35 minute profile with the experimental electrical carrier concentration profile at the corresponding time. We also show the fit between the calculated total boron concentration profile with the experimental SIMS profile by Hofker et al [2]. The agreement is quite good in both comparisons. We can also

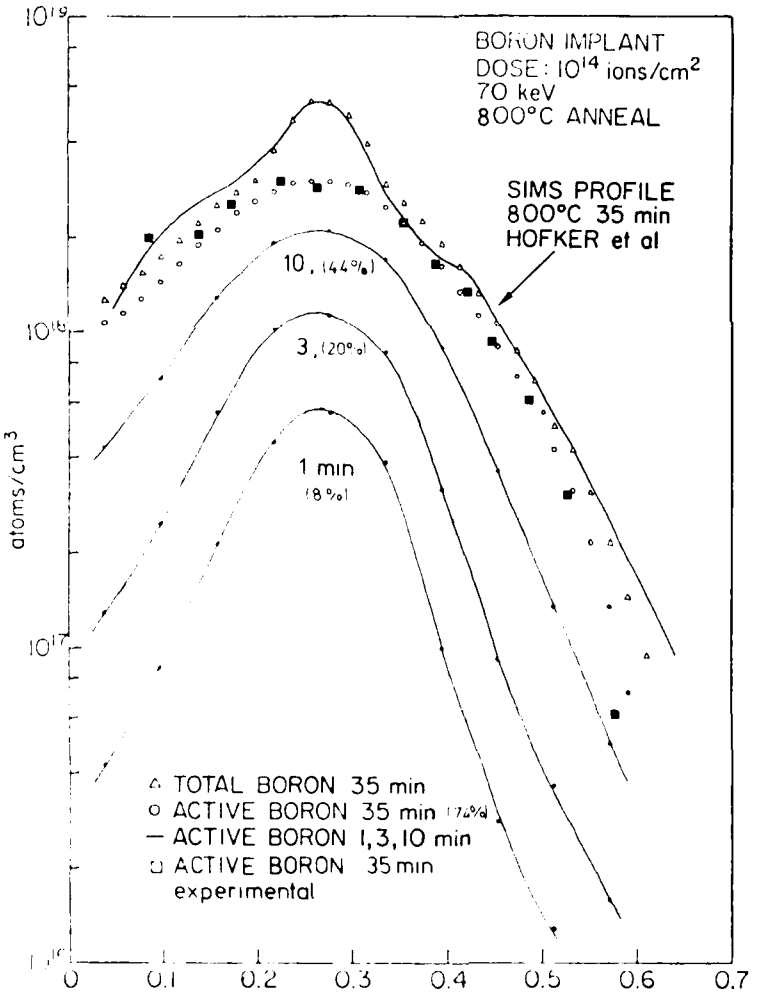

Fig. 22. THE ANNEALING OF A 10^{14} IONS/CM^2 DOSE B IMPLANT AT 800°C. The comparison of calculated and experimental results.

compare the electrical activation predicted by this calculation with the experimental activation curve by Seidel and MacRae in Fig. 23. We can see that again the zero initial electrical activity in this calculation is responsible for the discrepancy between the two curves at short annealing times. As in the previous instance, we attribute to room-temperature annealing the electrical activation of boron until the desired initial electrical activity is attained, and we compare the experimental annealing curve with the corrected calculated electrical activation curve. The corrected data points are represented by 'x's and they are obtained by shifting the time axis by t_o = 15 minutes. We can see now that the corrected calculated points are in agreement with the experimental curve.

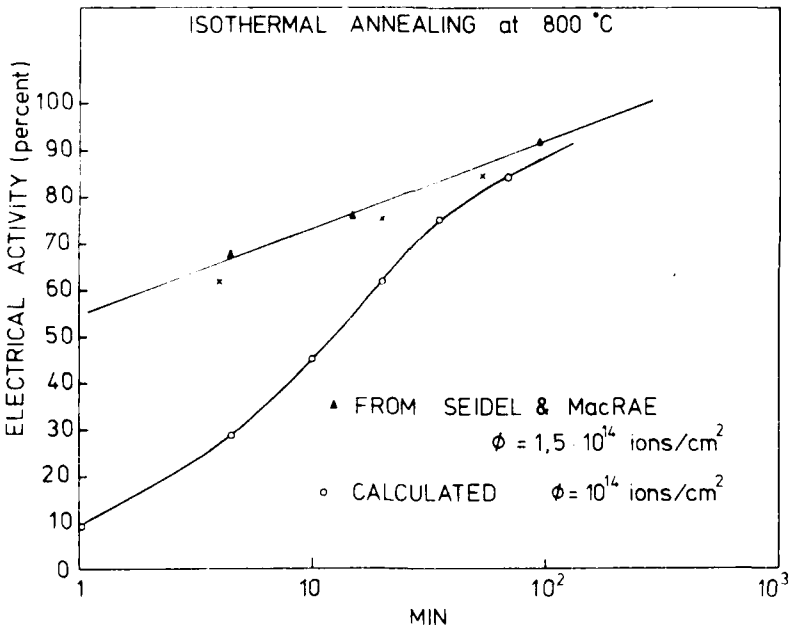

Fig. 23. THE COMPARISON OF CALCULATED ELECTRICAL ACTIVITY VERSUS TIME WITH THE EXPERIMENTAL ISOTHERMAL RESULT BY SEIDEL AND MacRAE. Dose: 10^{14} ions/cm^2, 800 °C.

Next, we show in Fig. 24 the result of the calculation performed with the same set of parameters for the 10^{15} ions/cm^2 dose annealed at the same temperature. In this figure, we show the comparison of the calculated total boron concentration with the experimental SIMS profile.

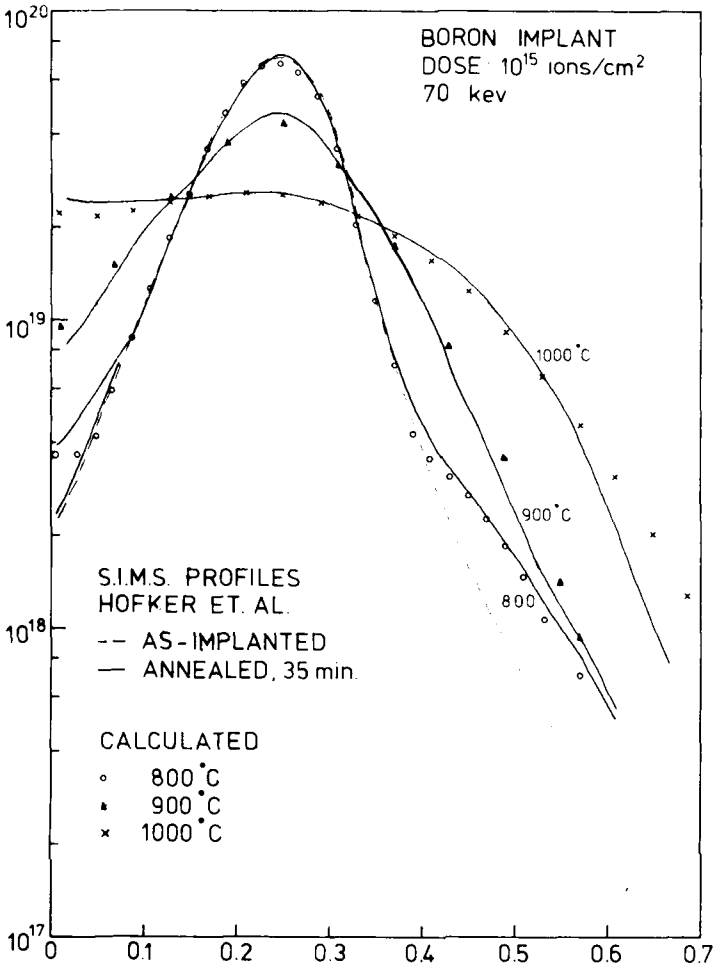

Fig. 24. THE ANNEALING OF A 10^{15} IONS/CM^2 DOSE B IMPLANT IN THE TEMPERATURE RANGE OF 800°C TO 1000°C.

We recall that with the higher dose implant the defect density is also higher and the fraction of immobile boron trapped by dislocation dipoles also increases. This larger fraction of immobile boron produces a more pronounced 'shoulder-like structure' in the annealed profile. We also include in this figure the calculated annealed boron profiles for 900°C and 1000°C to show that there is a significant change in the shape of the annealed profile as the annealing temperature is varied. The agreement of the calculated with the experimental results is quite good in all cases.

In summary, we have used the mathematical annealing model in conjunction with the set of parameters in Tables 6 and 7 to calculate the annealing of ion-implanted boron under conditions summarized in Table 3. These conditions include a variation of two orders of magnitude in implantation dose and annealing temperature in the range of 800°C to 1000°C. In the calculations, we use initial conditions and parameters that are in agreement with experiments pertinent to the annealing problem. The main group of parameters are obtained using procedures that are based on thermodynamic and physical considerations. In other instances, we use a single parameter to represent the composite effects of several phenomena. Naturally, more detailed modelling is possible in these cases but, based on the good agreement between the calculated and the experimental results, it is apparent that the selected set of parameters is representing indeed the major elements in the annealing problem under the conditions that we described.

Chapter IV

SUMMARY AND CONCLUSIONS

A. The Three Stream Diffusion Model

In the first chapter, we studied the annealing of ion-implanted boron into silicon and we reviewed the relevant experiments that are of central importance for the annealing problem. With this background, we then discuss a general diffusion model in which boron atoms interact with positively charged silicon vacancies to form BV-pairs. In this interpretation, the diffusion of boron becomes a weighted diffusion with contributions from a slow, electrically active fraction (substitutional boron) and a fast, electrically inactive fraction (the boron-vacancy pair). The presence of positive vacancies in the model has two important consequences. First, a large concentration of vacancies in excess of the equilibrium concentration level will modify (by virtue of the aforementioned reaction) the relative populations of the two forms of boron, hence altering the overall diffusion. Second, the concentration of positive vacancies in the silicon lattice is a function of the Fermi level in the bandgap. This Fermi level dependence is responsible for high concentration anomalies observed in diffusion experiments.

This basic three stream diffusion model is capable of predicting ordinary diffusion of boron, proton enhanced diffusion, and a number of important cases of annealing. In the ordinary diffusion problem, the prevalent fraction of substitutional boron under equilibrium conditions results in high electrical activity and slow diffusion. In the proton enhanced diffusion problem, the steady state proton beam produces an excess vacancy concentration, which in turn creates a large concentration of BV-pairs. This predominance of BV-pairs results then in low electrical activity and fast diffusion. A somewhat similar situation is found in the typical annealing cases of ion implanted boron. In these cases, the majority of the implanted boron ions react with nearby vacancies and form BV-pairs. Annealing proceeds then with the conversion of a large population of BV-pairs into substitutional boron. Consequently, during annealing, the redistribution of boron is characterized

AD-A159 133 A THEORETICAL APPROACH TO THE CALCULATION OF ANNEALED IMPURITY PROFILES O..(U) STANFORD UNIV CALIF SOLID-STATE ELECTRONICS LAB A CHU JUN 77 2/2

UNCLASSIFIED SU-SSEL-77-012 ECOM-77-2684-1 F/G 20/2 NL

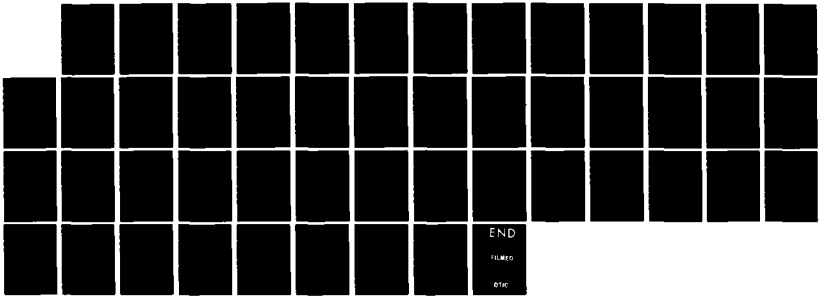

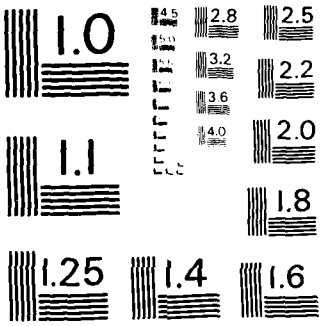

by an initial enhancement in diffusion that reduces to ordinary diffusion rates as the electrical activity increases to near 100%.

B. The Relation between Diffusion and Electrical Activity

The two forms of boron in this three stream diffusion model have dichotomous attributes. Namely, substitutional boron is electrically active and slow diffusing; on the other hand, the boron-vacancy pair is electrically inactive and fast diffusing. Because of this dichotomy and because the diffusion of the total boron is a weighted diffusion of these two species, a relation between diffusion and electrical activity ought to exist. We assume near 100% electrical activity in the selection of parameters to fit thermal diffusion experiments. This ensures that, when the abnormally high concentration of boron vacancy pairs that is produced by the implantation has annealed, the enhanced diffusion (associated with the initially low electrical act.) will relax to ordinary diffusion which is simply the near-thermal-equilibrium solution of the set of equations. The analytical analogue of this discussion is carried out in Appendix A. The boron and BV-pair equations are combined and the predominance of D_{BV} over D_B is used to arrive at a single approximated diffusion equation for total boron. In this equation, we can identify the overall diffusion coefficient D_{exp} with a product of D_{BV} and the fractional concentration of BV-pairs. Furthermore, the fractional concentration can be expressed in terms of electrical activity. Hence, we arrive at a diffusion coefficient (the only one accessible in an actual experiment, hence the subindex), which is a function of the electrical activity.

$$D_{exp} = D_{BV} \frac{C_{BV}}{C_{BV} + C_B} = D_{BV} \text{ (1 - electrical activity)} \qquad (6)$$

For instance, at the outset of the 900°C anneal, the assumed electrical activity is zero, and the value of D_{exp} is then initially equal to D_{BV}. During anneal, as the electrical activity increases, D_{exp} will decrease. Finally, when the electrical activity approaches 98%, D_{exp} will approach the value of $1.4\ 10^{-15}$ cm^2/sec, the ordinary diffusion coefficient of boron at 900°C measured in thermal diffusion experiments.

C. High Dose and Low Annealing Temperature Anomalies

In the typical annealing cases, the implantation dose is moderate and the annealing temperature is relatively high. These conditions ensure that the redistribution and electrical activation of boron evolves following the description in the preceding paragraph. However, when the implantation dose is increased sufficiently, the resultant impurity distribution in the substrate will exceed the solid solubility limit and a precipitated phase will form. Naturally, the presence of this immobile precipitated phase will strongly alter the redistribution and the electrical activation behavior of boron. A different situation arises when the annealing is performed at low temperature. In this case, many kinds of defects form, evolve, and interact during the anneal. The annealing temperature is an important parameter because processes have different activation energies and the selection of the temperature determines the duration and time sequence in the evolution of the defects and the likelihood of interactions between them. In particular, we are interested in defects that can interact with the implanted impurity. At 800°C, we have indications that the dislocation dipoles that form during annealing are capable of trapping boron atoms in their associated strain fields; hence, rendering the boron immobile and electrically inactive. For this reason, the redistribution profiles have special characteristics when the ion implanted boron is annealed at low temperature. The electrical activation in these cases is controlled by the release of boron from the strain fields as the dislocation dipoles anneal out. We wish to extend the three stream diffusion model to cover these high dose and low annealing temperature anomalies, since this constitutes a further test for the basic model.

D. The Model and the Parameters

The mathematical model for the annealing problem is basically a diffusion model extended to include the aforementioned anomalies. The equations express in mathematical terms the diffusion and possible interactions among the species. Consequently, the essence of the overall model lies in the modelling of each diffusion, each interaction, and the parameters associated with each phenomenon. In this respect, these elements

are the links to the physical world and, in particular, the plausibility of the values of the parameters is indeed an indicator of the validity of the model. For instance, the values of temperature dependent parameters should obey simple activation energy relations and they should be invariant when we calculate the annealing behavior of different dose boron implants annealed at the same temperature.

Figure 25 shows the temperature dependence of the parameters in the basic diffusion model. The horizontal axis is linear in units of inverse temperature in degrees Kelvin, and the vertical axis is a logarithmic

Fig. 25. THE TEMPERATURE DEPENDENCE OF PARAMETERS.

scale. The horizontal arrows adjacent to the lines give for each parameter the appropriate exponent to be read on the logarithmic scale. The straight lines in this semi-logarithmic representation indicate that the temperature dependence of the parameters follows indeed a simple activation energy relation. This result is extremely important, since it enables the determination of the set of parameters once the temperature is specified.

The remaining parameters are given in Table 7. In some cases, the modelling was not carried to the extent required to make the temperature dependence apparent. This is the case of the lifetime of vacancies, the vacancy generation time constant, and the time constants associated with the precipitation and dissolution of boron. For instance, the requirements on the latter parameters are for them to assume very small and very large values, respectively. In other cases, the parameters are chosen to represent the composite effects of very complex phenomena. Such is the case for the threshold concentration level for the trapping of boron by dislocation dipoles and the release of boron from these defects. In these cases, the representation is oversimplified and a more detailed model could be sought if necessary. However, based on the quality of the calculations in the preceding chapter, it is apparent that the present scheme captures the key features in the low annealing temperature and high dose cases as well.

E. The Initial Conditions

We wish to emphasize that the equations in conjunction with the parameter set constitute a diffusion model with provisions for high dose and low annealing temperature anomalies. But, to actually solve a particular problem, an ordinary diffusion, a proton-enhanced diffusion, or an anneal, we need, in addition, the set of appropriate initial conditions for the specific problem. In the preceding chapter, we solved nine cases of annealing with initial conditions for boron implanted into silicon at room temperature. The implantation condition is of importance because the damage produced by a low mass ion is light and there is room temperature annealing as the damage is being produced. Under these conditions, it is possible to assume that the initial vacancy

concentration is in thermal equilibrium in the silicon substrate. This assumption will certainly be inadequate for a liquid nitrogen implant or for the case of a heavy ion or a high dose implant that produces an amorphous damage layer.

F. Discussion

Let us examine a number of models reported in the literature. These models predict different aspects of the annealing problem that are included in our formulation. Table 9 is a summary of models proposed for the annealing or diffusion of boron in silicon. We list the number of species in the first column. In the second and third columns, we indicate whether the model is capable of predicting the redistribution or the electrical activation of boron during the anneal. In the fourth column, we list a representative source. And, the last column contains remarks pertinent to the particular model. It is apparent from the inspection of Table 9, that the proposed annealing model predicts both the redistribution and the electrical activation, as a realistic model should. It is also apparent that the proposed model is more complex. In this regard, we wish to offer the following discussion.

Our annealing model is devoted to the diffusion of boron and to the annealing of ion implanted boron under a wide range of implantation dose and annealing temperatures. For this reason, a substantial portion of this model is dedicated to the anomalies that arise when the implantation dose and annealing temperature vary over a wide range. In this regard, on one hand, it may be desirable to extend the model to cover other anomalies. And, the general nature of the numerical implementation of the solution enables additions to be made with minor modifications of the computer program. On the other hand, deletions could be appropriate under other circumstances. For instance, if the high dose and low annealing temperature cases are of little interest, then the three stream diffusion model with a subset of parameters will still predict ordinary diffusion, proton enhanced diffusion, and the typical annealing cases of boron implants at room temperature. This reduced model is still very important and attractive because, once the parameters associated with the anomalies are deleted, the remaining parameters have simple activation

Table 9

MODELS FOR ANNEALING OR DIFFUSION

Species	Prediction of Annealing Profiles	Prediction of Electrical Activation	Authors	Remarks
1	Yes	No	Widely used for comparison	Nonphysical--diffusion coefficient dependent on dose--temperature--annealing time
2	No	Yes	Seidel and MacRae [18]	For the prediction of the electrical activation
2	Yes	No	Hofker et al [2]	To obtain the structure in 10^{16} dose annealings
1	Yes	No	Fair et al [29]	Background effects of substrate doping and impurity concentration on diffusion
2	Yes	No	W. Nuyts and Van Overstraeten [30]	Includes electric field effect and predicts ordinary diffusion
1	Yes	No	Longini & Green [31] Crowder et al [8]	D/Di = P/Pi
1	Yes	Yes	Chu-Gibbons	Room temperature B implants Dose range: 10^{14} - 10^{16} ions/cm^2 Annealing temperature range: 800°C - 1000°C

energies and they are determined by the specification of a single variable: the temperature.

Lastly, we would like to elaborate on the boron-BV-pair reaction, the principal interaction in the three stream diffusion model. In the annealing problem, the spontaneous conversion of BV-pairs into substitutional boron is driven by the reaction rate, which is rather large during the anneal. From this viewpoint, it is apparent that the boron-BV-pair reaction is the dominant process in the annealing problem. However, in other problems, especially under thermal equilibrium when the boron-BV-pair reaction rate is small, it may be appropriate to reexamine the predominance of the boron-BV-pair reaction over other possible effects. For instance, depending on the nature of the problem and the features one wishes the model to predict, it may be necessary to consider effects such as the influence of internal electric fields or diffusion induced stresses due to the mismatch of the impurity atoms in the lattice.

G. Conclusion

The annealing model is capable of predicting boron impurity profiles under conditions of ordinary diffusion, proton enhanced diffusion, and radiation enhanced diffusion of the sort that occurs when boron is implanted at room temperature and subsequently annealed. In the latter case, the model also predicts the evolution of the electrically active boron as a function of space and time. In reference to practical implantation and annealing conditions, the model has been tested for all the cases in Table 2. In this wide range of dose and annealing temperatures, the most relevant case in device fabrication are in the lower left corner. The remaining cases are perhaps less important but not less interesting since the abnormalities are a real challenge to the annealing model. In calculating these cases, we show that by extending the basic approach it is possible to generalize the model to predict more complex situations. It is also remarked that this model and the associated parameter set are universal in the sense that the same equations and parameters are used in the prediction of ordinary diffusion, proton enhanced diffusion, and the annealing of ion-implanted boron into silicon at room temperature.

H. Suggestions for Future Work

It is apparent that this annealing model enables the use of the accurately calculated as-implanted profiles in the calculation of annealing profiles for the case of boron implants at room temperature. In this manner, the device designer can make a better use of the range calculations that are available for a large number of impurity-substrate combinations. From this viewpoint, it seems reasonable to suggest that perhaps similar annealing models can be developed for other commonly used impurities.

Phosphorus and arsenic are the most commonly used n-type dopants in silicon. It is generally accepted that their diffusion in silicon is also governed by a vacancy mechanism. Furthermore, a large body of work on ordinary diffusion, diffusion anomalies, lattice location, and annealing behavior of ion implanted phosphorus and arsenic is available in the technical literature. It is therefore likely that a careful review of relevant experiments will yield key attributes for the diffusion and the annealing of these impurities. In this regard, perhaps the subject of possible interactions between impurities and charged vacancies should be examined. Then, with some basic assumptions, the simplest model with the most essential attributes should be formulated and solved. Undoubtedly, many iterations of the described sequence will be necessary, and the availability of the 'diffusion solver' from this work will be useful.

We wish to highlight some similarities and differences between the suggested study and the case of boron. The diffusion of phosphorus and arsenic exhibit high concentration and background doping effects. Consequently, it is likely that the Fermi level dependence comes from interactions of the impurity with negatively charged vacancies. It is also possible that more than one kind of impurity-vacancy complexes coexist in the substrate and their different diffusive attributes give rise to anomalies in the diffusion profile. Certainly, the most important difference between the boron and the phosphorus or arsenic cases is the damage that results from the implantation. The heavy phosphorus or arsenic ions produce extended damage clusters in the lattice as the ions come to rest. In these cases, the room temperature annealing rate is

insufficient, and the individual damage clusters will overlap, producing an amorphous layer. During annealing, the implanted impurity will anneal in both the amorphous and crystalline regions following different behaviors. Meanwhile, the amorphous layer will also anneal. The regrowth of amorphous silicon layers is also a complicated matter. Backscattering experiments [44] indicate that the regrowth rate is dependent on the crystallographic direction, and it is modified by the doping effects of impurities.

Perhaps the problem should be addressed in three phases. A first phase devoted to the ordinary diffusion of phosphorus and arsenic and the most important diffusion anomalies. A second phase dedicated to the study of the regrowth of amorphous Si layers. The outcome of this study will certainly be useful for the understanding of the annealing behavior of boron that is implanted at liquid nitrogen temperature. And, lastly, in the third phase, the results of the first and second phases can be combined to develop an annealing model capable of predicting impurity profiles in the presence of an amorphous layer produced by the implantation.

Appendix A

THE NUMERICAL INTEGRATION OF THE COUPLED DIFFUSION EQUATIONS

In Chapter II, we formulated the annealing model which consists of a set of nonlinearly coupled partial differential equations. We will describe now the numerical integration of this mathematical problem. The solution consists of two distinct steps. First, we transform the set of Partial Differential Equations (PDE) into a larger set of Ordinary Differential Equations (ODE), and then we use GEARB [45], a FORTRAN subroutine package, to integrate the system of ordinary differential equations.

1. The Transformation of Partial Differential Equations into Ordinary Differential Equations

To illustrate this transformation, we will use the three stream diffusion model described in Eq. (A1). This simpler case is chosen for the purpose of illustrating the problem with a minimum of algebraic complexities.

$$\frac{\partial C_B}{\partial t} = D_B \frac{\partial^2 C_B}{\partial x^2} - K_o \frac{C_B C_{V^+}}{\tau} + \frac{C_{BV}}{\tau} \tag{A1a}$$

$$\frac{\partial C_{V^+}}{\partial t} = D_{V^+} \frac{\partial^2 C_{V^+}}{\partial x^2} - K_o \frac{C_B C_{V^+}}{\tau} + \frac{C_{BV}}{\tau} - \frac{\left(C_{V^+} - C_{V^+_{eq}}\right)}{\tau_V} \tag{A1b}$$

$$\frac{\partial C_{BV}}{\partial t} = D_{BV} \frac{\partial^2 C_{BV}}{\partial x^2} + \underbrace{K_o \frac{C_B C_{V^+}}{\tau}}_{\text{nonlinear coupling}} - \frac{C_{BV}}{\tau} \tag{A1c}$$

In this system of PDE, the dependent variables are: the concentrations of electrically active boron ($C_B(x,t)$), positive vacancies ($C_B(x,t)$), and BV-pairs ($C_{BV}(x,t)$). Time and space are the independent variables in this problem. The transformation under consideration is based on the elimination of the spatial variable by:

(a) the discretization of the space in N partitions

(b) the definition of new dependent variables

(c) the formulation of the problem in terms of the new variables

For example, first, the x-axis is divided into 33 partitions of width Δx. Second, we define the concentrations of active boron, positive vacancies, and BV-pairs in each one of the 33 partitions as new variables. Since 3 variables are associated with each partition, and there are 33 partitions, the total number of new dependent variables is 99. It is convenient to define a vector $\dot{y}$ composed of the new dependent variables, as is illustrated in Table A1. We obtain the system of ODE in terms of the new variables by rewriting Eq. (A1) for each one of the 33 partitions and by approximating the second partial derivative with the central differences [16] in Eq. (A2).

$$\frac{\partial^2 C^c}{\partial x^2} \simeq \frac{C^l - 2C^c + C^r}{\Delta x} \tag{A2}$$

In this equation, the superscripts l, c, and r denote left, center, and right, respectively; Δx is the width of the partition. The central difference approximation in Eq. (A2) is indicating explicitly that the second partial derivative of the variable C at the central partition is only referenced to the same variable C at the same location and at adjacent locations (left and right). Following these instructions and using Table A1 to express the new variables in place of the old ones, we obtain Eq. (A3), the system of 99 coupled ordinary differential equations.

$$\dot{y}_{(1)} = -2K_1 y_{(1)} + K_1 y_{(1)} - Ky_{(1)}y_{(2)} + K'y_{(3)}$$

$$\dot{y}_{(2)} = (-2K_2 - K_V)\, y_{(2)} + K_{(2)}y_{(5)} - Ky_{(1)}y_{(2)} + K'y_{(3)} + K_V'$$

$$\dot{y}_{(3)} = (-2K_3 - K')\, y_{(3)} + K_{(3)}y_{(6)} + Ky_{(1)}y_{(2)}$$

$$i = (1, 2, \ldots, 31) \tag{A3}$$

$$\dot{y}(3i+1) = K_1 y(3i-2) - 2K_1 y(3i+1) + K_1 y(3i+1)$$
$$- Ky(3i+1)\, y(3i+2) + K' y(3i+3)$$

$$\dot{y}(3i+2) = K_2 y(3i-1) - (2K_2 + K_V)\, y(3i+2) + K_2 y(3i+5)$$
$$- Ky(3i+1)\, y(3i+2) + K' y(3i+3) + K'_V$$

$$\dot{y}(3i+3) = K_3 y(3i) - (2K_3 + K')\, y(3i+3) + K_3 y(3i+6)$$
$$- Ky(3i+1)\, y(3i+2)$$

$$\dot{y}(97) = K_1 y(94) - 2K_1 y(97) - K_1 y(97)\, y(98) + K' y(99)$$

$$\dot{y}(98) = K_2 y(95) - (2K_2 + K_V)\, y(98) - Ky(97)\, y(98) + K' y(99) + K'_V$$

$$\dot{y}(99) = K_3 y(96) - (2K_3 + K')\, y(99) + Ky(97)\, y(98) \qquad \text{(A3) Cont.}$$

where

$$K_1 = \frac{D_B}{\Delta x^2} \qquad K = \frac{\text{Eq. Const.}}{\tau} \qquad K' = \frac{1}{\tau}$$

$$K_2 = \frac{D_V}{\Delta x^2} \qquad K_V = \frac{1}{\tau_V}$$

$$K_3 = \frac{D_{BV}}{\Delta x^2} \qquad K'_V = \frac{C_{V^+_{eq}}}{\tau_V}$$

In Eq. (A3), we assumed, for the sake of simplicity, that the values of the variables is zero outside of the spatial range of interest. In principle, the ordering of the components in the vector $\vec{y}$ (Table A1) is arbitrary, and other definitions of $\vec{y}$ would yield equivalent sets of ordinary differential equations. However, as we analyze the

```
C------ DMG IS THE VACANCY CONCENTRATION PROFILE CALCULATED FROM
C--     THE DISTRIBUTION OF ENERGY DEPOSITED INTO ATOMIC PROCESSES.
C--     J.F.GIBBONS, PROC. OF THE 5TH INT.CONF. ON ION IMPL.,THOUSAND
C--     OAKS, CA. GORDON AND BREACH PUBLISHERS.
C--         THIS DISTRIBUTION CORRESPONDS TO A 10**15 DOSE, 70 KEV
C--     BORON IMPLANT.
      DATA DMG /2.45D21,2.65D21,2.93D21,3.35D21,3.9D21,4.6D21,
     1          5.6D21,6.3D21,6.2D21,5.4D21,4.5D21,3.55D21,
     2          2.5D21,1.48D21,8.D20,4.5D20,2.3D20,1.D20,
     3          4.9D19,2.3D19,1.12D19,5.4D18,2.5D18,1.2D18,
     4          5.D17,2.9D17,1.4D17,6.7D16,3.1D16,1.4D16,
     5          6.D15,3.D15,1.5D15/,CD/33*0.D+00/
      M = 33
C------ TC IS THE TEMPERATURE OF THE ANNEAL OR DIFFUSION IN DEG.C.
      TC = K(7)
      DO 5 I = 1,33
    5 CA(I) = Y(3*I-2)
      CALL SIMS(M,TC,CA,CD,ECI,EC,EF,CVEQ,DELVAC)
C-----------------------------------------------------------
      YDOT(1) = -2.D0*K(1)*Y(1) + K(1)*Y(4) * 1.85D+00
     1          - K(4)*Y(1)*Y(2) +Y(3)*K(6)
      YDOT(2) =(-2.D0*K(2))*Y(2)+K(2)*Y(5)+K(2)*CVEQ(33)
     1         -K(4)*Y(1)*Y(2)+Y(3)*K(6)
     2         -K(5)* (Y(2)- CVEQ(1))
     4          +DEXP(-T/K(8)) * DMG(1) / K(8)
      YDOT(3) = -(2.D0*K(3)+K(6))*Y(3)+1.85D+00*K(3)*Y(6)+K(4)*Y(1)*Y(2)
      DO 10 I= 1, 31
        YDOT(3*I+1) = K(1)*Y(3*I-2)-2.D0*K(1)*Y(3*I+1)+K(1)*Y(3*I+4)
     2   -K(4)*Y(3*I+1)*Y(3*I+2)+Y(3*I+3)*K(6)
        YDOT(3*I+2) = K(2)*Y(3*I-1)-(2.D0*K(2))*Y(3*I+2)
     1  +K(2) *Y(3*I+5) -K(4)*Y(3*I+1)*Y(3*I+2)+Y(3*I+3)*K(6)
     2          -K(5) * ( Y(3*I+2) - CVEQ(I+1) )
     4           +DEXP(-T/K(8)) * DMG(I+1) / K(8)
        YDOT(3*I+3) = K(3)*Y(3*I)-(2.D0*K(3)+K(6))*Y(3*I+3)
     1  + K(3)*Y(3*I+6) +K(4)*Y(3*I+1)*Y(3*I+2)
```

```
      W0(99) = 0.D+00
      WRITE(6,145) DOSE, DOSEB,ACTIV,FVAL
  145 FORMAT(5X,8H DOSE = ,1PD14.7,3X,14HBORON SUBS. = ,1PD14.7,
     1       5X,14H ACTIVITY = ,1PD10.3,
     2       5X,8H FVAL = ,1PD23.16//)
C OUTPUT THE RESULT OF THE INTEGRATION
C----- THE OUTPUT LIST THE CONCENTRATIONS OF BORON, POSITIVE VACANCY
C----- BORON-VACANCY PAIR AND TOTAL BORON IN EACH PARTITION IN SPACE
C----- IN INCREASING ORDER FROM LEFT TO RIGHT .
      WRITE(6,150) TOUT,XINC,  DEPTH, (Z0(I), I = 1,132)
  150 FORMAT(5X,8H TIME = ,1PD10.3,4H SEC,10X,13H INCREMENT = ,1PD10.3,
     1          3H CM,10X,9H DEPTH = ,1PD12.3,3H CM//
     2       3(3X,5HBORON,3X,7HVACANCY,3X,7HBV PAIR,3X,7HB TOTAL,4X)//
     3       11(1P4D10.3,1X,1P4D10.3,1X,1P4D10.3/)///)
      WRITE (6,153) ( W0(I), I = 1,99)
  153 FORMAT (3(3X,5H  XI ,3X,7H SMALL ,3X,7H  BIG  )//
     1        11(1P3D10.3,1X,1P3D10.3,1X,1P3D10.3/)///)
      GO TO 105
  160 WRITE(6,170)  NSTEP,NFE,NJE
  170 FORMAT(//21H PROBLEM COMPLETED IN,I5,6H STEPS/
     1          21X,I5,14H F EVALUATIONS/
     2          21X,I5,14H J EVALUATIONS///)
  180 STOP
      END
      SUBROUTINE DIFFUN (N,T,Y,YDOT,K)
C USER SUPPLIED SUBROUTINE FOR GEAR B. K(1),K(2),K(3) ARE
C  SCALED DIFFUSION COEFFICIENTS. K(5) IS THE 1/VAC.LIFETIME
C  K(6)= 1/TIME CONSTANT, AND K(4) IS THE EQUILIBRIUM CONSTANT
C  DIVIDED BY THE TIME CONSTANT. K(7) IS THE TEMPERATURE IN
C  DEGRES CELCIUS AND K(8) IS THE TIME CONSTANT ASSOCIATED
C  WITH THE RELEASE OF VACANCIES FROM THE DAMAGE REGION.
      DOUBLE PRECISION T,Y,YDOT,K(1),DMG(33),TC,CA(33),CD(33),
     1                 ECI,EC(33),EF(33),CVEQ(33),DELVAC(33)
      INTEGER N
      DIMENSION Y(N),YDOT(N)
```

```
C ----     COMMON /GEAR5/ SAVE2(NMX)
C ----     COMMON /GEAR7/ IPIV(NMX)
C ----     -----
C ----     DIMENSION Y(NMX,13)
C ---- THE DIMENSION IN COMMON BLOCK GEAR6 IS CURRENTLY
C ---- SET TO 3100 = (2 ML + MU + 1) * N , IF THIS NUMBER
C ---- IS TO BE CHANGED TO A NUMBER NWMX, THEN THIS
C ---- DECLARATION SHOULD READ:
C ----     COMMON /GEAR6/ PW(NWMX)
C ---- ------------------------------------------------
      IF (INDEX.GE.0) GO TO 135
      WRITE(6,130) INDEX
  130 FORMAT(//26H ERROR RETURN WITH INDEX =,I3//)
      GO TO 160
C-----------------------SORT Y0  ----------------------
C----- THE VECTOR Z0 CONTAINS THE CONCENTRATIONS OF SUBSTITU-
C----- TIONAL BORON, POS. VACANCIES, BV-PAIRS AND TOTAL BORON.
  135 DO 140 I = 1,33
       Z0(4*I-3) = Y0(3*I -2)
       Z0(4*I-2) = Y0(3*I- 1)
       Z0(4*I-1) = Y0(3*I)
       Z0(4*I)   = Z0(4*I-3) + Z0(4*I-1)
       W0(3*I-2) = Z0(4*I-1)/Z0(4*I)
       FVAL = FVAL +((SIMS(I)-Z0(4*I))/1.D+18)**2
       DOSEB =  DOSEB + Z0(4*I-3)  * XINC
  140  DOSE =  DOSE + Z0(4*I) * XINC
      ACTIV =( DOSEB/DOSE ) * 100.D+00
C----- THE VECTOR W0 CONTAINS AUXILIARY RESULTS. THE USER MAY
C----- WISH TO MODIFY OR DELETE THEM.
      DO 142 I= 2,32
       W0(3*I-1) = ( W0(3*I+1) - W0(3*I-5) ) * Z0(4*I)
  142  W0(3*I)   = W0(3*I-2) * ( Z0(4*I+4) - Z0(4*I-4) )
      W0(2) = 0.D+00
      W0(3) = 0.D+00
      W0(98) = 0.D+00
```

```
      IF(TOUT.EQ.0.D00) GO TO 160
      IF (TOUT.EQ.1.D00) GO TO 35
      IF (TOUT.EQ.2.D00) GO TO 25
      DOSE = 0.D00
        SEB = 0.D+00
      FVAL = 0.D+00
      CALL ERRSET(208,256,-1,1)
      CALL DRIVEB(N,T0,H0,Y0,TOUT,EPS,MF,INDEX,ML,MU,PRN)
C ---- GEARB IS MODIFIED TO PASS THE PARAMETERS IN PRN TO THE
C----- SUBROUTINES DIFFUN AND PDB.
C ---- THE MODIFICATIONS CONSIST IN THE ADDITION OF THE VECTOR
C ---- PRN IN THE FOLLOWING SUBROUTINE, CALL AND DIMENSION
C ---- STATEMENTS:
C ---- SUBROUTINE DRIVEB(N,T0,H0,Y0,TOUT,EPS,MF,INDEX,ML,MU,PRN)
C ----  DOUBLE PRECISION PRN(1)
C ----  CALL STIFFB(Y, N0, PRN)
C ---- SUBROUTINE STIFFB(Y, N0, PRN)
C ----  DOUBLE PRECISION PRN(1)
C ----  CALL DIFFUN (N,T,Y,SAVE1,PRN)
C ----  CALL DIFFUN (N,T,Y,SAVE2,PRN)
C ----  CALL PSETB(Y, N0, CON, MITER, IER, PRN)
C ----  CALL DIFFUN (N,T,PW,SAVE1,PRN)
C ----  CALL DIFFUN (N,T,SAVE1,SAVE2,PRN)
C ---- SUBROUTINE PSETB(Y, N0, CON, MITER, IER, PRN)
C ----  DOUBLE PRECISION PRN(1)
C ----  CALL PDB (N,T,Y,PW,N0,ML,MU,PRN)
C ----  CALL DIFFUN (N,T,Y,SAVE1,PRN)
C ---- ------------------------------------------
C ---- THE MAXIMUM VALUE OF N IS CURRENTLY SET TO 100.
C ---- IF THIS NUMBER IS TO BE CHANGED TO A NUMBER NMX,
C ---- THEN THE DECLARATIONS IN DRIVEB SHOULD READ AS
C ---- AS FOLLOWS:
C ----     COMMON /GEAR2/ YMAX(NMX)
C ----     COMMON /GEAR3/ ERROR(NMX)
C ----     COMMON /GEAR4/ SAVE1(NMX)
```

```
C-----  THE PARAMETERS ARE DESCRIBED IN THE FORMAT STATEMENT 80
 60    READ(5,70)(X(I),I = 1,8)
 70    FORMAT( 4D10.3)
C-START AT COL 1 >+4.000D+00 8.000D+00 1.200D+01 NEXT CARD
C--PARAMETERS 'ECHO INPUT PARAMETERS TO OUTPUT'
       WRITE(6,80)  (X(I),I = 1,8)
 80    FORMAT(10X,11H PARAMETERS//
     1         5X,23H DIFF.COEF.(BORON)    = ,1PD10.3,10H CM**2/SEC/
     2         5X,23H DIFF.COEF.(VACANCY)  = ,1PD10.3,10H CM**2/SEC/
     3         5X,23H DIFF.COEF.(BV PAIR)  = ,1PD10.3,10H CM**2/SEC/
     4         5X,23H EQUIL.CONS.(B+V=BV)  = ,1PD10.3,6H CM**3/
     5         5X,23H REACTION TIME CONST  = ,1PD10.3,4H SEC/
     6         5X,23H VACANCY LIFETIME     = ,1PD10.3,4H SEC/
     7         5X,23H TEMPERATURE          = ,1PD10.3,6H DEG.C/
     8         5X,23H DAMAGE TIME CONSTANT =,1PD10.3,4H SEC///)
C-PARAMETER NORMALIZATION
       DO 90 I = 1,3
 90     PRN(I) = X(I) / ( XINC**2)
       PRN(4) = X(4)/X(5)
       PRN(5) = 1/ X(6)
       PRN(6) = 1/ X(5)
       PRN(7) = X(7)
       PRN(8) = X(8)
C--OUTPUT THE MODIFIED PARAMETERS USED IN DIFFUN AND PDB
       WRITE ( 6,100) (PRN(I),I = 1,8)
 100   FORMAT(53H MODIFIED PARAM. OF DIM. 1/SEC USED IN PROGRAM PRN(7)//
     1        1P8D10.3///)
C ---------------------- READ  TIMES  -------------------
C--EXAMPLE: START AT COLUMN #1 >+1.000D+00 NEXT CARD
C--THE LAST TIME IS AN INTEGER FLAG:
C       TOUT = 0  EXIT
C       TOUT = 1  CHANGE PARAMETER SET
C       TOUT = 2  CHANGE INITIAL PROFILES.
 105   READ(5,110)  TOUT
 110   FORMAT (D10.3)
```

```
 30   FORMAT(3D10.3)
C--EXAMPLE: START AT COLUMN #1 >+1.000D+00 2.000D+00 3.000D+00 NEXT
C----------CONSTRUCT Y0, THE INPUT VECTOR FOR DRIVEB,IN GEARB
C-----  DOSE,DOSEB ARE THE TOTAL BORON DOSE AND THE DOSE
C                  OF ACTIVE BORON IN #/CM**2
C------ ACTIV IS THE ELECTRICAL ACTIVITY IN PERCENT
C------ FVAL - A COST FUNCTION CALCULATED FROM THE COMPARISON
C       OF THE CALCULATED TOTAL BORON PROFILE WITH THE DESIRED
C       PROFILE.
C-----  H0 - STEP SIZE TO BE ATTEMTED FOR THE FIRST TIME
C-----  EPS - THE LOCAL ERROR TOLERANCE PARAMETER(SEE GEARB)
C-----  INDEX - AN INTEGER FLAG. FOR THE FIRST CALL: INDEX=1
 35   DOSE = 0.D00
      DOSEB = 0.D+00
      ACTIV = 0.D+00
      FVAL = 0.D+00
C----- CONSTRUCTION OF THE INPUT VECTOR Y0 FOR DRIVEB USING
C----- THE INITIAL CONDITIONS. THE VALUE ASSIGNED TO Y0(3*I-1)
C----- IS THE EQUILIBRIUM CONCENTRATION OF POSITIVE VACANCIES
C----- IN INTRINSIC SILICON AT 900 C.
      DO 40 I= 1,33
       Y0(3*I-2)=0.D+00
       Y0(3*I-1) = 1.250D+11
       Y0(3*I)   = B0(I)
 40    DOSE = DOSE + ( B0(I) + BV0(I) ) * XINC
      WRITE(6,145) DOSE, DOSEB, ACTIV
      H0=1.D-14
      EPS=1.D-4
      INDEX=1
C--ECHO INPUT TO OUTPUT ------Y0------
      WRITE(6,50) (Y0(I),I=1,99)
 50   FORMAT(10X,17H INITIAL PROFILES//
     2       3(5X,5HBORON,5X,7HVACANCY,5X,7HBV PAIR,5X)//
     3       11(1P3D12.3,1X,1P3D12.3,1X,1P3D12.3/)///)
C-----------------------READ PARAMETERS-------------------
```

```
      COMMON/GEAR9/HUSED,NQUSED,NSTEP,NFE,NJE
C-----------------------INITIALIZATION--------------------
C-----    XINC ------ SPATIAL INCREMENT IN CM.
C-----    N    ------ NUMBER OF POINTS = # SPECIES * # OF INCREMENTS
C-----    T0   ------ INITIAL VALUE OF TIME T IN SECONDS
C-----    MF   ------ BACKWARD DIFFERENTIATION FORMULA METHOD
C                     FOR THE INTEGRATION.
C-----    ML,MU ----- BAND-WIDTHS IN THE JACOBIAN MATRIX
C-----    DEPTH ----- NUMBER OF PARTITIONS * XINC
      XINC= 2.0D-6
      N=99
      T0=0.D00
      MF=21
      ML=3
      MU=3
      DEPTH =(33.0D00) * (XINC)
C------------------- READ DATE OF RUN ---------------------
      READ(5,10) MONTH ,DAY, YEAR
 10   FORMAT(I2,1X,I2,1X,I4)
C--EXAMPLE: START AT COL 1:03 12 1976
C---------------------- LABELS  --------------------------
      WRITE(6,20)  MONTH,DAY,YEAR
 20   FORMAT(39H BORON VACANCY PAIR DIFFUSIVE ANNEALING///
     1       10X,10H RUN#-----,10X,7H DATE : ,I2,1X,I2,1X,I4,
     2       10X,20H 3-STREAM DIFF.MODEL///)
C-------READ INITIAL PROFILES---------
C----- THE INITIAL CONCENTRATION PROFILES ARE IN #/CM**3
C--    B0 ------  THE AS IMPLANTED BORON PROFILE, OR A
C--               DIFFUSED PROFILE
C--    SIMS ----  THE TOTAL BORON PROFILE WE WISH TO COMPARE WITH
C--    THE USER CAN INPUT THE INITIAL PROFILES FOR THE POS.
C--    VACANCIES AND THE SUBSTITUTIONAL BORON BY MODIFYING
C--    READ STATEMENT NUMBER 25.
C---I WILL ALWAYS USE UNIFORM FORMAT D10.3 FOR ALL DOUBLE PRES.
 25   READ(5,30) ( B0(I), I = 1,33),(SIMS(I), I=1,33)
```

```
C-----   THIS IS A GENERAL PURPOSE VERSION OF THE 3-STREAM
C----- DIFFUSION MODEL FOR BORON IN SILICON. THE MODEL IS
C----- COMPOSED OF A MAIN PROGRAM AND 3 SUBROUTINES: DIFFUN,
C----- PDB AND SILS. DIFFUN IS THE SYSTEM OF ORDINARY DIFFE-
C----- RENTIAL EQUATIONS ASSOCIATED WITH THE DIFFUSION OF B.
C----- PDB CONTAINS THE NON-ZERO ELEMENTS OF THE JACOBIAN MA-
C----- TRIX. AND SILS IS A SUBROUTINE FOR THE CALCULATION OF
C----- THE FERMI-LEVEL AND CARRIER CONCENTRATIONS.
C-----    THIS GROUP OF SUBROUTINES IS INTENDED TO BE USED IN
C----- CONJUNCTION WITH GEARB, A SUBROUTINE PACKAGE FOR THE
C----- SOLUTION OF SYSTEMS OF ORD.DIFFERENTIAL EQ. WITH BANDED
C----- JACOBIAN, BY A.C.HINDMARSH (LAWRENCE LIVERMORE LAB,
C----- U.C. LIVERMORE, CA. MARCH 1975.
C-----     THE INPUTS TO THE DIFFUSION MODEL ARE: THE AS-
C----- IMPLANTED B PROFILE, A SIMS PROFILE THE USER WISHES
C----- TO APPROXIMATE, THE PARAMETERS AND THE TIMES AT WHICH
C----- THE OUTPUT ARE DESIRED. THE PRIMARY DAMAGE PROFILE IS
C----- ALSO REQUIRED IN THE DATA STATEMENT IN DIFFUN, IF THE
C----- PROBLEM IS AN ANNEAL OR A PROTON ENHANCED DIFFUSION.
C----- FOR THE CASE OF AN ORDINARY DIFFUSION THE DAMAGE
C----- PROFILE CAN BE REPLACED BY THE EQUILIBRIUM VACANCY
C----- CONCENTRATION OR ALTERNATIVELY, THE TIME CONSTANT
C----- ASSOCIATED WITH THE DAMAGE CAN BE SET TO A VERY LARGE
C----- VALUE,10D8 SECONDS.
C--------------DECLARATIONS--------------
      DOUBLE PRECISION B0(33),V0(33),BV0(33),
     1    BT(33),Z0(132), DEPTH,XINC,X(8),Y0(99),PRN(8),TOUT,TIME,TLAST,
     2    T0, H0, EPS, HUSED, DOSE, DOSEB,ACTIV,FVAL,SIMS(33),W0(99)
      INTEGER MONTH,DAY,YEAR,
     1        N, MF, INDEX, ML, MU, NQUSED, NSTEP, NFE,NJE
```

The user should send a blank magnetic tape, together with character, channel, and density specifications, and ask for the appropriate version of GEARB. For a complete description of GEARB and the user's instructions, the reader is referred to Ref. 45.

problems in which the stiffness is apparent, the use of the backward differentiation formula with the user supplied Jacobian is more efficient. The annealing problem falls into this category. In other problems, where the stiffness is only apparent in the later stage of the integration, it is possible to change the method of integration during the computation. The user need only to specify the initial step size of the integration. Thereafter, the package adjusts the step-size according to the error incurred in the integration. The communication with GEARB is performed through the subroutine DRIVEB by means of a CALL statement. The user supplies a MAIN PROGRAM and two subroutines: DIFFUN and PDB. The main program controls the input-output, initializes variables, selects the options, and performs the communication with DRIVEB. DIFFUN defines the system of ordinary differential equations [Eq. (A3)] and PDB is the Jacobian [Eq. (A6)] stored by diagonal lines. In the event that the Jacobian cannot be coded, it is possible to select an option that generates the Jacobian internally. The penalty associated with this option is, of course, a loss in efficiency. In our case, the sample codes that we list in the next section do contain the user supplied Jacobian.

It is apparent from this outline that the interface with GEARB has a modular structure. The definition of the mathematical problem is coded in DIFFUN and PDB, and the adaptation of the mathematical formulation to the particular problem is accomplished in the main program. For these reasons, the potential user will find that DIFFUN and PDB are of immediate use; however, he may wish to modify the main program, to alter the width of the partition, the step-size, the error control, etc., to suit his particular problem. In Section 3, we include the listing of the three stream diffusion model and the complete annealing model. GEARB is available in both single and double precision versions from:

Argonne Code Center
Argonne National Laboratory
9700 South Cass Avenue
Argonne, Illinois 60439
Telephone: (312) 739-7711, Ext. 1366

Schematically, the nonzero elements of the Jacobian are represented by 'x' in Table A2. And, the banded structure of this matrix is apparent.

Table A2

NONZERO ELEMENTS OF THE JACOBIAN

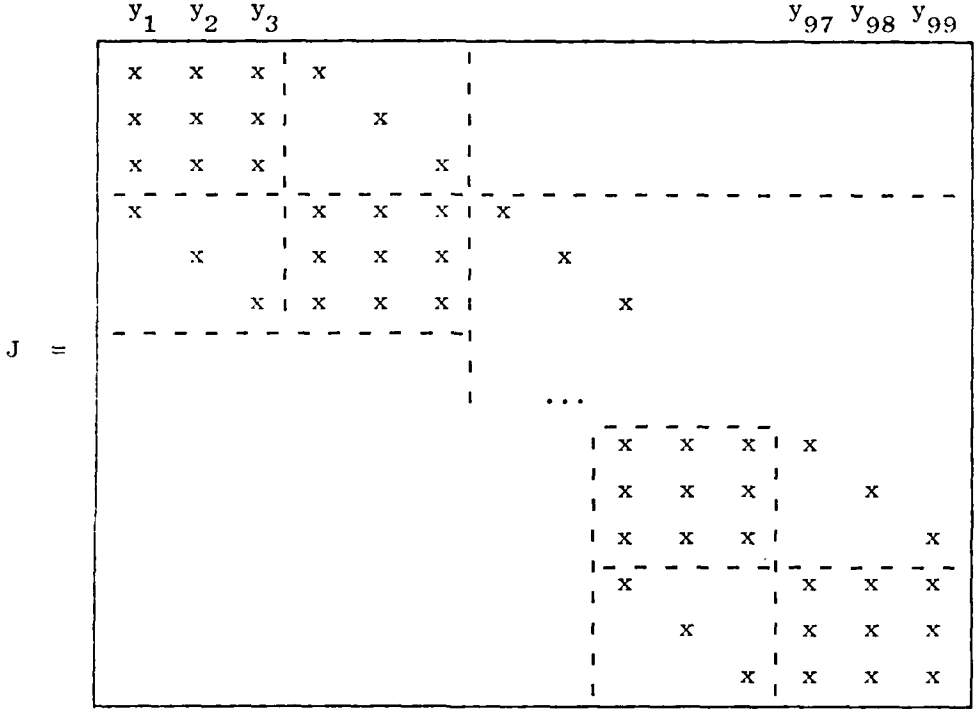

2. The Solution of the System of Ordinary Differential Equations

The numerical integration of the system of ordinary differential equations is performed on a digital computer using GEARB [15], a FORTRAN subroutine package. GEARB is composed of seven subroutines designed to solve systems of ordinary differential equations in which the Jacobian has a banded structure. This structure allows the storing of the elements of the Jacobian by diagonal lines, hence saving storage and computation time. The package offers several options with regard to the method of integration. For instance, the Adams method with functional iteration is recommended for nonstiff problems. On the other hand, for

$$J(3i + 1,3i + 3) = K'$$

$$J(3i + 1,3i - 2) = \begin{cases} 0 & i = 0 \\ K_1 & i > 0 \end{cases}$$

$$J(3i + 2,3i + 1) = -Ky(3i + 2)$$

$$J(3i + 2,3i + 2) = -2K_2 - Ky(3i + 1) - K_V$$

$$J(3i + 2,3i + 3) = K'$$

$$J(3i + 1,3i + 4) = \begin{cases} K_1 & i = 32 \\ 0 & i < 32 \end{cases}$$

$$J(3i + 2,3i + 5) = \begin{cases} K_2 & i < 32 \\ 0 & i = 32 \end{cases}$$

$$J(3i + 2,3i - 1) = \begin{cases} K_2 & 0 < i \\ 0 & i = 0 \end{cases}$$

$$J(3i + 3,3i + 1) = Ky(3i + 2)$$

$$J(3i + 3,3i + 2) = Ky(3i + 1)$$

$$J(3i + 3,3i + 3) = -2K_3 - K'$$

$$J(3i + 3,3i + 6) = \begin{cases} K_3 & i \quad 32 \\ 0 & i = 32 \end{cases}$$

$$J(3i + 3,3i) = \begin{cases} K_3 & i > 0 \\ 0 & i = 0 \end{cases}$$

(A6)
Cont.

Jacobian of the system, it will be apparent that this particular ordering of species in partitions does produce a set of ODE with a banded Jacobian in which the width o the band is small. And, such a system can be solved very efficiently since it does not require the storage of elements outside of the band.

It is more concise and convenient to use the vector notation in the description of the system of ordinary differential equations. For instance, Eq. (A3) can be expressed as:

$$\dot{y}_i = f_i(y_1, \ldots, y_j, \ldots, y_N) \qquad i(1, \ldots, N) \tag{A4}$$

where N is 99 in our example.

The Jacobian of the set of ordinary differential equations in Eq. (A4) has elements J_{ij} given by:

$$J_{ij} = \frac{\partial f_i}{\partial y_j} \tag{A5}$$

Hence,

$$J_{11} = -2K_1 - Ky(2) = \partial f_1/\partial y_1$$

$$J_{12} = -Ky(1) = \partial f_1/\partial y_2$$

$$J_{13} = K' = \partial f_1/\partial y_3$$

$$J_{14} = K_1 = \partial f_1/\partial y_4$$

$$\vdots \qquad \text{etc.}$$

And, in general, the nonzero elements of J are for $i = (0 \ldots 32)$:

$$J(3i + 1,3i + 1) = -2K_1 - Ky(3i + 2)$$

$$J(3i + 1,3i + 2) = -Ky(3i + 1) \tag{A6}$$

Table A1

DEFINITION OF THE VECTOR $\vec{y} = (y_1 \ \ldots \ y_{99})$

$$\dot{y}_i = f(y_1 \ \ldots \ y_{99}) \qquad i = (1 \ \ldots \ 99)$$

Partition	1			2			3			...	i			...	33		
Specie	B	V	BV	B	V	BV	B	V	BV	...	B	V	BV	...	B	V	BV
Concentration	$y_{(1)}$	$y_{(2)}$	$y_{(3)}$	$y_{(4)}$	$y_{(5)}$	$y_{(6)}$	$y_{(7)}$	$y_{(8)}$	$y_{(9)}$		$y_{(3i-2)}$	$y_{(3i-1)}$	$y_{(3i)}$		$y_{(98)}$	$y_{(98)}$	$y_{(99)}$

```
   10 CONTINUE
      YDOT(97) =K(1)*Y(94) -2.D0*K(1)*Y(97) + K(1) * 5.D+16
     1           -K(4)*Y(97)*Y(98)+Y(99)*K(6)
      YDOT(98)=K(2)*Y(95)-(2.D0*K(2))*Y(98)+K(2)*CVEQ(33)
     1          -K(4)*Y(97)*Y(98)+Y(99)* K(6)
     2           -K(5) * ( Y(98) - CVEQ(33) )
     4            +DEXP(-T/K(8)) * DMG(33) / K(8)
      YDOT(99) = K(3)*Y(96)-(2.D0*K(3)+K(6))*Y(99) +K(3)*5.D+14
     1            +K(4)*Y(97)*Y(98)
      RETURN
      END
      SUBROUTINE PDB(N,T,Y,PD,N0,ML,MU,K)
C-------------------------------------------------------------
C USER SUPPLIED SUBROUTINE FOR GEARB-ANALYTICAL JACOBIAN
C K(1),,K(2),K(3),ARE SCALED DIFFUSION COEFFICIENTS.K(5) IS THE
C INVERSE OF THE VACANCY LIFETIME. K(6) IS THE INVERSE OF THE
C REACTION TIME CONSTANT. K(4) IS THE EQUILIBRIUM CONSTANT DIVIDED
C BY THE REACTION TIME CONSTANT. K(7) IS THE TEMPERATURE IN DEG.
C CELCIUS. K(8) IS THE TIME CONSTANT ASSOCIATED WITH THE RELEASE
C OF VACANCIES FROM THE DAMAGE REGION.
C-------------------------------------------------------------
      DOUBLE PRECISION T, Y, PD, K(1),TC,CA(33),CD(33),
     1                 ECI,EC(33),EF(33),CVEQ(33),DELVAC(33)
      INTEGER N, N0,ML,MU
      DIMENSION Y(N),PD(N0,7)
      M = 33
C----- TC IS THE TEMPERATURE OF THE ANNEAL OR DIFFUSION IN DEG.C.
      TC = K(7)
      DO 5 I = 1,33
 5    CA(I) = Y(3*I-2)
      CALL SILS(M,TC,CA,CD,ECI,EC,EF,CVEQ,DELVAC)
      DO 10 I = 1, 97, 3
       PD(I,1) = K(1)
       PD(I,2) = 0
       PD(I,3) = 0
```

```
      PD(I,4) = -2.D0*K(1)-K(4)*Y(I+1)
      PD(I,5) = -K(4)*Y(I)
      PD(I,6) = K(6)
      PD(I,7) = K(1)
C THE ELEMENTS ABOVE WERE FOR THE FIRST SPECIE (BORON)
      PD(I+1,1) = K(2)
      PD(I+1,2) = 0
      PD(I+1,3) = -K(4)*Y(I+1) -K(5)*DELVAC((I+2)/3)
      PD(I+1,4) = -2.D0*K(2)-K(4)*Y(I)-K(5)
      PD(I+1,5) = K(6)
      PD(I+1,6) = 0
      PD(I+1,7) = K(2)
C THE ELEMENTS ABOVE ARE FOR THE SECOND SPECIE (VACANCY)
      PD(I+2,1) = K(3)
      PD(I+2,2) = K(4)*Y(I+1)
      PD(I+2,3) = K(4)*Y(I)
      PD(I+2,4) = -2.D0*K(3)-K(6)
      PD(I+2,5) = 0
      PD(I+2,6) = 0
      PD(I+2,7) = K(3)
C THE ELEMENTS ABOVE WERE FOR THE THIRD SPECIE(BV-PAIR)
   10 CONTINUE
      PD(1,7) = 1.85D+00 * K(1)
      PD(2,7) = 1.D+00 * K(2)
      PD(3,7) = 1.85D+00 * K(3)
      RETURN
C RECALL THAT THE UNUSED LOCATIONS IN PD,GIVEN BY
C I - ML <=J <=0  AND N< J <= I+MU, CAN BE FILLED
C ARBITRARILY. THIS SUBROUTINE IS TO BE USED WITH
C MITER = 1.
      END
      SUBROUTINE SILS(N,TC,CA,CD,ECI,EC,EF,CVEQ,DELVAC)
C-----THIS SUBROUTINE IS FOR SILICON,INPUT PARAMETERS ARE:
C-----      N ------------- # OF POINTS
C-----     TC ------------- TEMP. IN DEG.CELSIUS
```

```
C-----     CA ------------- ACCEPTOR IMPURITY CONCENTRATION
C-----     CD ------------- DONOR IMPURITY CONCENTRATION
C-----     OUTPUT PARAMETERS ARE:
C-----     ECI ------------ INTRINSIC CARRIER CONC,
C-----     EC ------------- MAJORITY CARRIER CONC,
C-----     EF ------------  FERMI LEVEL IN E.V. FROM THE
C-----                      MAJORITY BAND EDGE.
C-----    CVEQ IS THE EQUILIBRIUM CONC OF SINGLY CAHARGED VAC.
C-----    DELVEQ IS THE PARTIAL DERIVATIVE OF CVEQ RESPECT TO THE
C-----           IMPURITY CONCENTRATION
      IMPLICIT REAL*8(A-H,O-Z)
      DIMENSION CA(N),CD(N),EC(N),EF(N),CVEQ(N),DELVAC(N)
C-----  'ED' AND 'EA' ARE THE ENERGY LEVELS OF DONORS AND ACCEPTORS
      ED = 0.046D+00
      EA = 0.045D+00
C------TK IS THE TEMPERATURE IN DEGREES KELVIN.
      TK = TC + 2.7316D+02
C----- QVEQ  IS THE ACTIVATION ENERGY OF FORMATION OF VACANCIES
      QVEQ = 3.4D+00
C----- PEX  IS THE PRE-EXPONENTIAL FACTOR OF THE FORMATION OF VAC.
      PEX  = 5.D+25
C----- THE FOLLOWING ARE THE ENERGY LEVELS OF THE SINGLY CHARGED
C----- VACANCIES IN THE BAND-GAP REFERRED TO THE RESPECTIVE BAND-
C----- EDGES. P AND N STAND FOR POSITIVE AND NEGATIVE CHARGE-STATES.
      EVP = 3.557D-01
      EVN = 5.557D-01
C------ECI, FROM MORIN & MAITA
      ECI = 3.88D+16 * (TK ** 1.5D+00) * DEXP(-6.05D-01/(8.62D-05*TK))
      DO 10 I=1,N
      IF (CA(I).GE.CD(I)) GO TO 5
C-----  PARAMETERS FOR N-TYPE
      EV = EVN
       DSC = 5.421978D+15 * ( TK**1.5D+00)
       ECT = 2.D+00 * DSC * (CD(I)-CA(I)) / ( DSC+2.7D-01
     1           * (CD(I)-CA(I)) + 5.D-01 *CA(I) *DEXP(ED/(8.62D-05
```

```
     2           *TK))+ DSQRT((DSC - 2.7D-01 *(CD(I)-CA(I)) +
     3           5.D-01 * CA(I) * DEXP( ED/ (8.62D-05 * TK)))**2.D+00
     4           + 4.D+00 *5.D-01 *(DSC-2.7D-01*CA(I))*(CD(I)-CA(I))
     5           * DEXP(ED/(8.62D-05*TK))))
       IF (CA(I).LE.CD(I)) GO TO 9
C-----  PARAMETERS FOR P-TYPE
 5     EV = EVP
       DSC = 2.0163964D+15 * (TK ** 1.5D+00)
        ECT = 2.D+00 * DSC * (CA(I)-CD(I)) / ( DSC+2.7D-01
     1           * (CA(I)-CD(I)) + 2.D+00 *CD(I) *DEXP(EA/(8.62D-05
     2           *TK))+ DSQRT((DSC - 2.7D-01 *(CA(I)-CD(I)) +
     3           2.D+00 * CD(I) * DEXP( EA/ (8.62D-05 * TK)))**2.D+00
     4           + 4.D+00 *2.D+00 *(DSC-2.7D-01*CD(I))*(CA(I)-CD(I))
     5           * DEXP(EA/(8.62D-05*TK))))
 9      EC(I) = ECT/ 2.D+00 + DSQRT( ((ECT)/2.D+00)**2.D+00
     1                                + (ECI**2.D+00) )
       EF(I) = + 8.62D-05 * TK * DLOG( (DSC/EC(I)) -2.7D-01)
       CVEQ(I) = PEX * DEXP( -QVEQ/ (8.62D-05*TK))
     1        * DEXP( (EV-EF(I))/(8.62D-05*TK) )
 10    DELVAC(I) = CVEQ(I) * DSC* (1 + ECT/DSQRT(
     1             ( ECT/2.D+00)**2.D+00+(ECI**2.D+00)))
     2            / ( 2.D+00 * EC(I)*EC(I) * ( DSC/EC(I) - 2.7D-01))
       RETURN
       END
```

```
C-- THIS IS A GENERAL PURPOSE VERSION OF THE FOUR SPECIES DIFFUSION
C-- MODEL. THIS MODEL IS IN ESSENCE THE THREE STREAM DIFFUSION
C-- MODEL EXTENDED TO INCLUDE THE ANOMALIES ASSOCIATED WITH HIGH
C-- DOSE IMPLANTS AND LOW ANNEALING TEMPERATURES. THE NEW SPECIES
C-- IS THE IMMOBILE BORON WHICH IS ELECTRICALLY INACTIVE.  THIS
C-- MODEL IS COMPOSED OF A MAIN PROGRAM AND 3 SUBROUTINES: DIFFUN
C-- FUN AND SILS. THE STRUCTURE AND USAGE OF THIS CODE  IS COMPLETELY
C-- ANALOGOUS TO THE PRECEDING EXAMPLE. FOR THIS REASON WE ADVISE
C-- THE USER TO STUDY FIRST THE CODE FOR THE THREE STREAM DIFFUSION
C-- MODEL WHICH IS SIMPLER, AND THEN EXAMINE THIS CODE WHICH IS MORE
C-- COMPLEX BECAUSE OF THE ADDITIONAL INTERACTION TERMS AMONG THE
C-- SPECIES. THE NUMBER OF SPATIAL PARTITIONS IN THIS EXAMPLE IS 30,
C-- AND THERE ARE 4 SPECIES IN EACH PARTITION. CONSEQUENTLY THE NUMBER
C-- OF POINTS IS N=120.  IN GEARB THE MAXIMUM NUMBER OF POINTS IS
C-- PRESET TO 100,THEREFORE IT IS NECESSARY TO PERFORM THE MODIFICATIONS
C-  TO GEARB INDICATED IN THE COMMENT CARDS IN THE PRECEEDING EXAMPLE.
C-------------------------------------------------------------------
C---------------DECLARATIONS--------------
      IMPLICIT REAL*8(A-H,O-Z)
      INTEGER  MONTH,DAY,YEAR
      DOUBLE PRECISION B0(30),V0(30),BV0(30),
     1    Z0(120),Y0(120),SIMS(30),X(12),PRN(12)
      COMMON/GEARB/NUSED,NQUSED,NSTEP,NFE,NJE
C -- THIS IS THE SIMS PROFILE CORRESPONDING TO THE 70KEV BORON IMPLANTED
C -- TO THE DOSE OF 10D14 AND ANNEALED AT 800 C FOR 35MIN.(XINC=2.D-6CM)
      DATA SIMS/1.2D18,1.4D18,1.7D18,2.1D18,2.5D18,2.7D18,
     1          2.8D18,3.D18,3.3D18,3.9D18,4.85D18,5.2D18,
     2          4.75D18,4.15D18,3.55D18,3.D18,2.5D18,2.15D18,
     3          1.87D18,1.62D18,1.43D18,1.18D18,9.2D17,7.6D17,
     4          6.1D17,4.9D17,3.85D17,3.D17,2.3D17,1.7D17/
```

```
C------------------------INITIALIZATION----------------------
C -- THE LIST OF SYMBOLS IS GIVEN IN THE PRECEEDING EXAMPLE.
      XINC= 4.0D-6
      N=120
      T0=0.D00
      MF=21
      ML=4
      MU=4
      DEPTH =(30.0D00) * (XINC)
C-------------------- READ DATE OF RUN --------------------
      READ(5,10) MONTH ,DAY, YEAR
 10   FORMAT(I2,1X,I2,1X,I4)
C--EXAMPLE: START AT COL 1:03 12 1976
C------------------------   LABELS   --------------------------------
      WRITE(6,20)  MONTH,DAY,YEAR
 20   FORMAT(39H BORON VACANCY PAIR DIFFUSIVE ANNEALING///
     1        10X,10H RUN#_____,10X,7H DATE : ,I2,1X,I2,1X,I4,
     2        10X,20H FOUR SPECIES MODEL ///)
C-------READ INITIAL PROFILES---------
C -- THE INITIAL CONCENTRATION PROFILES ARE IN #/CM**3
C -- IN THIS PARTICULAR EXAMPLE THE INPUT PROFILE REQUESTED IS EITHER
C -- THE AS-IMPLANTED BORON PROFILE OR A DIFFUSED PROFILE TO BE USED AS
C -- THE INITIAL BORON VACANCY PROFILE. IN GENERAL, THE USER MAY WISH
C -- TO INPUT THE INITIAL PROFILES FOR EACH OF THE SPECIES. IF THIS IS
C -- CASE, THE READ STATEMENT NUMBER 25 SHOULD BE MODIFIED.
C---I WILL ALWAYS USE UNIFORM FORMAT D10.3 FOR ALL DOUBLE PRES.
 25   READ(5,30) ( B0(I), I = 1,30)
 30   FORMAT(3D10.3)
C -- EXAMPLE: START AL COLUMN #1 >+1.000D+00 2.000D+00 3.000D+00
C----------MAKE Y0
 35   DOSE = 0.D00
      DOSEB = 0.D+00
      ACTIV = 0.D+00
      EVAL = 0.D+00
      DO 40 I= 1,30
```

```
        Y0(4*I-3) = 0.D+00
        Y0(4*I-2)=1.25D+11
C -- THIS IS THE EQUILIBRIUM CONCENTRATION OF POSITIVE VACANCIES IN
C -- INTRINSIC SILICON.
        Y0(4*I)   = 0.D+00
        IF (I.GE.16) GO TO 37
        Y0(4*I-1) = B0(2*I-1)
        GO TO 40
  37    Y0(4*I-1) = 0.D+00
  40    DOSE = DOSE + ( Y0(4*I) + Y0(4*I-1) + Y0(4*I-3)) * XINC
       WRITE(6,145) DOSE,DOSEB,ACTIV
       B0=1.D-13
       EPS=1.D-4
       INDEX=1
C--ECHO INPUT TO OUTPUT ------Y0------
       WRITE(6,50) (Y0(I),I=1,120)
  50   FORMAT(10X,17H INITIAL PROFILES//
     2        3(3X,5HBORON,3X,7HVACANCY,3X,7HBV PAIR,3X,7HBPRECIP),/
     3        10(1P4D10.3,1X,1P4D10.3,1X,1P4D10.3/)///)
C-----------------------READ PARAMETERS-------------------
  60   READ(5,70)(X(I),I = 1,12)
C -- THE PARAMETERS ARE DESCRIBED IN THE FORMAT STETEMENT  80
  70   FORMAT( 3D10.3)
C-START AT COL 1 >+4.000D+00 8.000D+00 1.200D+01 NEXT CARD
C--PARAMETERS 'ECHO INPUT PARAMETERS TO OUTPUT'
       WRITE(6,80)  (X(I),I = 1,12)
  80   FORMAT(10X,11H PARAMETERS//
     1        5X,23H DIFF.COEF.(BORON)    = ,1PD10.3,10H CM**2/SEC/
     2        5X,23H DIFF.COEF.(VACANCY)  = ,1PD10.3,10H CM**2/SEC/
     3        5X,23H DIFF.COEF.(BV PAIR)  = ,1PD10.3,10H CM**2/SEC/
     4        5X,23H EQUIL.CONS.(B+V=BV)  = ,1PD10.3,6H CM**3/
     5        5X,23H REACTION TIME CONST  = ,1PD10.3,4H SEC/
     6        5X,23H VACANCY LIFETIME     = ,1PD10.3,4H SEC/
     7        5X,23H DAMAGE ANN. TIME CONS=,1PD10.3,4H SEC/
     8        5X,23H DISS./B.REL.TIME CONS=,1PD10.3,4H SEC/
```

```
     9         5X,23H ANNEAL TEMPERATURE  =,1PD10.3,8H CELSIUS/
     1         5X,23H SOLID SOLUBILITY     =,1PD10.3,8H #/CM**3/
     2         5X,23H PREC./B.TRAP. TIME CS=,1PD10.3,4H SEC/
     3         5X,23H CONC.THRESHLD OF D.D.=,1PD10.3,8H #/CM**3///)
C-PARAMETER NORMALIZATION
      DO 90 I = 1,3
 90    PRN(I) = X(I) / ( XINC**2)
      PRN(4) = X(4)/X(5)
      PRN(5) = 1/ X(6)
      PRN(6) = 1/ X(5)
      PRN(7) = X(7)
      PRN(8) = 1/X(8)
      PRN(9) = X(9)
      PRN(10) = X(10)
      PRN(11) = 1/X(11)
      PRN(12) = X(12)
C--OUTPUT THE MODIFIED PARAMETERS USED IN DIFFUN AND PDB
      WRITE ( 6,100) (PRN(I),I = 1,12)
 100  FORMAT(53H MODIFIED PARAM. OF DIM. 1/SEC USED IN PROGRAM PRN( )//
     1       4(1P3D10.3/)///)
C ---------------------- READ  TIMES  -------------------
C -- EXAMPLE: START AT COLUMN #1 >+1.000D+00 NEXT CARD
C -- THE LAST TIME IS A FLAG:
C         TOUT = 0.000D+00  -------->  EXIT
C         TOUT = 1.000D+00  -------->  CHANGE PARAMETER SET
C         TOUT = 2.000D+00  -------->  CHANGE INITIAL PROFILES
 105  READ(5,110)  TOUT
 110  FORMAT (D10.3)
      IF(TOUT.EQ.0.D00) GO TO 160
      IF (TOUT.EQ.1.D00) GO TO 35
      IF (TOUT.EQ.2.D+00) GO TO 25
      DOSE = 0.D00
      DOSEB = 0.D+00
      EVAL = 0.D+00
      CALL ERRSET(208,256,-1,1)
```

```
C -- RECALL TO MODIFY DRIVEB IN GEARB FOR N= 120 (NMX =120).
      CALL DRIVEB(N,T0,H0,Y0,TOUT,EPS,MF,INDEX,ML,MU,PRN)
      IF (INDEX.GE.0) GO TO 135
      WRITE(6,130) INDEX
 130  FORMAT(//26H ERROR RETURN WITH INDEX =,I3//)
      GO TO 160
C-----------------------SORT Y0  ----------------------
 135  DO 140 I = 1,30
C -- THE VECTOR Y0 CONTAINS THE SPECIES CORRESPONDING TO EACH OF
C -- THE 30 PARTITIONS. THE VECTOR Z0 IS AN AUXILIARY VECTOR
C -- CONTAINING THE DRIVING FORCES FOR THE BV-PAIR REACTION, THE
C -- PRECIPITATION, THE TOTAL BORON CONCENTRATION AND THE
C -- DIFFERENCE TO THE SIMS PROFILE. THE USER MAY WISH TO
C -- MODIFY OR DELETE THESE AUXILIARY RESULTS.
        Z0(4*I-3) = Y0(4*I-1) - Y0(4*I-3) * Y0(4*I-2) * X(4)
        Z0(4*I-2) = Y0(4*I-3) + Y0(4*I-1) - X(10)
        Z0(4*I-1) = Y0(4*I-3) - Y0(4*I-1) + Y0(4*I)
        Z0(4*I)   = SIMS(I) - Z0(4*I-1)
        FVAL = FVAL + ( (SIMS(I)-Z0(4*I))/1.D+18)**2
        DOSEB =  DOSEB + Y0(4*I-3) * XINC
 140    DOSE = DOSE + Z0(4*I-1) * XINC
       ACTIV =( DOSEB/DOSE ) * 100.D+00
       WRITE(6,145) DOSE, DOSEB,ACTIV,FVAL
 145   FORMAT(5X,8H DOSE = ,1PD14.7,3X,14HBORON SUBS. = ,1PD14.7,
     1        5X,14H % ACTIVITY = ,1PD10.3/
     2        5X,8H FVAL = ,1PD23.16//)
C ------     OUTPUT THE RESULTS OF THE INTEGRATION  --------------
C ----- THE OUTPUT LIST THE CONCENTRATIONS OF BORON, POSIVE VACANCY,
C ----- BORON-VACANCY PAIR AND IMMOBILE BORON IN EACH PARTITION IN SPACE
C ----- IN INCREASING ORDER FROM LEFT TO RIGHT.
C ----  THE AUXILIARY RESULTS ARE LISTED FOLLOWING THE SAME CRITERION.
       WRITE(6,150) TOUT,XINC,  DEPTH, (Y0(I), I = 1,120),(Z0(I),I=1,120)
 150   FORMAT(5X,8H TIME = ,1PD10.3,4H SEC,10X,13H INCREMENT = ,1PD10.3,
     1          3H CM,10X,9H DEPTH = ,1PD12.3,3H CM//
     2        3(3X,5HBORON,3X,7HVACANCY,3X,7HBV PAIR,3X,7HB PREC.,4X)//
```

```
     3        10(1P4D10.3,1X,1P4D10.3,1X,1P4D10.3,/)/
     2        3(3X,5HDR.FO,3X,7HPREC.FO,3X,7HB TOTAL,3X,7HB ERROR,4X)//
     3        10(1P4D10.3,1X,1P4D10.3,1X,1P4D10.3,/)///)
      GO TO 105
 160  WRITE(6,170)  NSTEP,NFE,NJE
 170  FORMAT(//21H PROBLEM COMPLETED IN,I5,6H STEPS/
     1          21X,I5,14H F EVALUATIONS/
     2          21X,I5,14H J EVALUATIONS//)
 180  STOP
      END
      SUBROUTINE DIFFUN (N,T,Y,YDOT,K)
C USER SUPPLIED SUBROUTINE FOR GEAR B. K(1),K(2),K(3) ARE
C  SCALED DIFFUSION COEFFICIENTS. K(5) IS THE 1/VACANCY LIFETIME
C  K(6)= 1/TIME CONSTANT, AND K(4) IS THE EQUILIBRIUM CONSTANT
C  DIVIDED BY THE TIME CONSTANT.
C K(7) IS THE DAMAGE TIME CONSTANT,K(8) IS 1/DISS.OR B.RELEASE TIME
C CONSTANT,K(9) IS THE ANNEALING TEMPERATURE,AND K(10) IS THE
C SOLID SOLUBILITY LIMIT FOR BORON IN SILICON. K(11) IS THE TIME
C CONSTANT ASSOCIATED WITH PRECIPITATION OR THE TRAPPING OF BORON
C BY DISLOCATION DIPOLES. K(12) IS THE TRESHOLD LEVEL FOR THE
C FORMATION OF DISLOCATION DIPOLES.
C DMG IS THE DAMAGE PROFILE USED FOR DISTRIBUTING THE VACANCY
C GENERATION SITES.
      IMPLICIT REAL*8(A-H,O-Z)
      DOUBLE PRECISION Y(N),YDOT(N),DMG(30),REAC(30),PREC(30),K(1)
     1          ,LD(30),CA(30),CD(30),EC(30),EF(30),CVEQ(30),DELVAC(30)
C -- THIS DAMAGE PROFILE CORRESPONDS TO A 70 KEV B IMPLANT, L0D14 DOSE
      DATA DMG/2.45D20,2.65D20,2.93D20,3.35D20,3.9D20,4.6D20,
     1          5.6D20,6.3D20,6.2D20,5.4D20,4.5D20,3.55D20,
     2          2.5D20,1.48D20,8.D19,4.5D19,2.3D19,1.D19,
     3          4.9D18,2.3D18,1.12D18,5.4D17,2.5D17,1.2D17,
     4          6.D16,2.9D16,1.4D16,6.7D15,3.1D15,1.4D15 ,CD/30*0.D+00/
C -- TC IS THE ANNEALING TEMPERATURE IN DEGREES CELSIUS.
      M = 30
      TC = K(9)
```

```
      DO 5 I = 1,30
 5    CA(I) = Y(4*I-3)
      CALL SILS(M,TC,CA,CD,ECI,EC,EF,CVEQ,DELVAC)
C-----------------------------------------------------------
      REAC(1) = K(6)*Y(3) - K(4)*Y(1)*Y(2)
      PREC(1) = -K(8) * Y(4)
      LD(1)   = 0.D+00
      IF (Y(3).GT.K(12))  LD(1) = K(11) *(Y(3) -K(12))
C     IF (Y(3).GT.K(12))  LD(1) = K(11) *(Y(3)*Y(3) -K(12)*K(12))
C -- THE PRECEDING CARD CORRESPONDS TO AN OPTIONAL SECOND ORDER
C -- KINETIC TERM
      IF (Y(3).GE.K(10)) PREC(1) = K(8) *(Y(3)-K(10))
      YDOT(1) = - K(1)*2.D+00*Y(1) + K(1)*2.D+00*Y(5)
     1          + REAC(1)
      YDOT(2) = -K(2)*2.D+00*Y(2) + K(2)*2.D+00*Y(6)
     1          + REAC(1) + PREC(1) - K(5)*(Y(2) - CVEQ(1) )
     2          + (2.D-02/K(7)) *DMG(1) *DEXP(-T/K(7))
      YDOT(3) = -K(3)*2.D+00*Y(3) + K(3)*2.D+00*Y(7)
     1          -REAC(1)  - PREC(1) -LD(1)
      YDOT(4) = PREC(1)             +LD(1)
C-----------------------------------------------------------
      DO 10 I = 8, 116, 4
       REAC(I/4) = K(6)*Y(I-1) - K(4)*Y(I-2)*Y(I-3)
       PREC(I/4) = -K(8) * Y(I)
      LD(I/4) = 0.D+00
      IF (Y(I-1).GT.K(12))  LD(I/4) = K(11) *(Y(I-1)-K(12))
C     IF (Y(I-1).GT.K(12))  LD(I/4) = K(11) *(Y(I-1)*Y(I-1)-K(12)*K(12))
C -- THE PRECEDING CARD CORRESPONDS TO AN OPTIONAL SECOND ORDER
C -- KINETIC TERM
      IF (Y(I-1).GE.K(10)) PREC(I/4) = K(8) *(Y(I-1)-K(10))
       YDOT(I-3) = K(1) * ( Y(I-7) - 2.D+00*Y(I-3) + Y(I+1) )
     1           + REAC(I/4)
       YDOT(I-2) = K(2) * ( Y(I-6) - 2.D+00*Y(I-2) + Y(I+2) )
     1           + REAC(I/4) + PREC(I/4)
     2           + (2.D-02/K(7)) *DMG(I/4) *DEXP(-T/K(7))
```

```
     3              - K(5) * ( Y(I-2) - CVEQ(I/4) )
       YDOT(I-1) = K(3) * ( Y(I-5) - 2.D+00*Y(I-1) + Y(I+3) )
     1              - REAC(I/4) - PREC(I/4) -LD(I/4)
 10    YDOT(I)   = PREC(I/4)                +LD(I/4)
C-----------------------------------------------------------------------
      REAC(30) = K(6)*Y(119) - K(4)*Y(118)*Y(117)
      PREC(30) = -K(8) * Y(120)
      LD(30)   = 0.D+00
      IF (Y(119).GT.K(12))  LD(30) = K(11) *(Y(119)-K(12))
C     IF (Y(119).GT.K(12))  LD(30) = K(11) *(Y(119)*Y(119)-K(12)*K(12))
C -- THE PRECEEDING CARD CORRESPONDS TO AN OPTIONAL SECOND ORDER
C -- KINETIC TERM
      IF (Y(119).GE.K(10)) PREC(30) = K(8) *(Y(119)-K(10))
      YDOT(117) = K(1) * ( Y(113) - 2.D+00*Y(117) + 1.D+15 )
     1            + REAC(30)
      YDOT(118) = K(2) * ( Y(114) - 2.D+00*Y(118) + 1.D+12)
     1            + REAC(30) + PREC(30)
     2            + (2.D-02/K(7)) *DMG(30) *DEXP(-T/K(7))
     3            -  K(5) * ( Y(118) - CVEQ(30) )
      YDOT(119) = K(3) * ( Y(115) - 2.D+00*Y(119) + 5.D+16)
     1            - REAC(30) - PREC(30) -LD(30)
      YDOT(120) = PREC(30)               +LD(30)
      RETURN
      END
      SUBROUTINE PDB(N,T,Y,PD,N0,ML,MU,K)
      IMPLICIT REAL*8(A-H,O-Z)
      DOUBLE PRECISION Y(N),PD(N0,9),K(1),LDF,
     1                 CA(30),CD(30),EC(30),EF(30),CVEQ(30),DELVAC(30)
      M = 30
      TC = K(9)
      DO 5 I = 1,30
 5    CA(I) = Y(4*I-3)
      CALL SILS(M,TC,CA,CD,ECI,EC,EF,CVEQ,DELVAC)
C-----------------------------------------------------------
      DO 10 I = 1, 117, 4
```

```
      SEL = 1.D+00
      IF (Y(I+3).GE.K(10)) SEL = 0.D+00
      LDF = 0.D+00
      IF (Y(I+2).GT.K(12)) LDF = 1.D+00
C-----------------B O R O N  SUBSTITUTIONAL ---------------
       PD(I,1) = K(1)
       PD(I,2) = 0.D+00
       PD(I,3) = 0.D+00
       PD(I,4) = 0.D+00
       PD(I,5) = -2.D+00 * K(1) - K(4) * Y(I+1)
       PD(I,6) = -K(4) * Y(I)
       PD(I,7) = + K(6)
       PD(I,8) = 0.D+00
       PD(I,9) = K(1)
C--------------------- V A C A N C Y  ----------------------
       PD(I+1,1) = K(2)
       PD(I+1,2) = 0.D+00
       PD(I+1,3) = 0.D+00
       PD(I+1,4) = -K(4) * Y(I+1) - K(5) * DELVAC((I+3)/4)
       PD(I+1,5) = - 2.D+00 * K(2) -  K(4)*Y(I)    -K(5)
       PD(I+1,6) = + K(6) + K(8) *(1.D+00 -SEL)
       PD(I+1,7) = - K(8) *SEL
       PD(I+1,8) = 0.D+00
       PD(I+1,9) = K(2)
C--------------------- BORON - VACANCY - PAIRS -----------
       PD(I+2,1) = K(3)
       PD(I+2,2) = 0.D+00
       PD(I+2,3) = + K(4) * Y(I+1)
       PD(I+2,4) = + K(4) * Y(I)
       PD(I+2,5) = - 2.D+00 * K(3) - K(6) - K(8) *(1.D+00 -SEL)
     1             - LDF  *K(11)
C    1             - LDF *2.D+00 *K(11) *Y(I+2)
C -- THE PRECEEDING CARD CORRESPONDS TO AN OPTIONAL SECOND ORDER
C -- KINETIC TERM
       PD(I+2,6) = + K(8) *SEL
```

```
        PD(I+2,7) = 0.D+00
        PD(I+2,8) = 0.D+00
        PD(I+2,9) = K(3)
C---------------------- BORON IMMOBILE -------------------
        PD(I+3,1) = 0.D+00
        PD(I+3,2) =  0.D+00
        PD(I+3,3) = 0.D+00
        PD(I+3,4) = + K(8) *(1.D+00 -SEL) +LDF  *K(11)
C       PD(I+3,4) = + K(8) *(1.D+00 -SEL) +LDF *2.D+00 *K(11) * Y(I+2)
C -- THE PRECEEDING CARD CORRESPONDS TO AN OPTIONAL SECOND ORDER
C -- KINETIC TERM
        PD(I+3,5) = - K(8) *SEL
        PD(I+3,6) = 0.D+00
        PD(I+3,7) = 0.D+00
        PD(I+3,8) = 0.D+00
 10     PD(I+3,9) = 0.D+00
C-------------------------------------------------------------
        PD(1,9) = 2.D+00 * K(1)
        PD(2,9) = 2.D+00 * K(2)
        PD(3,9) = 2.D+00 * K(3)
      RETURN
      END
      SUBROUTINE SILS(N,TC,CA,CD,ECI,EC,EF,CVEQ,DELVAC)
C-----THIS SUBROUTINE IS FOR SILICON,INPUT PARAMETERS ARE:
C-----      N ------------- # OF POINTS
C-----     TC ------------- TEMP. IN DEG.CELSIUS
C-----     CA ------------- ACCEPTOR IMPURITY CONCENTRATION
C-----     CD ------------- DONOR IMPURITY CONCENTRATION
C-----     OUTPUT PARAMETERS ARE:
C-----     ECI ------------ INTRINSIC CARRIER CONC,
C-----     EC ------------- MAJORITY CARRIER CONC,
C-----     EF ------------  FERMI LEVEL IN E.V. FROM THE
C-----                      MAJORITY BAND EDGE.
C-----    CVEQ IS THE EQUILIBRIUM CONC OF SINGLY CHARGED VAC.
C-----    DELVEQ IS THE PARTIAL DERIVATIVE OF CVEQ RESPECT TO THE
```

```
C-----           IMPURITY CONCENTRATION
      IMPLICIT REAL*8(A-H,O-Z)
      DIMENSION CA(N),CD(N),EC(N),EF(N),CVEQ(N),DELVAC(N)
C-----  'ED' AND 'EA' ARE THE ENERGY LEVELS OF DONORS AND ACCEPTORS
      ED = 0.046D+00
      EA = 0.045D+00
C------TK IS THE TEMPERATURE IN DEGREES KELVIN.
      TK = TC + 2.7316D+02
C----- QVEQ  IS THE ACTIVATION ENERGY OF FORMATION OF VACANCIES
      QVEQ = 3.4D+00
C----- PEX  IS THE PRE-EXPONENTIAL FACTOR OF THE FORMATION OF VAC.
      PEX  = 5.D+25
C----- THE FOLLOWING ARE THE ENERGY LEVELS OF THE SINGLY CHARGED
C----- VACANCIES IN THE BAND-GAP REFERRED TO THE RESPECTIVE BAND-
C----- EDGES. P AND N STAND FOR POSITIVE AND NEGATIVE CHARGE-STATES.
      EVP = 3.557D-01
      EVN = 5.557D-01
C------ECI, FROM MORIN & MAITA
      ECI = 3.88D+16 * (TK ** 1.5D+00) * DEXP(-6.05D-01/(8.62D-05*TK))
      DO 10 I=1,N
      IF (CA(I).GE.CD(I)) GO TO 5
C-----  PARAMETERS FOR N-TYPE
      EV = EVN
       DSC = 3.421978D+15 * ( TK**1.5D+00)
       ECT = 2.D+00 * DSC * (CD(I)-CA(I)) / ( DSC+2.7D-01
     1           * (CD(I)-CA(I)) + 5.D-01 *CA(I) *DEXP(ED/(8.62D-05
     2           *TK))+ DSQRT((DSC - 2.7D-01 *(CD(I)-CA(I)) +
     3           5.D-01 * CA(I) * DEXP( ED/ (8.62D-05 * TK)))**2.D+00
     4           + 4.D+00 *5.D-01 *(DSC-2.7D-01*CA(I))*(CD(I)-CA(I))
     5           * DEXP(ED/(8.62D-05*TK))))
       IF (CA(I).LE.CD(I)) GO TO 9
C-----  PARAMETERS FOR P-TYPE
 5     EV = EVP
       DSC = 2.0163964D+15 * (TK ** 1.5D+00)
       ECT = 2.D+00 * DSC * (CA(I)-CD(I)) / ( DSC+2.7D-01
```

```
     1           * (CA(I)-CD(I)) + 2.D+00 *CD(I) *DEXP(EA/(8.62D-05
     2           *TK))+ DSQRT((DSC - 2.7D-01 *(CA(I)-CD(I)) +
     3           2.D+00 * CD(I) * DEXP( EA/ (8.62D-05 * TK)))**2.D+00
     4           + 4.D+00 *2.D+00 *(DSC-2.7D-01*CD(I))*(CA(I)-CD(I))
     5           * DEXP(EA/(8.62D-05*TK))))
9      EC(I) = ECT/ 2.D+00 + DSQRT( ((ECT)/2.D+00)**2.D+00
     1                                + (ECI**2.D+00) )
       EF(I) = + 8.62D-05 * TK * DLOG( (DSC/EC(I)) -2.7D-01)
       CVEQ(I) = PEX * DEXP( -QVEQ/ (8.62D-05*TK))
     1       * DEXP( (EV-EF(I))/(8.62D-05*TK) )
10     DELVAC(I) = CVEQ(I) * DSC* (1 + ECT/DSQRT(
     1             ( ECT/2.D+00)**2.D+00+(ECI**2.D+00)))
     2           / ( 2.D+00 * EC(I)*EC(I) * ( DSC/EC(I) - 2.7D-01))
       RETURN
       END
```

Appendix B

CALCULATION OF AN EFFECTIVE DIFFUSION COEFFICIENT

Equations (B1) and (B2) are equations (A1a) and (A1c) in Appendix A rewritten in terms of fluxes, J_B and J_{BV}.

$$\frac{dC_B}{dt} = \frac{dJ_B}{dx} + \left(\frac{C_{BV} - k_o C_B C_V^+}{\tau}\right) \tag{B1}$$

$$\frac{dC_{BV}}{dt} = \frac{dJ_{BV}}{dx} - \left(\frac{C_{BV} - k_o C_B C_V^+}{\tau}\right) \tag{B2}$$

Addition of Eqs. (B1) and (B2) yields:

$$\frac{d}{dt}\,(C_B + C_{BV}) = \frac{d}{dx}\,(J_B + J_{BV}) \tag{B3}$$

Expressing the fluxes in terms of concentration gradients and diffussion coefficients, we obtain Eq. (B4).

$$J_B + J_{BV} = D_B \frac{\partial C_B}{\partial x} + D_{BV} \frac{\partial C_{BV}}{\partial x} \tag{B4}$$

For this equation, we can show that the last term dominates as follows: D_{BV} is much greater than D_B, at 900°C; their values are 7×10^{-14} and 1.6×10^{-21} cm^2/sec, respectively. At the outset of the anneal, C_{BV} C_B and $\partial C_{BV}/\partial x \gg \partial C_B/\partial x$, hence we can neglect the first term. As the annealing proceeds, the diffusion of boron will approach ordinary diffusion conditions, namely,

$$\left(\frac{\partial C_{BV}}{\partial x} \Big/ \frac{\partial C_B}{\partial x}\right) \sim \frac{C_{BV}}{C_B} \sim 0.02$$

The inequality between gradients has reversed; however, because D_{BV} is much greater than D_B, the last term still overwhelms the first one. We can then approximate the total flux as in Eq. (5):

$$J_B + J_{BV} \simeq D_{BV} \frac{\partial C_{BV}}{\partial x} \tag{B5}$$

We now let ξ be the fractional concentration of BV pairs, which is a function of the electrical activity:

$$\xi = \frac{C_{BV}}{C_{BV} + C_B} = 1 - \alpha \tag{B6}$$

Then,

$$C_{BV} = \xi(C_{BV} + C_B) \tag{B7}$$

and the gradient becomes:

$$\frac{\partial C_{BV}}{\partial x} = \frac{\partial \xi}{\partial x}(C_{BV} + C_B) + \xi \frac{\partial (C_{BV} + C_B)}{\partial x} \tag{B8}$$

We can now identify several situations in which the first term in Fig. (B8) is negligible in comparison with the last one. For instance, under equilibrium conditions, we can rewrite Eq. (3) in Section III as:

$$\frac{C_{BV}}{C_B} = k_o C_{V^+}$$

Then, substitution of the above equation in the expression for $1/\xi$ yields

$$\frac{1}{\xi} = 1 + \frac{C_B}{C_{BV}} = 1 + \frac{1}{k_o + C_{V^+}}$$

where

$$C_{V^+} = C_{V^0}(T) \exp \frac{E_{V^+} - E_F}{kT}$$

In general, the Fermi level, as a function of the acceptor concentration, will be a function of distance; however, for annealing temperatues

near 900°C and the boron concentration below ~10^{17} atoms/cm^3, this dependence is very weak, hence $C_{V+} \sim C_{V^0}$, $\partial\xi/\partial x \sim 0$, and the first term in Eq. (B8) is negligible. An analogous case arises when the annealing temperature is high, above 1100°C. In this case, the Fermi level is fixed in the middle of the bandgap.

Under nonequilibrium conditions, the comparison of the terms in Eq. (B8) can be performed numerically. For the typical annealing case in Table 3, the results of the calculation show that the approximation in Eq. (B8) is correct under nonequilibrium and equilibrium conditions, failing only under equilibrium conditions when the boron concentration is near and above 10^{18} atoms/cm^3. In other words, when the boron concentration is high and the Fermi level is a function of distance, $\partial\xi/\partial x$ may no longer be small.

For cases in which $d\xi/dx$ may be neglected, we may then simplify Eq. (B8) to

$$\frac{\partial C_{BV}}{\partial x} \simeq \xi \frac{\partial (C_{BV} + C_B)}{\partial x} \tag{B9}$$

Substitution of Eq. (B9) in Eq. (B5) and Eq. (B5) in Eq. (B3) then yields

$$\frac{d(C_B + C_{BV})}{dt} = (D_{BV} \cdot \xi) \frac{d^2(C_{BV} + C_B)}{\partial x^2} \tag{B10}$$

where $(D_{BV} \cdot \xi)$ can be identified with the overall diffusion coefficient D_{exp}. Hence,

$$D_{exp} = D_{BV}\xi = D_{BV}(1 - \alpha) \tag{B11}$$

REFERENCES

1. J. F. Gibbons, Proc. of the IEEE, 56, 3, March 1968, pp. 295-319; Proc. of the IEEE, 60, 9, Sep 1972, pp. 1062-1096.

2. W. K. Hofker, H. W. Werner, D. P. Oosthoek, and H. A. M. de Grefte, Appl. Phys., 2, Springer-Verlag, 1973, pp. 265-278.

3. E. Tanneu Baum, Solid State Electn., 2, 1961, p. 123.

4. P. A. Iles and B. Leibenhant, Solid State Electn., 5, 1962, p. 331.

5. V. K. Subashiev, A. P. Landsman, and A. A. Kukharskii, Sov. Phys. Solid State, 2, 1961, p. 2406.

6. S. Maekawa and T. Oshida, J. Phys. Soc. Japan, 19, 1964, p. 253.

7. K. H. Nicholas, Solid State Electn., 9, 1966, pp. 35-47.

8. B. L. Crowder, J. F. Ziegler, F. F. Morehead, and G. W. Cole, Proc. of the Third International Conf. on Ion Implantation in Semiconductors and Other Materials, edited by B. L. Crowder, Plenum Press, New York, 1973.

9. J. R. Anderson and J. F. Gibbons, Appl. Phys. Lett., 28, 4, 1976, p. 181.

10. T. J. Parker, J. Appl. Phys., 38, 9, 1967, pp. 3471-3477.

11. G. Fladda, K. Bjorkquist, L. Erikson, and D. Sigurd, Appl. Phys. Lett., 16, 8, Apr 1970.

12. J. R. Anderson and G. Thomas, private communication.

13. P. Baruch, J. Monnier, B. Blancherd, and C. Castaing, Proc. of the Third International Ion Implantation Conf., Yorktown Heights, edited by B. L. Crowder, Plenum Press, New York, 1973.

14. W. K. Hofker, H. W. Werner, D. P. Oosthoek, and N. J. Koeman, Appl. Phys., 4, Springer-Verlag, 1970, pp. 125-133.

15. J. V. Anderson, O. Andreasen, J. A. Davies, and E. Uggerhoj, Proc. of the First International Conf. on Ion Implantation in Semiconductors, Thousand Oaks, Calif., Gordon and Breach Pub., New York, 1970.

16. J. C. North and N. M. Gibson, Appl. Phys. Lett., 16, 3, Feb 1970.

17. R. W. Bicknell and R. M. Allen, Proc. of the First International Conf. on Ion Implantation in Semiconductors, Thousand Oaks, Calif., Gordon and Breach Pub., New York, 1970.

18. T. E. Seidel and A. U. MacRae, Proc. of the First International Conf. on Ion Implantation in Semiconductors, Thousand Oaks, Calif., Gordon and Breach Pub., New York, 1970.

19. To be published, jointly with T. Magee.

20. G. P. Pelous, D. P. Secrosnier, and P. Henoc, Ion Implantation in Semiconductors, edited by S. Namba, Plenum Press, New York, 1973.

21. R. W. Bicknell, Proc. Royal Soc. of London, Series A, 311, 1504, 1969.

22. L. T. Chadderton and F. H. Eisen, First International Conf. on Solid State in Semiconductors, Thousand Oaks, Calif., Gordon and Breach Pub., New York, 1970.

23. A. P. Karatsyuba, Vikurinny, Svrytchdova, T. P. Timashova, and V. V. Yudin, Proc. of the International Conf. at the U. of Reading, Jul 1972, published by Inst. of Physic, London, England.

24. M. Tamura, T. Ikeda, and N. Yoshikio, J. Appl. Phys. 40, 9, 1969.

25. L. J. Chen, K. Skshan, and G. Thomas, Phys. Stat. Solidi (A), 28, 1, 1975, p. 309.

26. E. Livine, J. Washburn, and G. Thomas, J. Appl. Phys., 38, 1, Jan 1967.

27. Seeger and Chick, Phys. Stat. Solidi, 29, 2, 1968, p. 455.

28. R. A. Swalin, J. Appl. Phys., 29, 4, 1958, p. 670.

29. R. B. Fair, J. Electrochem. Soc., 122, 6, Jun 1975.

30. W. Nuyts and Van Overstraeten, Phys. Stat. Solidi (A), 15, 1973, p. 329; 15, 1973, p. 455.

31. Longini and Greene, Phys. Rev., 102, 1956, p. 992.

32. C. Castaing, P. Baruch, J. P. Gailliard, G. Thomas, J. F. Gibbons, and J. R. Anderson, ESSDERC Conf., Grenoble, Sep 1975.

33. [illegible] J. Tan, B. S. Berry, and W. F. J. Frank, Proc. of the International Conf. on Ion Implantation in Semiconductors and [illegible]er Materials, Yorktown Heights, Plenum Press, New York, Dec 19[illegible]

34. B. Netange, M. Cherki, and P. Baruch, Appl. Phys. Lett., 20, 9, May 1972.

35. G. D. Watkins, Phys. Rev., 13, 6 Mar 1976.

36. W. Shockley and J. L. Moll, Phys. Rev., 119, 5, 1 Sep 1960.

37. T. E. Seidel and A. U. MacRae, Trans. of Metallurgical Soc. of AIME, 245, Mar 1969, pp. 491-498.

38. D. K. Brice, Proc. of the First International Conf. on Ion Implantation in Semiconductors, Thousand Oaks, Calif., Gordon and Breach Pub., New York, 1970.

39. J. E. Westmoreland, J. W. Meyer, F. H. Eisen, and B. Welch, Appl. Phys. Lett., 15, 9, Nov 1969.

40. J. M. Fairfield and B. J. Masters, J. Appl. Phys., 38, 5, Jul 1967.

41. J. S. Blakemore, Semiconductor Statistics, Mac Millan, New York, 1962.

42. T. Tsuchimoto and T. Tokuyama, Proc. of the First International Conf. on Ion Implantation in Semiconductors, Thousand Oaks, Calif., Gordon and Breach Pub., New York, 1970.

43. G. L. Vick and K. M. Whittle, J. Electrochem. Soc., 116, 8, 1969, p. 1112.

44. L. Csepregi, J. W. Mayer, and T. W. Sigmon, Phys. Lett., 54 A, 2, 25 Aug 1975; Appl. Phys. Lett., 29, 2, 15 Jul 1976; E. F. Kennedy, L. Csepregi, J. W. Meyer, and T. W. Sigmon, Proc. of the Fifth International Conf. on Ion Implantation in Semiconductors, Boulder, Colo., Aug 1976.

45. A. C. Hindmarsh, Report UCID-30059, Lawrence Livermore Lab., University of California, Livermore, Calif., Mar 1975.

46. R. D. Richtmeyer and K. W. Morton, Difference Methods for Initial Value Problems, New York Interscience Publishers, 1967, Chap. 8.

END

FILMED

11-85

DTIC